Dispersive construction of two-loop $P \to \pi\pi\pi (P = K, \eta)$ amplitudes

K. Kampf,[1,*] M. Knecht,[2,†] J. Novotný,[1,‡] and M. Zdráhal[1,§]

[1]*Institute of Particle and Nuclear Physics, Faculty of Mathematics and Physics, Charles University, V Holešovičkách 2, CZ-180 00 Prague 8, Czech Republic*

[2]*Centre de Physique Théorique, CNRS/Aix-Marseille Univ./Univ. du Sud Toulon-Var (UMR 7332) CNRS-Luminy Case 907, 13288 Marseille Cedex 9, France*

(Received 8 December 2019; accepted 24 February 2020; published 29 April 2020)

We present and develop a general dispersive framework allowing us to construct representations of the amplitudes for the processes $P\pi \to \pi\pi$, $P = K, \eta$, valid at the two-loop level in the low-energy expansion. The construction proceeds through a two-step iteration, starting from the tree-level amplitudes and their S and P partial-wave projections. The one-loop amplitudes are obtained for all possible configurations of pion masses. The second iteration is presented in detail in the cases where either all masses of charged and neutral pions are equal or for the decay into three neutral pions. Issues related to analyticity properties of the amplitudes and of their lowest partial-wave projections are given particular attention. This study is introduced by a brief survey of the situation, for both experimental and theoretical aspects, of the decay modes into three pions of charged and neutral kaons and of the eta meson.

DOI: 10.1103/PhysRevD.101.074043

I. INTRODUCTION

Our experimental knowledge of the Dalitz-plot structures of the amplitudes for the processes $P \to \pi\pi\pi$ has substantially improved during the last decades, for $P = K^{\pm}$ [1–7], $P = K_L$ [8], or $P = \eta$ [9–18]. This situation is likely to improve further still in the future [19,20]. The sizes of the collected data samples in the case of the charged kaons, for instance, outgrow by orders of magnitude those that were available before. This general increase in statistics has prompted various theoretical studies [21–43] of these decay modes, often with an emphasis on isospin-breaking contributions. Indeed, from the theoretical point of view, these processes are interesting because they provide access to fundamental quantities. For instance, the rates for the decays $\eta \to \pi\pi\pi$, which are forbidden in the isospin limit, offer a good possibility to determine the value of the quark mass ratio

$$R = \frac{m_s - \hat{m}}{m_d - m_u}, \tag{1.1}$$

where m_u, m_d, and m_s denote the masses of the three lightest quark flavors, while $\hat{m} = (m_u + m_d)/2$. Furthermore, the processes with two neutral pions in the final state exhibit the so-called cusp effect, which contains information on the $\pi\pi$ scattering lengths in the S-wave. Concerning this last aspect, in particular, the decay modes $K^{\pm} \to \pi^{\pm}\pi^0\pi^0$ and $K_L \to 3\pi^0$ have already been studied from this point of view by the NA48 [1,6] and KTeV [8] collaborations, respectively. The first attempts to measure the same effects in the decays of the η meson into three neutral pions have also been reported [12].[1]

Traditionally, the processes $P \to \pi\pi\pi$ are most of the time being analyzed with a polynomial parametrization (in terms of slopes and curvatures in appropriately chosen Dalitz-plot variables) of the amplitude, and theoretical expressions have often been given in this form as well. It is clear that the study of nonanalytic features of the amplitude, like a cusp, cannot be done within such a simple framework. The aim of the work presented in this article is, therefore, the construction of a model-independent form of two-loop amplitudes of the processes mentioned above that is valid up to two loops in the low-energy expansion and that exhibits the correct unitarity parts coming from the $\pi\pi$ intermediate states. These are the only states that, up to that order, give rise to nonanalytic structures in the

*kampf@ipnp.mff.cuni.cz
†Marc.Knecht@cpt.univ-mrs.fr
‡novotny@ipnp.mff.cuni.cz
§zdrahal@ipnp.mff.cuni.cz

[1]Depending on the process, the cusp can be more or less pronounced, and therefore more or less easy to measure. A criterion allowing one to estimate the "visibility" of the cusp in the different processes mentioned above has been proposed and discussed in Ref. [36].

corresponding decay amplitudes. Other two-meson intermediate states correspond to more remote thresholds for the $P\pi \to \pi\pi$ scattering amplitudes that, inside the decay region, can be quite appropriately approximated and described by a polynomial. Intermediate states with more than two mesons occur only at higher orders in the chiral expansion, and will, therefore, not be considered here. Our aim is, however, to include isospin-breaking effects induced by the mass difference between charged and neutral pions, without which no cusp would be seen in the decay distribution. Note that the effects of electromagnetic interactions other than those leading to isospin breaking in the meson masses, i.e., exchanges of virtual photons between charged states and photon emission, are not included in the construction. A more complete discussion of this aspect is given in Sec. 2.1 of Ref. [44].

Our construction is adapted from the "reconstruction theorem," first established in Ref. [45] for the case of the $\pi\pi$ amplitude in the isospin limit. The authors of Ref. [45] have shown that, up to two loops in the chiral expansion, the analytical form of the amplitude is completely fixed by general properties like relativistic invariance, unitarity, analyticity, and crossing, supplemented by chiral counting for the partial waves. Isospin symmetry was also invoked, but its role merely served to reduce the scattering amplitudes in the various channels to a single amplitude. The construction of the analytical expression of the $\pi\pi$ amplitude in this framework was then implemented explicitly in Ref. [46]. The method is, however, more general and allows for several extensions. First, it also applies to the scattering amplitudes involving other pseudoscalar mesons [47]. Next, it generalizes in a straightforward manner to the situation without isospin symmetry, the main difference being that several independent amplitudes will be involved in order to describe the different channels [44]. Finally, it also applies to other observables, like form factors [44,48,49]. The present work extends the general method of the reconstruction theorem of Ref. [45] to the amplitudes of the scattering processes $P\pi \to \pi\pi$, $P = K^{\pm}, K_L, K_S, \eta$, in the threshold region. The amplitudes for the decay processes $P \to 3\pi$ are then obtained by analytic continuation below the threshold and inside the physical decay region in the Mandelstam plane.

This is the first article devoted to the presentation of the details of the construction of such analytical expressions for the decay amplitudes $P \to \pi\pi\pi$ up to two loops in the low-energy expansion. In the present article, we give the full isospin-breaking result for all the amplitudes only at the one-loop level, while at the first stage, the expressions of the two-loop amplitudes are only worked out in the limit where the masses of the neutral and charged pions are equal. This allows describing some general features of our construction in a simpler framework without having to deal, in addition, with several kinematic complications that arise only when the intermediate- and final-state pions have unequal masses. Incidentally, this is the framework that we have used in Ref. [36], devoted to the analysis of the decay of the η meson into three pions. We also plan to update the latter analysis, taking more recent data [15,16,18] into account, but this will be left for a separate work [50]. A rather simple extension of this framework, though, allows dealing with isospin breaking in the pion masses in the case of the decay channels into three neutral pions, which we will treat in a second stage in the present article. The results where all isospin-breaking effects due to the mass difference between neutral and charged pions are included up to two loops when the final state contains also charged pions will be discussed in a forthcoming paper [51]. We also do not address the possible violation of CP invariance, for instance, in the $K \to \pi\pi\pi$ processes, although it could be straightforwardly incorporated into our framework if necessary.

The outline of this paper is then as follows. In the next section, we briefly summarize all the processes in question and list the existing studies of the last few years. Section III recalls the main aspects and content of the reconstruction theorem and introduces our notation. In Sec. IV, we write the results of the first iteration of the reconstruction theorem for the $\pi\pi$ scattering and the $P\pi \to \pi\pi$ amplitudes. Section V then gives the result of the second iteration in the limit where the charged and neutral pion masses are identical. These results are extended, for the decay modes into three neutral pions, to the situation where the difference in the pion masses is taken into account in Sec. VI. The final section is devoted to a summary and conclusions. In order not to overload the main text with too many technical issues and lengthy expressions, some of them have been gathered in four Appendixes.

Some aspects of this work have also been discussed in earlier preliminary reports [52–54]. A comprehensive account with more details on some of the technical aspects can also be found in Ref. [55].

II. PROCESSES IN QUESTION

Our analysis covers the following list of processes:

$$K^{\pm} \to \pi^0\pi^0\pi^{\pm}, \tag{2.1a}$$

$$K^{\pm} \to \pi^{\pm}\pi^{\pm}\pi^{\mp}, \tag{2.1b}$$

$$K_L \to \pi^0\pi^0\pi^0, \tag{2.1c}$$

$$K_L \to \pi^+\pi^-\pi^0, \tag{2.1d}$$

$$K_S \to \pi^+\pi^-\pi^0, \tag{2.1e}$$

$$\eta \to \pi^0\pi^0\pi^0, \tag{2.1f}$$

$$\eta \to \pi^+\pi^-\pi^0. \tag{2.1g}$$

The natural framework for describing the amplitudes of these processes is three-flavor chiral perturbation theory [56], extended, in the case of kaon decays, to also include the weak nonleptonic decays [57]. At the lowest order, the corresponding amplitudes are simply first-order polynomials in the Mandelstam variables. Here, as already mentioned, we will ignore CP-violating contributions, so that the coefficients of these lowest-order polynomials are real. The computation of higher orders meets technical complications, as well as the necessity to consider an increasing number of low-energy constants, which then need to be determined independently.

In the rest of this section, we are going to describe the present situation for the three types of processes, the decay of a charged or of a neutral CP-odd kaon into three pions, the similar decay modes of the η meson, and finally the decay into three pions of a neutral CP-even kaon.

A. $K^{\pm}$ and K_L^0 decays into three pions

These decay amplitudes were computed using the framework of chiral perturbation theory up to next-to-leading order (NLO) already in 1991 [58], at that time ignoring all the isospin-breaking effects. Explicit expressions for the one-loop amplitudes in the isospin limit have been given in Ref. [21]. The most comprehensive work also including isospin breaking, but still stopping at NLO only, is contained in the series of papers [22–24].

The interest for these processes has risen after the observation of a unitarity cusp in the event distribution with respect to the invariant mass of two neutral pions by the NA48 Collaboration [1]. In Ref. [26], this cusp is proposed as a potentially clean method allowing for the determination of the combination $a_0 - a_2$ of $\pi\pi$ scattering lengths. Elaborations on this idea appeared in Ref. [27]. Assuming a simplified analytic structure of the amplitude and using unitarity of the scattering matrix allows expressing the decay amplitude in the vicinity of the cusp as an expansion in the scattering lengths a_i. In Ref. [28], the same assumptions are made, but in addition, the isospin symmetric NLO result of chiral perturbation theory is used as an input for the real parts of the amplitudes.

It was pointed out by the authors of Refs. [29,31,37] that the correct analytic structure of the amplitudes should be more complicated than described in Refs. [27,28], and they have constructed a representation of the amplitude within the framework of nonrelativistic effective field theory, based on a combined expansion in both the scattering lengths and a formal nonrelativistic parameter ε. This expansion is considered to remain valid over the whole decay region, although the pions emitted at the edge of the decay region are already relativistic. Finally, taking advantage of working within a Lagrangian formulation, the effects of real and virtual photons could also be accounted for [33] within this nonrelativistic framework.

B. η decays into three pions

The decay modes $\eta \to \pi^+\pi^-\pi^0$ and $\eta \to \pi^0\pi^0\pi^0$ are $\Delta I = 1$ transitions, and thus require isospin breaking. The latter is provided by two sources, electromagnetic interactions on the one hand and the quark mass difference $m_d - m_u$ on the other hand. As far as the former is concerned, contributions of the order $\mathcal{O}(e^2E^0)$ vanish [59,60], and corrections of the order $\mathcal{O}(e^2 m_q)$, $q = u$, d, s to the decay rate were found to be quite small [61,62]. Thus, to a very good approximation, the amplitudes for the decay modes of the η meson into three pions are proportional to the isospin-breaking quark mass difference $m_d - m_u$, e.g., $A^{\eta\to\pi^+\pi^-\pi^0}(s,t,u) = (\sqrt{3}/4R) f(s,t,u)$, with the quark-mass ratio R already defined in (1.1). Measuring the corresponding decay rates thus directly gives information on $m_d - m_u$, provided one knows $f(s,t,u)$ sufficiently well.

The amplitude $f(s,t,u)$ has been computed in the chiral expansion, at orders $\mathcal{O}(E^2)$ [60,63], $\mathcal{O}(E^4)$ [64], and $\mathcal{O}(E^6)$ [30]. The convergence is, however, slow, due to strong $\pi\pi$ rescattering effects. Furthermore, the two-loop expression involves many unknown $\mathcal{O}(E^6)$ low-energy constants. The very long complete analytical expression of the $\mathcal{O}(E^6)$ amplitude has not been published, but is available as a Fortran code from the authors of Ref. [30]. Other approaches have, therefore, been considered in order to improve the situation. For instance, a more compact explicit representation of $f(s,t,u)$ at next-to-next-to-leading order (NNLO) can also be worked out [35] within the nonrelativistic framework mentioned above. Notice, however, that in the center of the Dalitz plot, the momenta of the outgoing pions in the rest frame of the decaying particle, which count as order $\mathcal{O}(\varepsilon)$, can already represent 90% of their rest energy, which is counted as order $\mathcal{O}(1)$.

Alternatively, the iterative resummation of the $\pi\pi$ rescattering effects can be handled numerically in a dispersive framework [65,66]. In this second approach, one writes unitarity relations with $\pi\pi$ intermediate states and constructs dispersion relations of the Khuri-Treiman type [67–73]. The amplitude is then obtained by finding the numerically fixed-point solution of these relations. The determination of the subtraction constants arises from matching [65,66] with the NLO results of chiral perturbation theory. A more recent analysis [40] within this framework uses instead information from the chiral perturbation theory calculation at NNLO of Ref. [30].

All these studies, but the one of Ref. [35], address the description of the amplitude $f(s,t,u)$ in the isospin limit, thus leaving out the possibility to discuss the effect of the cusp in the $\pi^0\pi^0$ invariant mass of the decay of the η into three neutral pions. Isospin-breaking effects in $f(s,t,u)$ can also be naturally included in the relativistic approach we will develop in the present work.

C. K_S decay into three pions

Our procedure can easily be applied as well to the CP-conserving part of the decay amplitude for the decay $K_S \to \pi^+\pi^-\pi^0$. Nevertheless, the corresponding branching ratio is very small, which makes it difficult to measure the energy dependence of the decay distribution, although some measurements exist [74,75]. Therefore, the only parameter connected with this process that has been measured recently [76] is the amplitude of the CP-conserving component of the decay $K_S \to \pi^+\pi^-\pi^0$ relative to $K_L \to \pi^+\pi^-\pi^0$. From the theoretical point of view, this process is also covered by the chiral perturbation theory computations up to NLO presented in Refs. [21–24].

III. GENERAL STRUCTURE OF THE TWO-LOOP AMPLITUDES

As mentioned above, we will obtain the amplitudes $\mathcal{M}(s_1, s_2, s_3)$ describing the decay processes

$$P(k) \to \pi(p_1)\pi(p_2)\pi(p_3) \tag{3.1}$$

from an analytic continuation into the subthreshold region of the amplitude $\mathcal{M}(s,t,u)$ of a corresponding scattering process of the type

$$P(k)\pi(p_1) \to \pi(p_2)\pi(p_3), \tag{3.2}$$

where $k^2 = M_P^2$, $p_i^2 = M_i^2$. In the first case, the variables are defined as usual, $s_i = (k-p_i)^2$, whereas in the scattering region, we take $s=(k+p_1)^2$, $t=(k-p_2)^2$, $u=(k-p_3)^2$. These variables satisfy $s_1+s_2+s_3 = 3s_0$ and $s+t+u = 3s_0$, respectively, where

$$3s_0 = M_P^2 + M_1^2 + M_2^2 + M_3^2. \tag{3.3}$$

Notice that, depending on the phase convention used for the various states, this analytic continuation does not necessarily boil down to a mere substitution of the variables (s,t,u) by (s_1,s_2,s_3), but can also generate an additional phase for the amplitude. We shall specify our convention in that matter later in this section. For the time being, we use a rather generic notation, in order to keep the discussion as general as possible. Later on, when considering specific processes, we shall refine the notation according to our needs (see in particular Tables I and III below, which also specify the phase conventions and the notation we will use for the various meson masses).

From a practical point of view, and in order not to obscure the line of reasoning with analyticity issues connected with the fact that $M_P > 3M_\pi$, it is useful, at a first stage, to replace M_P by a fictitious mass $\bar{M}_P$, somewhat lower than $3M_{\pi^0}$, or than $3M_\pi$ if isospin-breaking effects are neglected.[2] Then, the amplitudes possess the usual analyticity properties. In particular, they are real analytic [77]. After the construction of the two-loop amplitude for this fictitious process is completed, one can perform an analytic continuation in $\bar{M}_P^2$ toward its physical value, provided it is endowed with a small positive imaginary part δ, $\bar{M}_P^2 \to M_P^2 + i\delta$. The issues related to this analytic continuation will be discussed in Sec. V and Appendix B. Notice simply, at this stage, that in the course of this process, real analyticity is lost, and the real and imaginary parts of the amplitude along its cuts actually become complex dispersive and absorptive parts, respectively; i.e., schematically,

$$\begin{aligned}\mathrm{Re}\mathcal{M}(s) \to \mathrm{Disp}\mathcal{M}(s) &= \frac{1}{2}[\mathcal{M}(s+i0) + \mathcal{M}(s-i0)],\\ \mathrm{Im}\mathcal{M}(s) \to \mathrm{Abs}\mathcal{M}(s) &= \frac{1}{2i}[\mathcal{M}(s+i0) - \mathcal{M}(s-i0)],\end{aligned} \tag{3.4}$$

where 0 indicates an infinitesimal positive number. In order to keep the notation simple, we will continue denoting the mass of the meson P by M_P, even when it is smaller than

TABLE I. For each process under consideration, we show the amplitude $\mathcal{M}(s,t,u)$, and the corresponding amplitude $\mathcal{M}_u(s,t,u)$ in the crossed u-channel that appears in the dispersion relation (3.5). The penultimate column gives the appropriate crossing phase ϵ, and the last column displays, for each process, the quantity $3s_0$. Here, M_π and M_K denote the charged pion and kaon masses, respectively. CP violation is ignored so that the same amplitude describes the CP-conjugate processes. On the other hand, we keep the distinction between the masses of the neutral kaons K_L and K_S.

Process	$\mathcal{M}$	$\mathcal{M}_u$	ϵ	$3s_0$
$K^\pm\pi^\pm \to \pi^\pm\pi^\pm$	$\mathcal{M}_{++}$	$\mathcal{M}_{+-}$	$+1$	$M_K^2 + 3M_\pi^2$
$K^\pm\pi^\mp \to \pi^\pm\pi^\mp$	$\mathcal{M}_{+-}$	$\mathcal{M}_{++}$	$+1$	$M_K^2 + 3M_\pi^2$
$K^\pm\pi^\mp \to \pi^0\pi^0$	$\mathcal{M}_x$	$\mathcal{M}_{0+}$	-1	$M_K^2 + M_\pi^2 + 2M_{\pi^0}^2$
$K^\pm\pi^0 \to \pi^0\pi^\pm$	$\mathcal{M}_{0+}$	$\mathcal{M}_x$	-1	$M_K^2 + M_\pi^2 + 2M_{\pi^0}^2$
$K_L\pi^0 \to \pi^\pm\pi^\mp$	$\mathcal{M}_x^L$	$\mathcal{M}_{+0}^L$	-1	$M_{K_L}^2 + 2M_\pi^2 + M_{\pi^0}^2$
$K_L\pi^\pm \to \pi^\pm\pi^0$	$\mathcal{M}_{+0}^L$	$\mathcal{M}_x^L$	-1	$M_{K_L}^2 + 2M_\pi^2 + M_{\pi^0}^2$
$K_L\pi^0 \to \pi^0\pi^0$	$\mathcal{M}_{00}^L$	$\mathcal{M}_{00}^L$	$+1$	$M_{K_L}^2 + 3M_{\pi^0}^2$
$K_S\pi^0 \to \pi^+\pi^-$	$\mathcal{M}_x^S$	$\mathcal{M}_{+0}^S$	-1	$M_{K_S}^2 + 2M_\pi^2 + M_{\pi^0}^2$
$K_S\pi^+ \to \pi^+\pi^0$	$\mathcal{M}_{+0}^S$	$\mathcal{M}_x^S$	-1	$M_{K_S}^2 + 2M_\pi^2 + M_{\pi^0}^2$
$\eta\pi^0 \to \pi^\pm\pi^\mp$	$\mathcal{M}_x^\eta$	$\mathcal{M}_{+0}^\eta$	-1	$M_\eta^2 + 2M_\pi^2 + M_{\pi^0}^2$
$\eta\pi^\pm \to \pi^\pm\pi^0$	$\mathcal{M}_{+0}^\eta$	$\mathcal{M}_x^\eta$	-1	$M_\eta^2 + 2M_\pi^2 + M_{\pi^0}^2$
$\eta\pi^0 \to \pi^0\pi^0$	$\mathcal{M}_{00}^\eta$	$\mathcal{M}_{00}^\eta$	$+1$	$M_\eta^2 + 3M_{\pi^0}^2$

[2]The fact that the kaons are also unstable through their decay into two pions is irrelevant here since this feature would only start to play a role beyond the orders in the low-energy expansion we are considering. The η meson is stable with respect to decay into two pions if CP is conserved, which we have already assumed to be the case.

$3M_\pi$. This slight abuse of notation should not cause any confusion. Let us also point out that, even for values of M_P lower than $3M_\pi$, the analytic properties of the partial-wave projections are more involved than, say, in the $\pi\pi$ case, where, besides the s-channel unitarity cut, there is only a left-hand cut coming from the unitarity cut in the u channel. In the case of the $P\pi \to \pi\pi$ partial-wave projections, additional circular cuts can be present. For a more complete discussion, we refer the reader to Refs. [78] and [68].

In order to proceed with the construction of the scattering amplitudes $\mathcal{M}(s,t,u)$, we write, keeping the preceding discussion in mind and following Ref. [45], thrice subtracted, fixed-t, dispersion relations[3]

$$\begin{aligned}\mathcal{M}(s,t,u) &= a(t) + (s-u)b(t) + (s-u)^2 c(t) \\ &+ \frac{s^3}{\pi}\int_{s_{\rm thr}}^{\infty}\frac{dx}{x^3}\frac{\mathrm{Abs}\mathcal{M}(x,t,3s_0-x-t)}{x-s} \\ &+ \frac{u^3}{\pi}\int_{u_{\rm thr}}^{\infty}\frac{dx}{x^3}\frac{\epsilon\mathrm{Abs}\mathcal{M}_u(x,t,3s_0-x-t)}{x-u},\end{aligned} \tag{3.5}$$

where $a(t)$, $b(t)$, and $c(t)$ are arbitrary subtraction functions, whereas $s_{\rm thr}$ and $u_{\rm thr}$ denote the thresholds in the corresponding channels. In the presence of anomalous thresholds, the corresponding discontinuities should be included. Otherwise, $s_{\rm thr}$ and $u_{\rm thr}$ are fixed by unitarity. In this expression, ϵ denotes a crossing phase, which depends on the phase convention adopted for the various amplitudes; see Table I. We have chosen a phase convention that reduces to the one of Condon and Shortley in the isospin limit. In practice, this amounts to having a minus sign for the crossing of a charged pion, whereas the crossing of a neutral pion generates no phase. Furthermore, $\mathcal{M}_u(s,t,u)$ denotes the amplitude in the crossed u-channel. The latter obeys a similar dispersion relation, with subtraction functions $a_u(t)$, $b_u(t)$, and $c_u(t)$, and with $\mathcal{M}$ replacing $\mathcal{M}_u$ in the u-channel integral.

Notice that for the applications we have in mind, we need only to assume that the above dispersion relations are valid in the region of the kinematic variables where the chiral expansion makes sense. Then, they merely embody the analyticity properties of the corresponding amplitudes constructed by the usual Feynman diagram method in the field-theoretic framework of chiral perturbation theory. Thus, from this point of view, their existence is actually not an issue in this context. This link with Feynman diagrams will also provide the basis for the analytic continuation in M_P^2, which has been discussed previously.

The next step consists in writing, for each amplitude $\mathcal{M}(s,t,u)$ in Table I, a decomposition of the form

$$\mathcal{M}(s,t,u) = 16\pi[t_0(s) + 3t_1(s)\cos\tilde{\theta}] + \mathcal{M}_{\ell\geq 2}(s,t,u), \tag{3.6}$$

where $t_0(s)$ and $t_1(s)$ denote the partial waves for angular momentum ℓ equal to 0 and 1, respectively. The contributions from higher partial waves are contained in $\mathcal{M}_{\ell\geq 2}(s,t,u)$. The scattering angle is given by

$$\cos\tilde{\theta} = \frac{1}{2K_{P1;23}(s)}\left[2t + s - 3s_0 + \frac{\Delta_{P1}\Delta_{23}}{s}\right] \tag{3.7}$$

with $\Delta_{P1} \equiv M_P^2 - M_1^2$ and $\Delta_{23} \equiv M_2^2 - M_3^2$. The function $K_{P1;23}(s)$ is defined by

$$K_{P1;23}^2(s) = \frac{1}{4s^2}\lambda_{P1}(s)\lambda_{23}(s), \tag{3.8}$$

where $\lambda_{P1}(s) = \lambda(s, M_P^2, M_1^2)$, $\lambda_{23}(s) = \lambda(s, M_2^2, M_3^2)$ are expressed in terms of the Källen or triangle function $\lambda(x,y,z) \equiv x^2 + y^2 + z^2 - 2xy - 2xz - 2yz$. We will refer to $K_{P1;23}(s)$ as the Kacser function since it generalizes the function introduced in Ref. [68] to the case where the mass difference between neutral and charged pions is not neglected. The Kacser function $K_{P1;23}(s)$ as an analytic function of s is unambiguously defined by its cuts, which are conventionally placed at the real axis[4] and by the values of (3.8) as long as s corresponds to the scattering region, $s \geq (M_P + M_1)^2$. Eventually, we need to continue the amplitude analytically to lower values of s. This will require a careful study of the analytic properties of $K_{P1;23}(s)$ in the complex s plane for the different configurations of pion masses in Secs. V and VI. The same also applies to the partial-wave projections $t_0(s)$ and $t_1(s)$. For $s \geq (M_P + M_1)^2$, they are defined as usual by the integrals

$$t_\ell(s) = \frac{1}{32\pi}\int_{-1}^{+1} d\cos\tilde{\theta}(\cos\tilde{\theta})^\ell \mathcal{M}(s,t,u), \quad \ell = 0,1. \tag{3.9}$$

In order to construct the analytic continuations of the partial waves outside of the region of definition consisting of the portion of the real axis $s \geq (M_P + M_1)^2$, the contour of integration in Eq. (3.9) needs to be appropriately deformed in the complex plane. This issue, which is rather well documented in the literature [68,79,80] in the case where all

[3]Due to the Froissart bound and Regge phenomenology, two subtractions are enough to ensure convergence of the dispersion integrals [65,66]. However, as shown in Ref. [45], in order to obtain a representation that correctly accounts for all two-loop contributions, it is necessary to start from oversubtracted dispersion relations. Two subtractions would be enough, though, for the purpose of constructing a representation of the amplitudes valid at one loop only. We will make implicit use of this last remark in Sec. IV.

[4]For the case $M_P > M_1 + M_2 + M_3$, the cuts correspond to the intervals $((M_2 - M_3)^2, (M_2 + M_3)^2)$ and $((M_P - M_1)^2, (M_P + M_1)^2)$.

the pions have equal masses, requires a careful discussion, and we address it when considering the second iteration of the construction process in Sec. V (see also Appendix A). For the moment, however, we proceed with our general outline. To that effect, it is necessary to use our knowledge about the dominant chiral behavior of the various quantities appearing in Eq. (3.6). For the dispersive and absorptive parts of the lowest partial-wave projections, we have

$$\begin{aligned} &\mathrm{Disp}t_{\ell=0,1}(s) = \mathcal{O}(E^2), \qquad &&\mathrm{Disp}\mathcal{M}_{\ell\geq 2} = \mathcal{O}(E^4), \\ &\mathrm{Abs}t_{\ell=0,1}(s) = \mathcal{O}(E^4), \qquad &&\mathrm{Abs}\mathcal{M}_{\ell\geq 2} = \mathcal{O}(E^8). \end{aligned} \tag{3.10}$$

Therefore, up to order $\mathcal{O}(E^6)$, only the S and P waves contribute to the absorptive parts of the dispersion relations. Imposing the crossing relations, the subtraction function reduces to a polynomial $\mathcal{P}(s,t,u)$ of at most third order in the Mandelstam variables [45]. The amplitudes eventually take the form

$$\mathcal{M}(s,t,u) = \mathcal{P}(s,t,u) + \mathcal{U}(s,t,u) + \mathcal{O}(E^8), \tag{3.11}$$

where $\mathcal{U}(s,t,u)$ denotes the nonanalytic unitarity part,

$$\begin{aligned} \mathcal{U}(s,t,u) = 16\pi[&\mathcal{W}_0(s) + 3(t-u)\mathcal{W}_1(s) \\ &+ \mathcal{W}_0^t(t) + 3(u-s)\mathcal{W}_1^t(t) \\ &+ \mathcal{W}_0^u(u) + 3(t-s)\mathcal{W}_1^u(u)]. \end{aligned} \tag{3.12}$$

The functions $\mathcal{W}_\ell(s)$, $\ell = 0, 1$ are analytic in the complex s plane, except for a right-hand cut, with discontinuities provided by the absorptive parts along this same cut of the partial-wave projections, for instance,

$$\begin{aligned} \mathrm{Abs}\mathcal{W}_0(s) &= \left[\mathrm{Abs}t_0(s) + 3\frac{\Delta_{P1}\Delta_{23}}{s}\frac{\mathrm{Abs}t_1(s)}{2K_{P1;23}(s)}\right]\theta(s-s_{\mathrm{thr}}), \\ \mathrm{Abs}\mathcal{W}_1(s) &= \frac{\mathrm{Abs}t_1(s)}{2K_{P1;23}(s)}\theta(s-s_{\mathrm{thr}}). \end{aligned} \tag{3.13}$$

Similar properties hold for the other functions $\mathcal{W}_\ell^{t,u}(s)$, but their absorptive parts are now given in terms of the partial waves of the amplitudes in the crossed channels. The absorptive parts (3.13) do not completely fix the functions $\mathcal{W}_{0,1}(s)$. Without loss of generality, we shall require that they satisfy the asymptotic conditions [46]

$$\lim_{|s|\to\infty} \mathcal{W}_0(s)/s^4 = 0, \qquad \lim_{|s|\to\infty} \mathcal{W}_1(s)/s^3 = 0 \tag{3.14}$$

up to arbitrary polynomials in s, of at most third order for $\mathcal{W}_0$ or at most second order for $\mathcal{W}_1$, which are absorbed into $\mathcal{P}(s,t,u)$. Note that, even after the implementation of these conditions, the ambiguity in the single-variable polynomials is not entirely fixed; however, the form of $\mathcal{P}(s,t,u)$ is unique (up to inconsequential ambiguities stemming from the condition $s+t+u = 3s_0$).

TABLE II. Expressions, for each $P\pi \to \pi\pi$ scattering amplitude, of the functions occurring in the representation of Eq. (3.12) in terms of a set of 13 independent functions. The amplitudes involving the η meson have the same structure as those involving the K_L meson, and follow upon replacing the label L by η.

$\mathcal{M}$	$\mathcal{W}_0$	$\mathcal{W}_1$	$\mathcal{W}_0^t$	$\mathcal{W}_1^t$	$\mathcal{W}_0^u$	$\mathcal{W}_1^u$
$\mathcal{M}_{++}$	$\mathcal{W}_{++}$		$\mathcal{W}_{+-}^{(0)}$	$\mathcal{W}_{+-}^{(1)}$	$\mathcal{W}_{+-}^{(0)}$	$\mathcal{W}_{+-}^{(1)}$
$\mathcal{M}_{+-}$	$\mathcal{W}_{+-}^{(0)}$	$\mathcal{W}_{+-}^{(1)}$	$\mathcal{W}_{+-}^{(0)}$	$-\mathcal{W}_{+-}^{(1)}$	$\mathcal{W}_{++}$	
$\mathcal{M}_x$	$\mathcal{W}_x$		$-\mathcal{W}_{0+}^{(0)}$	$-\mathcal{W}_{0+}^{(1)}$	$-\mathcal{W}_{0+}^{(0)}$	$-\mathcal{W}_{0+}^{(1)}$
$\mathcal{M}_{0+}$	$\mathcal{W}_{0+}^{(0)}$	$\mathcal{W}_{0+}^{(1)}$	$\mathcal{W}_{0+}^{(0)}$	$-\mathcal{W}_{0+}^{(1)}$	$-\mathcal{W}_x$	
$\mathcal{M}_x^L$	$\mathcal{W}_{L;x}$		$-\mathcal{W}_{L;+0}^{(0)}$	$-\mathcal{W}_{L;+0}^{(1)}$	$-\mathcal{W}_{L;+0}^{(0)}$	$-\mathcal{W}_{L;+0}^{(1)}$
$\mathcal{M}_{+0}^L$	$\mathcal{W}_{L;+0}^{(0)}$	$\mathcal{W}_{L;+0}^{(1)}$	$\mathcal{W}_{L;+0}^{(0)}$	$-\mathcal{W}_{L;+0}^{(1)}$	$-\mathcal{W}_{L;x}$	
$\mathcal{M}_{00}^L$	$\mathcal{W}_{L;00}$		$\mathcal{W}_{L;00}$		$\mathcal{W}_{L;00}$	
$\mathcal{M}_x^S$		$\mathcal{W}_{S;x}^{(1)}$	$\mathcal{W}_{S;+0}^{(0)}$	$\mathcal{W}_{S;+0}^{(1)}$	$-\mathcal{W}_{S;+0}^{(0)}$	$-\mathcal{W}_{S;+0}^{(1)}$
$\mathcal{M}_{+0}^S$	$\mathcal{W}_{S;+0}^{(0)}$	$\mathcal{W}_{S;+0}^{(1)}$	$-\mathcal{W}_{S;+0}^{(0)}$	$\mathcal{W}_{S;+0}^{(1)}$		$-\mathcal{W}_{S;x}^{(1)}$

These expressions form the content of the reconstruction theorem in the present context. Notice that, depending on the symmetries of the amplitude $\mathcal{M}(s,t,u)$, these functions are not all independent. Actually, making use of the arbitrariness of the various functions $\mathcal{W}_{0,1}(s)$, one can achieve that $\mathcal{U}(s,t,u)$ and $\mathcal{P}(s,t,u)$ separately have the same s, t, u symmetries as the full amplitude $\mathcal{M}(s,t,u)$. Finally, as far as their structure is concerned, the amplitudes of the processes involving the η meson can be obtained from those involving the K_L meson, upon changing the corresponding labels. We thus need to consider only 13 distinct functions, which we choose as indicated in Table II. Note that a given process involves at most only three distinct functions.

It remains to transform these dispersive representations into a tool that will lead to an explicit construction of the two-loop amplitudes. For this, it is necessary to specify the input for the absorptive parts of the partial waves that appear in these expressions. This input will be provided by unitarity. Up to and including two-loop order, these absorptive parts result only from intermediate states composed of two pseudoscalar mesons, $\pi\pi$, $K\pi$, $\eta\pi$, etc. Except for the $\pi\pi$ case, the singularities induced by these intermediate states are far from the central region of the Dalitz plot that describes the $P \to \pi\pi\pi$ decay processes. For a description of the latter, and of the corresponding unitarity cusps due to the $\pi\pi$ intermediate states, it is, therefore, not necessary to explicitly retain the intermediate states corresponding to these higher thresholds. Their contributions can be expanded in powers of the Mandelstam variables divided by the square of a scale, which is at least equal to the kaon (or eta) mass, so that they will appear only in the polynomial contributions to the amplitudes. Of course, this approximation would not be suitable if we intended to

describe the scattering processes $P\pi \to \pi\pi$ themselves. If necessary, the formalism to be described below could actually be extended to the full set of possible two-meson states. Therefore, we have (recall that only the values $\ell = 0, 1$ need to be considered)

$$\mathrm{Abs}t_\ell^{i\to f}(s) = \sum_k \frac{1}{S_k}\frac{\lambda_k^{1/2}(s)}{s} t_\ell^{i\to k}(s)[f_\ell^{f\to k}(s)]^* \theta(s - s_k^{\mathrm{thr}}). \tag{3.15}$$

The sum goes over all the possible two-pions intermediate states k, $f_\ell^{f\to k}(s)$ denotes the partial-wave projection of the corresponding $\pi\pi$ scattering amplitude $f \to k$, while S_k is the symmetry factor, $S_k = 2$ for identically charged pions, and $S_k = 1$ otherwise. Note that for $\ell = 1$, one always has $S_k = 1$. Furthermore, s_k^{thr} denotes the threshold at which the channel k opens, and $\lambda_k(s)$ is the triangle function that describes the corresponding phase space. There are only three possibilities, $s_k^{\mathrm{thr}} = 4M_\pi^2, (M_\pi + M_{\pi^0})^2, 4M_{\pi^0}^2$, depending on the channel under consideration [M_π (M_{π^0}) denotes the mass of the charged (neutral) pion].

Thus, as was to be expected, in order to complete our program, we need to consider at the same time the amplitudes $A(s,t,u)$ for the scattering processes $\pi(p_1)\pi(p_2) \to \pi(p_3)\pi(p_4)$ in the various channels, but only at lowest and at next-to-leading orders. It can be achieved following the same path as for the $P\pi \to \pi\pi$ amplitudes. The construction of the amplitudes $A(s,t,u)$ in the presence of isospin breaking has already been described in Ref. [44], so we can remain brief, and refer the reader to this reference for details. The starting point is again provided by thrice subtracted, fixed-t, dispersion relations satisfied by the amplitudes $A(s,t,u)$,

$$\begin{aligned} A(s,t,u) &= a(t) + (s-u)b(t) + (s-u)^2 c(t) \\ &\quad + \frac{s^3}{\pi}\int_{s_{\mathrm{thr}}}^\infty \frac{dx}{x^3}\frac{\mathrm{Im}A(x,t,\Sigma - x - t)}{x - s} \\ &\quad + \frac{u^3}{\pi}\int_{u_{\mathrm{thr}}}^\infty \frac{dx}{x^3}\frac{\epsilon \mathrm{Im}A_u(x,t,\Sigma - x - t)}{x - u}, \end{aligned} \tag{3.16}$$

where $a(t)$, $b(t)$, and $c(t)$ are arbitrary subtraction functions, Σ stands for the sum of the squared masses of the pions appearing in the process, and s_{thr} and u_{thr} denote the thresholds in the corresponding channels. Although, in order not to overburden the notation at this stage, we have used the same symbols, these last quantities can, of course, be different from the ones appearing in Eq. (3.5). Table III shows the notation that will be used in the sequel when specific channels are considered.

We now decompose the various amplitudes $A(s,t,u)$ such as to single out the lowest, S and P, partial waves,

TABLE III. For each $\pi\pi$ scattering process, the table shows the amplitude $A(s,t,u)$ and the corresponding amplitude $A_u(s,t,u)$ in the crossed u-channel, which appears in the dispersion relation (3.16). The penultimate column gives the appropriate crossing phase ϵ, and the last column displays, for each process, the quantity $s+t+u$. Here, M_π denotes the charged pion mass, and $\Sigma_\pi \equiv M_\pi^2 + M_{\pi^0}^2$.

Process	A	A_u	ϵ	$s+t+u$
$\pi^\pm\pi^\mp \to \pi^\pm\pi^\mp$	A_{+-}	A_{++}	$+1$	$4M_\pi^2$
$\pi^\pm\pi^\pm \to \pi^\pm\pi^\pm$	A_{++}	A_{+-}	$+1$	$4M_\pi^2$
$\pi^\pm\pi^0 \to \pi^\pm\pi^0$	A_{+0}	A_{+0}	$+1$	$2\Sigma_\pi$
$\pi^\pm\pi^0 \to \pi^0\pi^\pm$	A_{0+}	A_x	-1	$2\Sigma_\pi$
$\pi^\pm\pi^\mp \to \pi^0\pi^0$	A_x	A_{0+}	-1	$2\Sigma_\pi$
$\pi^0\pi^0 \to \pi^0\pi^0$	A_{00}	A_{00}	$+1$	$4M_{\pi^0}^2$

$$A(s,t,u) = 16\pi[f_0(s) + 3f_1(s)\cos\theta] + \mathcal{A}_{\ell\geq 2}(s,t,u), \tag{3.17}$$

where the scattering angle is given by a formula analogous to (3.7),

$$\cos\theta = \frac{s(t-u) + \Delta_{12}\Delta_{34}}{\lambda_{12}^{1/2}(s)\lambda_{34}^{1/2}(s)} \tag{3.18}$$

with $\Delta_{ij} \equiv M_i^2 - M_j^2$, M_i and M_j being pion masses, so that now the only possibilities are $\Delta_{ij} = 0, \pm\Delta_\pi, \Delta_\pi \equiv M_\pi^2 - M_{\pi^0}^2$. Likewise, $\lambda_{ij}(s)$ is the Källen function involving the pion masses M_i and M_j. The dominant chiral behavior of these various pieces is given as in Eq. (3.10), with now $f_{0,1}(s)$ and $A_{\ell\geq 2}$ replacing $t_{0,1}(s)$ and $\mathcal{M}_{\ell\geq 2}$, respectively, so that again, only the S and P waves contribute to the absorptive parts of the dispersion relations up to order $\mathcal{O}(E^6)$. After imposing crossing, the amplitudes $A(s,t,u)$ eventually take the form

$$A(s,t,u) = P(s,t,u) + U(s,t,u) + \mathcal{O}(E^8), \tag{3.19}$$

where $U(s,t,u)$ is the nonanalytic unitarity part,

$$\begin{aligned} U(s,t,u) &= 16\pi[W_0(s) + 3(t-u)W_1(s) \\ &\quad + W_0^t(t) + 3(u-s)W_1^t(t) \\ &\quad + W_0^u(u) + 3(t-s)W_1^u(u)], \end{aligned} \tag{3.20}$$

and $P(s,t,u)$ is a polynomial of at most third order in the Mandelstam variables with the same s, t, u symmetries as the amplitude $A(s,t,u)$. Because of crossing relations among subsets of the $\pi\pi$ amplitudes, it is possible to express all the functions that appear in the representations of the type (3.20) in terms of only seven distinct functions, which we denote as $W_{00}(s)$, $W_x(s)$, $W_{++}(s)$, $W_{+-}^{(0)}(s)$, $W_{+-}^{(1)}(s)$, $W_{+0}^{(0)}(s)$, $W_{+0}^{(1)}(s)$. How these functions contribute

TABLE IV. Expressions, for each $\pi\pi$ scattering amplitude, of the functions occurring in the representation of Eq. (3.20) in terms of the set of seven distinct functions.

A	W_0	W_1	W_0^t	W_1^t	W_0^u	W_1^u
A_{+-}	$W_{+-}^{(0)}$	$W_{+-}^{(1)}$	$W_{+-}^{(0)}$	$-W_{+-}^{(1)}$	W_{++}	
A_{++}	W_{++}		$W_{+-}^{(0)}$	$W_{+-}^{(1)}$	$W_{+-}^{(0)}$	$W_{+-}^{(1)}$
A_{+0}	$W_{+0}^{(0)}$	$W_{+0}^{(1)}$	W_x		$W_{+0}^{(0)}$	$W_{+0}^{(1)}$
A_{0+}	$W_{+0}^{(0)}$	$-W_{+0}^{(1)}$	$W_{+0}^{(0)}$	$W_{+0}^{(1)}$	W_x	
A_x	$-W_x$		$-W_{+0}^{(0)}$	$W_{+0}^{(1)}$	$-W_{+0}^{(0)}$	$W_{+0}^{(1)}$
A_{00}	W_{00}		W_{00}		W_{00}	

to the various amplitudes can be gathered from Table IV. The functions $W_\ell(s)$, $\ell = 0, 1$, are analytic in the complex s plane, except for a right-hand cut, with discontinuities given by the appropriate partial waves, e.g.,[5]

$$\begin{aligned}\mathrm{Abs}W_0(s) &= [\mathrm{Abs}f_0(s) + 3\frac{\Delta_{12}\Delta_{34}}{\lambda_{12}^{1/2}(s)\lambda_{34}^{1/2}(s)}\mathrm{Abs}f_1(s)] \\ &\quad\times\theta(s-s_{\mathrm{thr}}), \\ \mathrm{Abs}W_1(s) &= \frac{s}{\lambda_{12}^{1/2}(s)\lambda_{34}^{1/2}(s)}\mathrm{Abs}f_1(s)\theta(s-s_{\mathrm{thr}}).\end{aligned} \tag{3.21}$$

These discontinuities are again provided by unitarity,

$$\mathrm{Abs}f_\ell^{i\to f}(s) = \sum_k \frac{1}{S_k}\frac{\lambda_k^{1/2}(s)}{s} f_\ell^{i\to k}(s)[f_\ell^{f\to k}(s)]^\star\theta(s-s_k^{\mathrm{thr}}). \tag{3.22}$$

For reasons already explained above, only the contributions of two-pion intermediate states need to be retained.

Within the framework we have just presented, the amplitudes for the processes $P\pi \to \pi\pi$ and $\pi\pi \to \pi\pi$ form a closed set. This framework also allows for a two-step iterative construction of the corresponding amplitudes to two loops, along the lines described in detail in Ref. [46]. The essential information is provided by the chiral counting of the partial waves, Eq. (3.10) for the amplitudes $\mathcal{M}(s,t,u)$, and similar relations [44–46] for the $\pi\pi$ scattering amplitudes. Indeed, at lowest order, these amplitudes, being $\mathcal{O}(E^2)$, are real first-order polynomials in the Mandelstam variables, entirely saturated by the S and P partial waves,

$$\begin{aligned}f_\ell(s) &= \mathrm{Disp}f_\ell(s) + \mathcal{O}(E^4) = \varphi_\ell(s) + \mathcal{O}(E^4), \\ t_\ell(s) &= \mathrm{Disp}t_\ell(s) + \mathcal{O}(E^4) = \tilde{\varphi}_\ell(s) + \mathcal{O}(E^4),\end{aligned} \tag{3.23}$$

for $\ell = 0, 1$. Subsequently, they provide the discontinuities of the $\ell = 0, 1$ partial waves along the unitarity cut at order $\mathcal{O}(E^4)$,

$$\begin{aligned}\mathrm{Abs}f_\ell^{i\to f}(s) &= \sum_k \frac{1}{S_k}\frac{\lambda_k^{1/2}(s)}{s}\varphi_\ell^{i\to k}(s)\varphi_\ell^{k\to f}(s) \\ &\quad\times\theta(s-s_k^{\mathrm{thr}}) + \mathcal{O}(E^6), \\ \mathrm{Abs}t_\ell^{i\to f}(s) &= \sum_k \frac{1}{S_k}\frac{\lambda_k^{1/2}(s)}{s}\tilde{\varphi}_\ell^{i\to k}(s)\varphi_\ell^{k\to f}(s) \\ &\quad\times\theta(s-s_k^{\mathrm{thr}}) + \mathcal{O}(E^6),\end{aligned} \tag{3.24}$$

from which the one-loop amplitudes can be constructed, up to an ambiguity which reduces to a polynomial of at most second order in the Mandelstam variables. From these one-loop expressions, one may now compute the order $\mathcal{O}(E^4)$ dispersive parts of the lowest partial waves,

$$\begin{aligned}\mathrm{Disp}f_\ell(s) &= \varphi_\ell(s) + \psi_\ell(s) + \mathcal{O}(E^6), \\ \mathrm{Disp}t_\ell(s) &= \tilde{\varphi}_\ell(s) + \tilde{\psi}_\ell(s) + \mathcal{O}(E^6),\end{aligned} \tag{3.25}$$

for $s \geq s_{\mathrm{thr}}$, which in turn will provide the corresponding absorptive parts at order $\mathcal{O}(E^6)$,

$$\begin{aligned}\mathrm{Abs}f_\ell^{i\to f}(s) &= \sum_k \frac{1}{S_k}\frac{\lambda_k^{1/2}(s)}{s}\varphi_\ell^{i\to k}(s)[\varphi_\ell^{k\to f}(s) + 2\psi_\ell^{k\to f}(s)] \\ &\quad\times\theta(s-s_k^{\mathrm{thr}}) + \mathcal{O}(E^8), \\ \mathrm{Abs}t_\ell^{i\to f}(s) &= \sum_k \frac{1}{S_k}\frac{\lambda_k^{1/2}(s)}{s}\{\tilde{\varphi}_\ell^{i\to k}(s)[\varphi_\ell^{k\to f}(s) + \psi_\ell^{k\to f}(s)] \\ &\quad + \tilde{\psi}_\ell^{i\to k}(s)\varphi_\ell^{k\to f}(s)\} \\ &\quad\times\theta(s-s_k^{\mathrm{thr}}) + \mathcal{O}(E^8).\end{aligned} \tag{3.26}$$

These equations follow from Eq. (3.15), from the chiral counting of the partial waves, combined with T invariance and the fact that real analyticity holds for the $\pi\pi$ scattering amplitudes, so that the quantities $\varphi_\ell(s)$ and $\psi_\ell(s)$ in Eq. (3.25) are real. Note that the contributions of the absorptive parts of the amplitudes on the right-hand sides of these equations cancel, and so there appear effectively just the dispersive parts of the partial waves. From (3.26), one can then obtain the full two-loop amplitudes. This construction is unique up to a polynomial contribution of at most third order in the Mandelstam variables, with coefficients that remain finite in the limit of vanishing pion masses. The main point of this discussion is that in order to obtain the full two-loop expressions of the amplitudes, only the dispersive parts of the one-loop S and P partial waves need to be computed directly. Extracting these partial-wave projections from the

[5]Although real analyticity is preserved for the $\pi\pi$ scattering amplitudes, even in the presence of isospin breaking, in order to uniformize the notation, we also call the real and imaginary parts dispersive and absorptive parts, respectively.

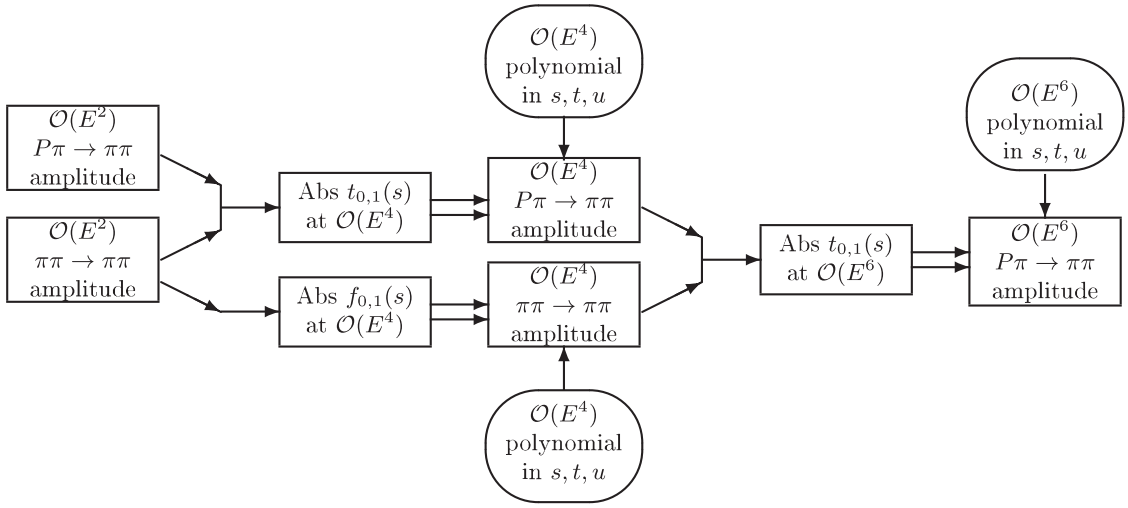

FIG. 1. Schematic representation of the iterative two-steps reconstruction procedure for the $P\pi \to \pi\pi$ amplitudes. The absorptive part (of partial waves) denoted by Abs is defined in Eq. (3.4).

corresponding one-loop amplitudes, however, constitutes also the most demanding difficulty in this reconstruction procedure, the main steps of which are summarized in Fig. 1.

Let us close this general overview by briefly specifying the link with the usual framework of the three-flavor chiral perturbation theory [56]. The latter considers an expansion in the Mandelstam variables s, t, u and in the light-quark masses, all counting as order $\mathcal{O}(E^2)$. In the approach presented here, the expansion is in the Mandelstam variables and in the meson masses, which also count as order $\mathcal{O}(E^2)$. In the chiral perturbation framework, amplitudes are worked out upon computing all the relevant Feynman diagrams generated, at a given order, by the effective Lagrangian, including tree-level and tadpole diagrams. In the dispersive approach followed here, the absorptive parts of the Feynman diagram are accounted for by the unitarity part $\mathcal{U}(s,t,u)$ [or $U(s,t,u)$], whereas their dispersive parts contribute both to $\mathcal{U}(s,t,u)$ and $\mathcal{P}(s,t,u)$ [or $U(s,t,u)$ and $P(s,t,u)$]. At two loops, these diagrams correspond to the two topologies illustrated in Fig. 2, and describe direct rescattering (diagram on the left) and rescattering in the crossed channels (diagram on the right). Contributions from tree or tadpole diagrams are accounted for solely by the subtraction polynomial $\mathcal{P}(s,t,u)$ [or $P(s,t,u)$].

IV. FIRST ITERATION

In this section, we construct the one-loop expressions of the amplitudes for $\pi\pi$ scattering and for the $P\pi \to \pi\pi$ decay

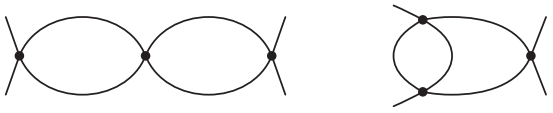

FIG. 2. The two-loop topologies that contribute to the absorptive parts.

processes, thus fulfilling the first step in our program. As a starting point, we need the lowest-order expressions of the corresponding amplitudes, which are, according to chiral counting, of order $\mathcal{O}(E^2)$. It means that they are first-order polynomials in the Mandelstam variables, with coefficients that remain finite in the chiral limit. In the case of the $\pi\pi$ amplitudes, for instance, this leads to

$$A(s,t,u) = 16\pi\left[\mathrm{a} + \mathrm{b}\,\frac{s-\mu_+}{F_\pi^2} + \mathrm{c}\,\frac{t-u-\mu_-}{F_\pi^2}\right] + \mathcal{O}(E^4), \tag{4.1}$$

where a, b, and c are constants, F_π denotes the decay constant of the charged pion, with $F_\pi = f_\pi/\sqrt{2} = 92.28(10)$ MeV from [81], and $\mu_\pm$ specify some reference point in the Mandelstam plane. In the chiral limit, a and $\mu_\pm$ vanish, while b and c remain nonzero and finite, so that the corresponding amplitudes satisfy the current-algebra consistency conditions [82,83]. Besides, from a practical point of view, the subtraction points $\mu_\pm$ should lie in the region of the Mandelstam plane where it makes sense to apply the chiral expansion, but are otherwise arbitrary. Their choice will depend on the applications one has in mind, and will also determine the interpretation of the parameters a, b, and c.

For instance, in Ref. [46], the reference point was chosen to be the center of the Dalitz plot ($\mu_+ = 4M_\pi^2/3$, $\mu_- = 0$ in the isospin limit), which led to the interpretation of these parameters as subthreshold coefficients. It might be an appropriate choice if one wants to discuss quantities for which the expansion in light quark masses converges rapidly. Table V shows the corresponding parameters for the $\pi\pi$ scattering amplitudes in the various channels. For later use, we have defined values for μ_+ ($\mu_- = 0$ in all cases) even in the case where b vanishes. Notice also that in the cases where there are two identical pions in the

TABLE V. Definition of the parameters a, b, and c of Eq. (4.1) for each $\pi\pi$ scattering process, in the case where one opts for a description in terms of subthreshold parameters. In these expressions, we have defined $\Sigma_\pi \equiv M_\pi^2 + M_{\pi^0}^2$, and $\mu_- = 0$ in all cases. Also shown are the expressions, in terms of the independent quantities $\lambda_{+-}^{(1)}$, $\lambda_{+-}^{(2)}$, $\lambda_x^{(1)}$, $\lambda_x^{(2)}$, and $\lambda_{00}^{(1)}$, of the constants $\lambda_{s,t,u}$ appearing in the subtraction polynomials $P(s,t,u)$ at one-loop order defined in Eq. (4.17).

A	$16\pi a F_\pi^2/M_{\pi^0}^2$	$16\pi b$	$16\pi c$	μ_+	λ_s	λ_t	λ_u
A_{+-}	$2\alpha_{+-}/3$	$\beta_{+-}/2$	$\gamma_{+-}/2$	$4M_\pi^2/3$	$\lambda_{+-}^{(1)} + \lambda_{+-}^{(2)}$	$\lambda_{+-}^{(1)} + \lambda_{+-}^{(2)}$	$2\lambda_{+-}^{(2)}$
A_{++}	$2\alpha_{++}/3$	$-\beta_{++}$	0	$4M_\pi^2/3$	$2\lambda_{+-}^{(2)}$	$\lambda_{+-}^{(1)} + \lambda_{+-}^{(2)}$	$\lambda_{+-}^{(1)} + \lambda_{+-}^{(2)}$
A_{+0}	$\alpha_{+0}/3$	$-\beta_{+0}/2$	$+\gamma_{+0}/2$	$2\Sigma_\pi/3$	$+\lambda_x^{(2)}$	$+\lambda_x^{(1)}$	$+\lambda_x^{(2)}$
A_{0+}	$\alpha_{+0}/3$	$-\beta_{+0}/2$	$-\gamma_{+0}/2$	$2\Sigma_\pi/3$	$+\lambda_x^{(2)}$	$+\lambda_x^{(2)}$	$+\lambda_x^{(1)}$
A_x	$-\alpha_x/3$	$-\beta_x$	0	$2\Sigma_\pi/3$	$-\lambda_x^{(1)}$	$-\lambda_x^{(2)}$	$-\lambda_x^{(2)}$
A_{00}	α_{00}	0	0	$4M_{\pi^0}^2/3$	$3\lambda_{00}^{(1)}$	$3\lambda_{00}^{(1)}$	$3\lambda_{00}^{(1)}$

initial and/or final state, Bose symmetry implies that the coefficient c vanishes. All these parameters are not independent since all the amplitudes involving a given total number of, say, charged pions are related by crossing. In terms of the parameters of Table V, these relations read

$$\begin{aligned}
\alpha_{+-} &= \alpha_{++} + \mathcal{O}(E^2), & \alpha_{+0} &= \alpha_x + \mathcal{O}(E^2),\\
\beta_{+-} &= \beta_{++} + \mathcal{O}(E^2), & \beta_{+0} &= \beta_x + \mathcal{O}(E^2),\\
\gamma_{+-} &= \beta_{++} + \mathcal{O}(E^2), & \gamma_{+0} &= \beta_x + \mathcal{O}(E^2).
\end{aligned} \tag{4.2}$$

It is, however, more convenient to treat these quantities as independent in a first stage, and to make the replacement, including the corrections from higher orders indicated above, only at the end of the calculation. It will also help to visualize the origin of various contributions in the higher-order expressions of the amplitudes.

On the other hand, subthreshold parameters are not observables that are particularly suited for the discussion of experimental data on $\pi\pi$ scattering. Furthermore, since the aim of the present study is to provide a parametrization of the $P \to \pi^0\pi^0\pi$ amplitudes which displays the dependence of the cusp on the $\pi\pi$ scattering lengths, the latter appears, in this context, as a better choice of parameters. In this case, $\mu_\pm$ are to be chosen such as to correspond to the threshold values of s, t, and u. In order that the parameters a in (4.1) retain their meaning as scattering lengths up to the two-loop level, the subtraction polynomials have to be adjusted appropriately. How this can be done has been described in Appendix F of Ref. [44]. The various parameters that enter the $\pi\pi$ amplitudes at the lowest order are shown in Table VI. Again, there are crossing relations among subsets of them. These relations, with next-to-leading corrections included, are also displayed in Appendix F of Ref. [44]. Notice that the normalization of the scattering lengths differs by a factor of 2 from the one usually adopted. The definition used here is in agreement with the normalization of the partial-wave projections in Eq. (3.17). However, when expressing these scattering lengths in terms of the two S-wave scattering lengths a_0^0 and a_0^2 in the isospin limit, we shall use, for the latter, the familiar normalization. According to Eqs. (2.18), (2.21), and (2.22) of Ref. [84], at order $\mathcal{O}(E^2)$, these relations read[6]

$$\begin{aligned}
a_{+-} &= \frac{2}{3}a_0^0 + \frac{1}{3}a_0^2 - 2a_0^2\frac{\Delta_\pi}{M_\pi^2},\\
a_{++} &= 2a_0^2 - 2a_0^2\frac{\Delta_\pi}{M_\pi^2},\\
a_{+0} &= a_0^2 - a_0^2\frac{\Delta_\pi}{M_\pi^2},\\
a_x &= -\frac{2}{3}a_0^0 + \frac{2}{3}a_0^2 + a_0^2\frac{\Delta_\pi}{M_\pi^2},\\
a_{00} &= \frac{2}{3}a_0^0 + \frac{4}{3}a_0^2 - \frac{2}{3}(a_0^0 + 2a_0^2)\frac{\Delta_\pi}{M_\pi^2},
\end{aligned} \tag{4.3}$$

where Δ_π was defined after Eq. (3.18).

In the case of the $P \to \pi\pi\pi$ amplitudes, we shall adopt a parametrization more akin to the usual description of their Dalitz-plot structure in terms of, say, slopes and curvatures

TABLE VI. Definition of the parameters a, b, and c of Eq. (4.1) for each $\pi\pi$ scattering process, in the case where one opts for a description in terms of scattering lengths.

A	a	b	c	μ_+	μ_-
A_{+-}	a_{+-}	b_{+-}	c_{+-}	$4M_\pi^2$	0
A_{++}	a_{++}	b_{++}	0	$4M_\pi^2$	0
A_{+0}	a_{+0}	b_{+0}	$+c_{+0}$	$(M_\pi + M_{\pi^0})^2$	$-(M_\pi - M_{\pi^0})^2$
A_{0+}	a_{+0}	b_{+0}	$-c_{+0}$	$(M_\pi + M_{\pi^0})^2$	$+(M_\pi - M_{\pi^0})^2$
A_x	a_x	b_x	0	$4M_\pi^2$	0
A_{00}	a_{00}	0	0	$4M_{\pi^0}^2$	0

[6]Our quantities a_0^0 and a_0^2 correspond to those denoted as $(a_0^0)_{\rm str}$ and $(a_0^2)_{\rm str}$, respectively, in Ref. [84].

with respect to appropriately chosen kinematic variables. Details will be provided in Sec. IV B.

A. $\pi\pi$ scattering

Since the construction of the $\pi\pi$ scattering amplitudes with $M_\pi \neq M_{\pi^0}$ has already been discussed at some length in Refs. [44,48], our account will remain brief. First, we need to notice that at one loop, the discontinuities of these functions are given by Eqs. (3.21) and (3.24). It is a straightforward matter to extract the corresponding order $\mathcal{O}(E^2)$ S and P partial waves $\varphi_\ell(s)$, $\ell = 0, 1$, from the general representation (4.1) of the lowest-order $\pi\pi$ scattering amplitudes:

$$\varphi_0(s) = \mathrm{a} + \mathrm{b}\frac{s-\mu_+}{F_\pi^2} - \frac{\mathrm{c}}{F_\pi^2}\left(\mu_- + \frac{\Delta_{12}\Delta_{34}}{s}\right),$$
$$\varphi_1(s) = \frac{\mathrm{c}}{3F_\pi^2}\frac{\lambda_{12}^{1/2}(s)\lambda_{34}^{1/2}(s)}{s}. \tag{4.4}$$

In view of the form of $\varphi_1(s)$, it is useful to remember, as evidenced by Eqs. (3.21) and (3.24), that the discontinuities only involve the combination (in hopefully self-explanatory notation)

$$\frac{\varphi_1^{i\to k}(s)\varphi_1^{k\to f}(s)}{\lambda_i^{1/2}(s)\lambda_f^{1/2}(s)} = \frac{\mathrm{c}^{i\to k}\mathrm{c}^{f\to k}}{9F_\pi^4}\frac{\lambda_k(s)}{s}. \tag{4.5}$$

One then obtains the following expressions:

$$W_{00}(s) = 16\pi\left\{\frac{1}{2}[\varphi_0^{00}(s)]^2\bar{J}_0(s) + [\varphi_0^{x}(s)]^2\bar{J}(s)\right\} + \mathcal{O}(E^6), \tag{4.6}$$

$$W_{x}(s) = -16\pi\varphi_0^{x}(s)\left[\frac{1}{2}\varphi_0^{00}(s)\bar{J}_0(s) + \varphi_0^{+-}(s)\bar{J}(s)\right] + \mathcal{O}(E^6), \tag{4.7}$$

$$W_{+0}^{(0)}(s) = 16\pi\left\{\frac{\mathrm{c}_{+0}^2}{3F_\pi^4}\Delta_\pi^2\left[1 - 2\frac{\Sigma_\pi}{s} - 3\frac{\Delta_\pi^2}{s^2}\right] + [\varphi_0^{+0}(s)]^2\right\}\bar{J}_{\pm0}(s) + 16\pi\frac{4\mathrm{c}_{+0}^2\Delta_\pi^4}{3F_\pi^4 s^2}\bar{\bar{J}}_{\pm0}(s) + \mathcal{O}(E^6), \tag{4.8}$$

$$W_{+0}^{(1)}(s) = 16\pi\frac{\mathrm{c}_{+0}^2}{9F_\pi^4}\frac{\lambda_{\pm0}(s)}{s}\bar{J}_{\pm0}(s) + \mathcal{O}(E^6), \tag{4.9}$$

$$W_{++}(s) = 16\pi\frac{1}{2}[\varphi_0^{++}(s)]^2\bar{J}(s) + \mathcal{O}(E^6), \tag{4.10}$$

$$W_{+-}^{(0)}(s) = 16\pi\left\{[\varphi_0^{+-}(s)]^2\bar{J}(s) + \frac{1}{2}[\varphi_0^{x}(s)]^2\bar{J}_0(s)\right\} + \mathcal{O}(E^6), \tag{4.11}$$

$$W_{+-}^{(1)}(s) = 16\pi\frac{\mathrm{c}_{+-}^2}{9F_\pi^4}(s - 4M_\pi^2)\bar{J}(s) + \mathcal{O}(E^6). \tag{4.12}$$

Here, $\bar{J}_0(s)$, $\bar{J}(s)$, and $\bar{J}_{\pm0}(s)$ denote the dispersive integrals[7]

$$\bar{J}_0(s) = \frac{s}{16\pi^2}\int_{4M_{\pi^0}^2}^{\infty}\frac{dx}{x}\frac{1}{x-s-\mathrm{i}0}\sigma_0(x),$$
$$\bar{J}(s) = \frac{s}{16\pi^2}\int_{4M_{\pi}^2}^{\infty}\frac{dx}{x}\frac{1}{x-s-\mathrm{i}0}\sigma(x),$$
$$\bar{J}_{\pm0}(s) = \frac{s}{16\pi^2}\int_{(M_{\pi^\pm}+M_{\pi^0})^2}^{\infty}\frac{dx}{x}\frac{1}{x-s-\mathrm{i}0}\frac{\lambda_{\pm0}^{1/2}(x)}{x}, \tag{4.13}$$

with

$$\sigma_0(s) = \sqrt{1-\frac{4M_{\pi^0}^2}{s}}, \qquad \sigma(s) = \sqrt{1-\frac{4M_{\pi}^2}{s}}, \tag{4.14}$$

and $\lambda_{\pm0}(s) = \lambda(s, M_\pi^2, M_{\pi^0}^2)$. Finally,

$$\bar{\bar{J}}(s) \equiv \bar{J}(s) - s\bar{J}'(0), \tag{4.15}$$

and

$$\Sigma_\pi \equiv M_\pi^2 + M_{\pi^0}^2. \tag{4.16}$$

The subtraction polynomials have the following form at the one-loop order (cf. also footnote 3):

$$P(s,t,u) = 16\pi\left[\mathrm{a} + \mathrm{b}\frac{s-\mu_+}{F_\pi^2} + \mathrm{c}\frac{t-u-\mu_-}{F_\pi^2}\right] - w + \frac{\lambda_s}{F_\pi^4}\left(s - \frac{3}{2}\mu_+\right)^2 + \frac{\lambda_t}{F_\pi^4}\left(t - \frac{3}{2}\mu_+\right)^2 + \frac{\lambda_u}{F_\pi^4}\left(u - \frac{3}{2}\mu_+\right)^2 + \mathcal{O}(E^6). \tag{4.17}$$

Crossing and Bose symmetry (when applicable) restrict to 5 the number of constants $\lambda_{s,t,u}$ that are independent. Their

[7]These functions are dispersive representations of the two-point one-loop integrals subtracted at $s = 0$,

$$J(p^2; m_1, m_2) = \frac{1}{i}\int\frac{d^4k}{(2\pi)^4}\frac{1}{k^2 - m_1^2}\frac{1}{(k-p)^2 - m_2^2},$$
$$\bar{J}(s; m_1, m_2) = J(s; m_1, m_2) - J(0; m_1, m_2)$$

with $\bar{J}(s) = \bar{J}(s; M_\pi, M_\pi)$, $\bar{J}_0(s) = \bar{J}(s; M_{\pi^0}, M_{\pi^0})$, $\bar{J}_{\pm0}(s) = \bar{J}(s; M_\pi, M_{\pi^0})$. Their closed forms are given, e.g., in Ref. [64]. We also use

$$\bar{J}(0) = 0, \qquad \bar{J}_0(4M_{\pi^0}^2) = \frac{1}{8\pi^2} = \bar{J}_{\pm0}(\mu_+) + \bar{J}_{\pm0}(\mu_-).$$

expressions in terms of the independent parameters introduced in Ref. [44] are shown in Table V. These expressions also apply to the case where one opts for the parametrization in terms of scattering lengths, and the constraints coming from the crossing properties have already been accounted for. The contribution denoted by w is not a new parameter, but is expressed in terms of the ones already present. In the case one chooses to retain the parametrization in terms of the subthreshold parameters, w is fixed so as to reproduce the expressions for the polynomials given in Ref. [44], which were themselves constructed so that they reproduce the polynomial part of the $\pi\pi$ amplitude in the isospin limit as given in Ref. [46]. Explicitly, this means

$$w_{+0} = -w_x = \frac{\Delta_\pi^2}{F_\pi^4} \times \lambda_x^{(1)} + \mathcal{O}(E^6), \tag{4.18}$$

and $w = 0$ in the remaining cases. For the parametrization in terms of scattering lengths, the value of w is simply

$$w = \frac{\lambda_s}{4}\frac{\mu_+^2}{F_\pi^4} + \frac{\lambda_t}{F_\pi^4}\left(t_{\rm thr} - \frac{3}{2}\mu_+\right)^2 + \frac{\lambda_u}{F_\pi^4}\left(u_{\rm thr} - \frac{3}{2}\mu_+\right)^2 + {\rm Re}U(\mu_+, t_{\rm thr}, u_{\rm thr}) + \mathcal{O}(E^6), \tag{4.19}$$

with $t_{\rm thr} - u_{\rm thr} = \mu_-$ and the values for μ_+ and μ_- as given in Table VI. This choice of w, therefore, ensures that the parameter a in Eq. (4.1) indeed corresponds to the scattering length, i.e.,

$${\rm Re}A(\mu_+, t_{\rm thr}, u_{\rm thr}) \equiv 16\pi {\rm a} + \mathcal{O}(E^6). \tag{4.20}$$

At next-to-leading order, the constraints arising from the crossing property read

$${\rm c}_{+-} = {\rm b}_{+-}, \qquad {\rm b}_{++} + 2{\rm b}_{+-} = 0, \tag{4.21}$$

$${\rm a}_{+-} - {\rm a}_{++} + \frac{4M_{\pi^\pm}^2}{F_\pi^2}{\rm b}_{++} = \frac{2}{\pi}({\rm a}_{+-})^2 - \frac{({\rm a}_{++})^2}{\pi} + \frac{2}{\pi}\frac{\lambda_{+-}^{(2)} - \lambda_{+-}^{(1)}}{F_\pi^4}M_\pi^4 + 16\pi\frac{({\rm a}_x)^2}{2}{\rm Re}\bar{J}_0(4M_\pi^2), \tag{4.22}$$

$${\rm c}_{+0} = -{\rm b}_{+0}, \tag{4.23}$$

$${\rm b}_x - 2{\rm b}_{+0} = \frac{3}{16\pi}\frac{\lambda_x^{(2)} - \lambda_x^{(1)}}{F_\pi^2}(M_\pi - M_{\pi^0})(3M_\pi + M_{\pi^0}), \tag{4.24}$$

and

$${\rm a}_x + {\rm a}_{+0} - 4\frac{M_{\pi^\pm}^2}{F_\pi^2}{\rm b}_x = \frac{2}{\pi}{\rm a}_x{\rm a}_{+-} + \frac{2}{\pi}{\rm a}_{+0}^2 + 16\pi\frac{{\rm a}_x{\rm a}_{00}}{2}{\rm Re}\bar{J}_0(4M_\pi^2) - 16\pi\frac{4}{3}\frac{{\rm b}_x^2}{F_\pi^4}M_\pi^2\Delta_\pi^2\bar{J}'(0) - 32\pi\left({\rm a}_x^2 - 4M_\pi^2{\rm a}_x\frac{{\rm b}_x}{F_\pi^2} + \frac{8}{3}\frac{{\rm b}_x^2}{F_\pi^4}M_\pi^4\right)\bar{J}_{\pm 0}(-\Delta_\pi) - \frac{M_\pi^2}{\pi}\frac{\lambda_x^{(2)}(3M_\pi^2 - M_{\pi^0}^2) - 2\lambda_x^{(1)}M_{\pi^0}^2}{F_\pi^4}. \tag{4.25}$$

B. $P\pi \to \pi\pi$ scattering

The implementation of the first iteration for the amplitudes of the processes $P\pi \to \pi\pi$ follows rather closely the previous case of $\pi\pi$ scattering, so that the main use of this section is to establish the notation in a more precise way. The starting point is now given by the order $\mathcal{O}(E^2)$ expressions for the amplitudes in Table I that are (anti) symmetric under exchange of t and u, which we now parametrize in the following form:

$$\begin{aligned}
\mathcal{M}_{++}(s,t) &= A_{++} + B_{++}\frac{s - s_0}{F_\pi^2},\\
\mathcal{M}_{x}(s,t) &= A_{x} + B_{x}\frac{s - s_0}{F_\pi^2},\\
\mathcal{M}_{x}^L(s,t) &= A_{x}^L + B_{x}^L\frac{s - s_0}{F_\pi^2},\\
\mathcal{M}_{00}^L(s,t) &= A_{00}^L,\\
\mathcal{M}_{x}^S(s,t) &= B_{x}^S\frac{t - u}{F_\pi^2}.
\end{aligned} \tag{4.26}$$

The crossing property then furnishes the remaining amplitudes

$$\begin{aligned}
\mathcal{M}_{+-}(s,t) &= A_{++} - \frac{B_{++}}{2F_\pi^2}[(s - s_0) + (t - u)],\\
\mathcal{M}_{0+}(s,t) &= -A_{x} + \frac{B_{x}}{2F_\pi^2}[(s - s_0) + (t - u)],\\
\mathcal{M}_{+0}^L(s,t) &= -A_{x}^L + \frac{B_{x}^L}{2F_\pi^2}[(s - s_0) + (t - u)],\\
\mathcal{M}_{+0}^S(s,t) &= \frac{B_{x}^S}{2F_\pi^2}[3(s - s_0) - (t - u)].
\end{aligned} \tag{4.27}$$

The value of s_0 depends on the process under consideration; see (3.3). We have not written the amplitudes describing the two processes involving the η meson. As far as their structure is concerned, they can be obtained in what follows from the amplitudes involving the K_L meson, upon replacing the mass of the latter by the mass of the

former, and upon changing the notation for the coefficients appearing in the polynomial part (e.g., A_x^η instead of A_x^L, and so on). The computation of the $\mathcal{O}(E^2)$ S and P partial waves $\tilde{\varphi}_\ell(s)$, $\ell = 0, 1$, from the amplitudes (4.26) and (4.27), presents no particular difficulty, and we merely display the resulting expressions,[8]

$$\begin{aligned}
\tilde{\varphi}_0^{++}(s) &= \frac{1}{16\pi}\left[A_{++} + \frac{B_{++}}{F_\pi^2}\left(s - \frac{M_K^2}{3} - M_\pi^2\right)\right],\\
\tilde{\varphi}_0^{+-}(s) &= \frac{1}{32\pi}\left[2A_{++} - \frac{B_{++}}{F_\pi^2}\left(s - \frac{M_K^2}{3} - M_\pi^2\right)\right],\\
\tilde{\varphi}_1^{+-}(s) &= -\frac{B_{++}}{48\pi}\frac{K_{K\mp;\pm\mp}(s)}{F_\pi^2},
\end{aligned} \tag{4.28}$$

$$\begin{aligned}
\tilde{\varphi}_0^{x}(s) &= \frac{1}{16\pi}\left[A_x + \frac{B_x}{3F_\pi^2}(3s - M_K^2 - M_\pi^2 - 2M_{\pi^0}^2)\right],\\
\tilde{\varphi}_0^{0+}(s) &= -\frac{A_x}{16\pi} - \frac{B_x}{96\pi F_\pi^2}\left[M_K^2 + M_\pi^2 + 2M_{\pi^0}^2\right.\\
&\quad \left. - 3s - \frac{3}{s}(M_K^2 - M_{\pi^0}^2)\Delta_\pi\right],\\
\tilde{\varphi}_1^{0+}(s) &= \frac{B_x}{48\pi}\frac{K_{K0;0\pm}(s)}{F_\pi^2},
\end{aligned} \tag{4.29}$$

$$\begin{aligned}
\tilde{\varphi}_0^{L;x}(s) &= \frac{1}{16\pi}\left[A_x^L + \frac{B_x^L}{3F_\pi^2}(3s - M_{K_L}^2 - 2M_\pi^2 - M_{\pi^0}^2)\right],\\
\tilde{\varphi}_0^{L;+0}(s) &= -\frac{A_x^L}{16\pi} - \frac{B_x^L}{96\pi F_\pi^2}\left[M_{K_L}^2 + 2M_\pi^2 + M_{\pi^0}^2\right.\\
&\quad \left. - 3s + \frac{3}{s}(M_{K_L}^2 - M_\pi^2)\Delta_\pi\right],\\
\tilde{\varphi}_1^{L;+0}(s) &= \frac{B_x^L}{48\pi}\frac{K_{K_L\pm;\pm 0}(s)}{F_\pi^2},
\end{aligned} \tag{4.30}$$

$$\tilde{\varphi}_0^{L;00}(s) = \frac{1}{16\pi}A_{00}^L, \tag{4.31}$$

$$\begin{aligned}
\tilde{\varphi}_1^{S;x}(s) &= \frac{B_x^S}{24\pi}\frac{K_{K_S0;+-}(s)}{F_\pi^2},\\
\tilde{\varphi}_0^{S;+0}(s) &= \frac{B_x^S}{32\pi F_\pi^2}\left[3s - M_{K_S}^2 - 2M_\pi^2 - M_{\pi^0}^2\right.\\
&\quad \left. + \frac{1}{s}(M_{K_S}^2 - M_\pi^2)\Delta_\pi\right],\\
\tilde{\varphi}_1^{S;+0}(s) &= -\frac{B_x^S}{48\pi}\frac{K_{K_S\pm;\pm 0}(s)}{F_\pi^2}.
\end{aligned} \tag{4.32}$$

[8]The remark made in Eq. (4.5) above also applies to the product $\tilde{\varphi}_1^{i\to k}(s)\varphi_1^{k\to f}(s)$. In addition, when referring to the Kacser function for a definite process, we denote the pions by their charges, e.g., $K_{K_L\pm;\pm 0}(s)$ or $K_{K\mp;00}(s)$, and so on. For a generic case, we write just $K(s)$.

In the case $P = K^\pm$, there are two independent channels to consider, one involving charged pions only and the other involving two neutral pions. The structure of the corresponding two-loop amplitudes, as inferred from the reconstruction theorem, is given by

$$\begin{aligned}
\mathcal{M}_{++}(s,t,u) &= \mathcal{P}_{++}(s,t,u) + 16\pi\mathcal{W}_{++}(s)\\
&\quad + 16\pi[\mathcal{W}_{+-}^{(0)}(t) + 3(u-s)\mathcal{W}_{+-}^{(1)}(t)]\\
&\quad + 16\pi[\mathcal{W}_{+-}^{(0)}(u) + 3(t-s)\mathcal{W}_{+-}^{(1)}(u)] + \mathcal{O}(E^8),
\end{aligned} \tag{4.33}$$

and

$$\begin{aligned}
\mathcal{M}_{x}(s,t,u) &= \mathcal{P}_{x}(s,t,u) + 16\pi\mathcal{W}_{x}(s)\\
&\quad + 16\pi[\mathcal{W}_{0+}^{(0)}(t) + 3(u-s)\mathcal{W}_{0+}^{(1)}(t)]\\
&\quad + 16\pi[\mathcal{W}_{0+}^{(0)}(u) + 3(t-s)\mathcal{W}_{0+}^{(1)}(u)] + \mathcal{O}(E^8).
\end{aligned} \tag{4.34}$$

The various functions that appear in these expressions have discontinuities that are given by unitarity. At the one-loop order, and when restricted to two-pions intermediate states, these read [cf. Eqs. (3.13) and (3.24)]

$$\begin{aligned}
\mathrm{Abs}\mathcal{W}_{++}(s) &= \frac{1}{2}\sigma(s)\tilde{\varphi}_0^{++}(s)\varphi_0^{++}(s)\theta(s-4M_\pi^2) + \mathcal{O}(E^6),\\
\mathrm{Abs}\mathcal{W}_{+-}^{(0)}(s) &= \left\{\sigma(s)\tilde{\varphi}_0^{+-}(s)\varphi_0^{+-}(s)\theta(s-4M_\pi^2)\right.\\
&\quad \left. + \frac{1}{2}\sigma_0(s)\tilde{\varphi}_0^{x}(s)\varphi_0^{x}(s)\theta(s-4M_{\pi^0}^2)\right\} + \mathcal{O}(E^6),\\
\mathrm{Abs}\mathcal{W}_{+-}^{(1)}(s) &= \sigma(s)\frac{\tilde{\varphi}_1^{+-}(s)\varphi_1^{+-}(s)}{2K_{K\mp;\pm\mp}(s)}\theta(s-4M_\pi^2) + \mathcal{O}(E^6),\\
\mathrm{Abs}\mathcal{W}_{x}(s) &= \left\{\frac{1}{2}\sigma_0(s)\tilde{\varphi}_0^{x}(s)\varphi_0^{00}(s)\theta(s-4M_{\pi^0}^2)\right.\\
&\quad \left. + \sigma(s)\tilde{\varphi}_0^{+-}(s)\varphi_0^{x}(s)\theta(s-4M_\pi^2)\right\} + \mathcal{O}(E^6),\\
\mathrm{Abs}\mathcal{W}_{0+}^{(0)}(s) &= \frac{\lambda_{\pm 0}^{1/2}(s)}{s}\left\{\varphi_0^{+0}(s)\tilde{\varphi}_0^{0+}(s)\right.\\
&\quad \left. - 3\frac{\Delta_\pi(M_K^2 - M_{\pi^0}^2)}{s}\frac{\varphi_1^{+0}(s)\tilde{\varphi}_1^{0+}(s)}{2K_{K0;0\pm}(s)}\right\}\\
&\quad \times\theta(s-(M_\pi+M_{\pi^0})^2) + \mathcal{O}(E^6),\\
\mathrm{Abs}\mathcal{W}_{0+}^{(1)}(s) &= \frac{\lambda_{\pm 0}^{1/2}(s)}{s}\frac{\varphi_1^{+0}(s)\tilde{\varphi}_1^{0+}(s)}{2K_{K0;0\pm}(s)}\\
&\quad \times\theta(s-(M_\pi+M_{\pi^0})^2) + \mathcal{O}(E^6).
\end{aligned} \tag{4.35}$$

Up to a polynomial ambiguity, this fixes then these functions to read

$$\mathcal{W}_{++}(s) = 16\pi\frac{1}{2}\tilde{\varphi}_0^{++}(s)\varphi_0^{++}(s)\bar{J}(s) + \mathcal{O}(E^6),$$
$$\mathcal{W}_{+-}^{(0)}(s) = 16\pi\left\{\tilde{\varphi}_0^{+-}(s)\varphi_0^{+-}(s)\bar{J}(s) + \frac{1}{2}\tilde{\varphi}_0^{x}(s)\varphi_0^{x}(s)\bar{J}_0(s)\right\} + \mathcal{O}(E^6),$$
$$\mathcal{W}_{+-}^{(1)}(s) = -\frac{B_{++}\mathrm{c}_{+-}}{18F_\pi^4}(s-4M_\pi^2)\bar{J}(s) + \mathcal{O}(E^6), \tag{4.36}$$

and

$$\mathcal{W}_{x}(s) = 16\pi\left[\frac{1}{2}\tilde{\varphi}_0^{x}(s)\varphi_0^{00}(s)\bar{J}_0(s) + \tilde{\varphi}_0^{+-}(s)\varphi_0^{x}(s)\bar{J}(s)\right] + \mathcal{O}(E^6),$$
$$\mathcal{W}_{0+}^{(0)}(s) = \left\{-\frac{B_x\mathrm{c}_{+0}}{6F_\pi^4}\left[1-2\frac{M_\pi^2+M_{\pi^0}^2}{s}-3\frac{\Delta_\pi^2}{s^2}\right]\times(M_K^2-M_{\pi^0}^2)\Delta_\pi + 16\pi\varphi_0^{+0}(s)\tilde{\varphi}_0^{0+}(s)\right\}\bar{J}_{\pm0}(s) - \frac{2B_x\mathrm{c}_{+0}}{3F_\pi^4}\frac{(M_K^2-M_{\pi^0}^2)\Delta_\pi^3}{s^2}\bar{\bar{J}}_{\pm0}(s) + \mathcal{O}(E^6),$$
$$\mathcal{W}_{0+}^{(1)}(s) = \frac{B_x\mathrm{c}_{+0}}{18F_\pi^4}\frac{\lambda_{\pm0}(s)}{s}\bar{J}_{\pm0}(s) + \mathcal{O}(E^6). \tag{4.37}$$

We may proceed similarly in the case of the reactions with $P = K_L$ (or η). The amplitude for $K_L\pi^0 \to \pi^\mp\pi^\pm$ reads

$$\mathcal{M}_x^L(s,t,u) = \mathcal{P}_{L;x}(s,t,u) + 16\pi\mathcal{W}_{L;x}(s) - 16\pi\left[\mathcal{W}_{L;+0}^{(0)}(t) + 3(u-s)\mathcal{W}_{L;+0}^{(1)}(t)\right] - 16\pi\left[\mathcal{W}_{L;+0}^{(0)}(u) + 3(t-s)\mathcal{W}_{L;+0}^{(1)}(u)\right] + \mathcal{O}(E^8), \tag{4.38}$$

whereas for $K_L\pi^0 \to \pi^0\pi^0$, we obtain

$$\mathcal{M}_{00}^L(s,t,u) = 16\pi[\mathcal{W}_{L;00}(s) + \mathcal{W}_{L;00}(t) + \mathcal{W}_{L;00}(u)] + \mathcal{P}_{L;00}(s,t,u) + \mathcal{O}(E^8). \tag{4.39}$$

At the one-loop order, the various functions that appear in these expressions are given as

$$\mathcal{W}_{L;x}(s) = 16\pi\left[\frac{1}{2}\tilde{\varphi}_0^{L;00}(s)\varphi_0^{x}(s)\bar{J}_0(s) + \tilde{\varphi}_0^{L;x}(s)\varphi_0^{+-}(s)\bar{J}(s)\right] + \mathcal{O}(E^6),$$
$$\mathcal{W}_{L;+0}^{(0)}(s) = \left\{\frac{B_x^L\mathrm{c}_{+0}}{6F_\pi^4}\left[1-2\frac{M_\pi^2+M_{\pi^0}^2}{s}-3\frac{\Delta_\pi^2}{s^2}\right]\times(M_{K_L}^2-M_\pi^2)\Delta_\pi + 16\pi\varphi_0^{+0}(s)\tilde{\varphi}_0^{L;+0}(s)\right\}\bar{J}_{\pm0}(s) + \frac{2B_x^L\mathrm{c}_{+0}}{3F_\pi^4}\frac{(M_{K_L}^2-M_\pi^2)\Delta_\pi^3}{s^2}\bar{\bar{J}}_{\pm0}(s) + \mathcal{O}(E^6),$$
$$\mathcal{W}_{L;+0}^{(1)}(s) = \frac{B_x^L\mathrm{c}_{+0}}{18F_\pi^4}\frac{\lambda_{\pm0}(s)}{s}\bar{J}_{\pm0}(s) + \mathcal{O}(E^6), \tag{4.40}$$

and

$$\mathcal{W}_{L;00}(s) = 16\pi\left[\frac{1}{2}\tilde{\varphi}_0^{L;00}(s)\varphi_0^{00}(s)\bar{J}_0(s) + \tilde{\varphi}_0^{L;x}(s)\varphi_0^{x}(s)\bar{J}(s)\right] + \mathcal{O}(E^6). \tag{4.41}$$

At the same one-loop accuracy, the polynomial contributions to the four amplitudes that we have just discussed, namely $\mathcal{M}_{++}$, $\mathcal{M}_x$, $\mathcal{M}_x^L$, $\mathcal{M}_{00}^L$, can be written as (cf. footnote 3)

$$\mathcal{P}(s,t,u) = A + B\frac{s-s_0}{F_\pi^2} + C\frac{(s-s_0)^2}{F_\pi^4} + \frac{D}{F_\pi^4}[(t-s_0)^2 + (u-s_0)^2] + \mathcal{O}(E^6), \tag{4.42}$$

putting appropriate labels on the coefficients, e.g., A_{++}, A_x, and so on. In the case of $\mathcal{P}_{00}^L(s,t,u)$, the additional restrictions $B_{00}^L = 0$ and $C_{00}^L = D_{00}^L$, due to Bose symmetry, apply. These coefficients are in one-to-one correspondence with the Dalitz-plot parameters of the $K \to \pi\pi\pi$ amplitudes.

Finally, it remains to discuss the case $P = K_S$ briefly. The corresponding two-loop amplitude for the process $K_S\pi^0 \to \pi^+\pi^-$ has the form

$$\mathcal{M}_x^S(s,t,u) = \mathcal{P}_{S,x}(s,t,u) + 48\pi(t-u)\mathcal{W}_{S;x}^{(1)}(s) + 16\pi[\mathcal{W}_{S;+0}^{(0)}(t) + 3(u-s)\mathcal{W}_{S;+0}^{(1)}(t)] - 16\pi[\mathcal{W}_{S;+0}^{(0)}(u) + 3(t-s)\mathcal{W}_{S;+0}^{(1)}(u)] + \mathcal{O}(E^8). \tag{4.43}$$

At the one-loop order, the functions involved in this expression read

$$\mathcal{W}_{S;x}^{(1)}(s) = \frac{B_x^S\mathrm{c}_{+0}}{9F_\pi^4}(s-4M_\pi^2)\bar{J}(s) + \mathcal{O}(E^6), \tag{4.44}$$

and

$$\mathcal{W}^{(0)}_{S;+0}(s) = \left\{ -\frac{B^S_x \mathrm{c}_{+0}}{6F_\pi^4}\left[1 - 2\frac{M_\pi^2 + M_{\pi^0}^2}{s} - 3\frac{\Delta_\pi^2}{s^2}\right] \times (M_{K_S}^2 - M_\pi^2)\Delta_\pi + 16\pi\varphi_0^{+0}(s)\tilde{\varphi}_0^{S;+0}(s)\right\}\bar{J}_{+0}(s) - \frac{2B^S_x \mathrm{c}_{+0}}{3F_\pi^4}\frac{(M_{K_S}^2 - M_\pi^2)\Delta_\pi^3}{s^2}\bar{\bar{J}}_{+0}(s) + \mathcal{O}(E^6),$$

$$\mathcal{W}^{(1)}_{S;+0}(s) = -\frac{B^S_x \mathrm{c}_{+0}}{18F_\pi^4}\frac{\lambda_{+0}(s)}{s}\bar{J}_{+0}(s) + \mathcal{O}(E^6). \quad (4.45)$$

The one-loop subtraction polynomial, in this case, is given by

$$\mathcal{P}^S_x(s,t,u) = \frac{t-u}{F_\pi^2}\left[B^S_x + D^S_x\frac{s_0 - s}{F_\pi^2}\right] + \mathcal{O}(E^6). \quad (4.46)$$

Again, B^S_x and D^S_x are related to Dalitz-plot parameters of the $K_S \to \pi^0\pi^+\pi^-$ amplitude.

V. SECOND ITERATION: EQUAL-MASS PIONS

The construction of the scattering amplitudes for the $\pi\pi \to \pi\pi$ and $P\pi \to \pi\pi$ processes could be performed in a rather straightforward manner at next-to-leading order: from the expressions of their discontinuities at one loop, the various functions $W(s)$ and $\mathcal{W}(s)$ have been obtained up to an ambiguity consisting in polynomials of at most second order in the Mandelstam variables. The resulting amplitudes at one loop display the correct analytic properties expected at this order, and satisfy all required crossing relations. In order to proceed toward obtaining two-loop expressions for all the $P\pi \to \pi\pi$ amplitudes, it is necessary to supplement the subtraction polynomials with $\mathcal{O}(E^6)$ terms. For $\mathcal{M}_{++}$, $\mathcal{M}_x$, $\mathcal{M}^L_x$, $\mathcal{M}^L_{00}$, we take the generic form[9]

$$\mathcal{P}(s,t,u) = A + B\frac{s-s_0}{F_\pi^2} + C\frac{(s-s_0)^2}{F_\pi^4} + \frac{D}{F_\pi^4}[(t-s_0)^2 + (u-s_0)^2] + E\frac{(s-s_0)^3}{F_\pi^6} + \frac{F}{F_\pi^6}[(t-s_0)^3 + (u-s_0)^3] + \mathcal{O}(E^8) \quad (5.1)$$

with appropriate labels. Due to the Bose symmetry, in the case of $\mathcal{P}^L_{00}(s,t,u)$, the additional constraint $F^L_{00} = E^L_{00}$ holds [in addition to the restrictions discussed after (4.42)]. For $\mathcal{M}^S_x$, the polynomial is

$$\mathcal{P}^S_x(s,t,u) = \frac{t-u}{F_\pi^2}\left[B^S_x + D^S_x\frac{s_0-s}{F_\pi^2} + E^S_x\frac{(s_0-s)^2}{F_\pi^4} + \frac{F^S_x}{F_\pi^4}((s_0-t)^2 + (s_0-u)^2)\right] + \mathcal{O}(E^8). \quad (5.2)$$

Then, we start from the discontinuities of the functions $\mathcal{W}(s)$ that hold at this order, as given by Eqs. (3.13), (3.21), and (3.26). For instance, for the amplitude $\mathcal{W}_{L;00}(s)$, it gives

$$\mathrm{Abs}\mathcal{W}_{L;00}(s) = \frac{\sigma_0(s)}{2}[\tilde{\varphi}_0^{L;00}(s)\varphi_0^{00}(s) + \tilde{\varphi}_0^{L;00}(s)\psi_0^{00}(s) + \tilde{\psi}_0^{L;00}(s)\varphi_0^{00}(s)]\theta(s-4M_{\pi^0}^2) + \sigma(s)[\tilde{\varphi}_0^{L;x}(s)\varphi_0^{x}(s) + \tilde{\varphi}_0^{L;x}(s)\psi_0^{x}(s) + \tilde{\psi}_0^{L;x}(s)\varphi_0^{x}(s)]\theta(s-4M_\pi^2) + \mathcal{O}(E^8). \quad (5.3)$$

As illustrated by this example, schematically these expressions now involve, in addition to the lowest-order partial waves represented by the functions $\varphi(s)$ and $\tilde{\varphi}(s)$, the one-loop dispersive part $\psi(s)$ $[\tilde{\psi}(s)]$ of the $\pi\pi \to \pi\pi$ ($P\pi \to \pi\pi$) S and P partial-wave projections. These are to be obtained from the one-loop expressions of these amplitudes that have just been computed in the preceding section. As compared to the leading-order case, their expressions at the next-to-leading order are much more complicated. In the case of the $\pi\pi$ scattering amplitudes, the difficulty is purely algebraic, and explicit formulas can be obtained in rather closed forms [44,48]. They essentially generalize the results obtained in the case without isospin breaking [46] to the situation where the pion mass difference is taken into account. In the case of the $P\pi \to \pi\pi$ amplitudes, the situation is somewhat more involved, due to the existence, in the central region of the Mandelstam plane, of a bounded region corresponding to the decay process $P \to \pi\pi\pi$. This feature makes the analytic properties of the amplitude less simple, and requires a more elaborate analysis. In particular, when performing the partial-wave projection by the usual integration over the variable t, one has to be careful to find the appropriate prescription for deforming the path of integration in order to avoid any singularity. The situation has been well studied in the case that corresponds to the isospin limit: the masses of the three particles in the final state (i.e., pions for the cases at hand), but also in the intermediate states, are identical. As explained before, the appropriate procedure consists in starting from the situation where $M_P < 3M_{\pi^0}$, so that the decay region disappears. In this case, dispersion relations exist under the usual conditions, and one can proceed as outlined in Fig. 1. After that, one performs the analytic continuation in the mass, $M_P^2 \to M_P^2 + i\delta$, to the region where $M_P > 3M_{\pi^0}$ [68,79,80]. In practice, this analytic continuation is provided by the prescription to deform the contour of integration in the partial-wave projection. We

[9]Note that in Ref. [36] for the case of $P = \eta$, we have used the same form of the polynomial with a different normalization of the coefficients $A^\eta_x, \ldots, F^\eta_x$ and $A^\eta_{00}, \ldots, E^\eta_{00}$.

show in Appendix A that this prescription, which was shown to give the correct result in the limit of equal-mass pions, also provides the appropriate prescription for the processes involving three neutral external pions, even when there appear pairs of heavier charged pions as intermediate states. The more general situation, with also charged pions in the external states, and lighter neutral pions as intermediate states, involves anomalous thresholds and requires a dedicated study. It will be the subject of a subsequent article [51]. Therefore, our analysis in this section is restricted to the case of equal-mass pions, in both final and intermediate states. The common pion mass will be taken as M_π, the mass of the charged pion. The case $P\pi^0 \to \pi^0\pi^0$, $P = K_L, \eta$, with $M_{\pi^0} \neq M_\pi$, will be considered in the next section.

For equal-mass pions, the discontinuities of the functions $\mathcal{W}(s)$ at next-to-leading order take the schematic form [in the case of the functions $\mathcal{W}^{(1)}(s)$, an additional factor $1/2K(s)$ is understood]

$$\mathrm{Abs}\mathcal{W}(s) \sim \sigma(s)[\tilde{\varphi}(s)\varphi(s) + \tilde{\varphi}(s)\psi(s) + \tilde{\psi}(s)\varphi(s)]. \quad (5.4)$$

This leads to the following convenient decomposition of the functions $\mathcal{W}(s)$ at two loops,

$$\mathcal{W}(s) = \mathcal{W}^{1\,\mathrm{loop}}(s) + \mathcal{W}^{\pi\pi}(s) + \mathcal{W}^{P\pi}(s), \quad (5.5)$$

where each term results from the corresponding term in the preceding decomposition of $\mathrm{Abs}\mathcal{W}(s)$. The preceding section was devoted to the evaluation of the NLO amplitudes $\mathcal{W}^{1\,\mathrm{loop}}(s)$, with $\mathrm{Abs}\mathcal{W}^{1\,\mathrm{loop}}(s) \sim \sigma(s)\tilde{\varphi}(s)\varphi(s)$. The next two terms give the contribution at NNLO, and their computation[10] will be addressed in turn in the remainder of the present section. The results for $\mathcal{W}^{\pi\pi}(s)$ can be found in Sec. V A [cf. (5.13)–(5.16)], whereas those for $\mathcal{W}^{P\pi}(s)$ are listed in Appendix D. Note that for $P = \eta$, we reproduce the expressions that were implicitly used (and the general structure of which was shown) already in Sec. IV of Ref. [36].

A. NLO $\pi\pi$ partial waves and the functions $\mathcal{W}^{\pi\pi}(s)$

In the case where the pions have all a common mass M_π, the partial-wave projections at one loop $\psi_\ell(s)$, $\ell = 0, 1$, for $\pi\pi$ scattering were already worked out quite some time ago in Ref. [46]. We will use the expressions as given in Ref. [44], with which we also share the normalization. The partial-wave projections in the various channels are expressed as combinations, weighted by the appropriate Clebsh-Gordan coefficients, of the isospin projections $\psi_I(s)$, $I = 0, 1, 2$, e.g., (with the Condon and Shortley phase convention),

$$\begin{pmatrix} \psi_0^{++} \\ \psi_0^{+-} \\ \psi_0^{x} \\ \psi_0^{+0} \\ \psi_0^{00} \end{pmatrix} = \begin{pmatrix} 0 & 1 \\ \frac{1}{3} & \frac{1}{6} \\ -\frac{1}{3} & \frac{1}{3} \\ 0 & \frac{1}{2} \\ \frac{1}{3} & \frac{2}{3} \end{pmatrix} \begin{pmatrix} \psi_0 \\ \psi_2 \end{pmatrix}, \quad (5.6)$$

whereas $\psi_1^{+-} = \psi_1^{+0} = \psi_1/2$. The isospin projections $\psi_I(s)$ themselves are expressed in the form

$$\psi_I(s) = 2\frac{M_\pi^4}{F_\pi^4}\sqrt{\frac{s}{s-4M_\pi^2}}\sum_{i=0}^{4}\xi_I^{(i)}(s)k_i(s), \quad (5.7)$$

where the functions $k_i(s)$ read, for $s \geq 4M_\pi^2$,

$$\begin{aligned} k_0(s) &= \frac{1}{16\pi}\sqrt{\frac{s-4M_\pi^2}{s}}, \qquad k_1(s) = \frac{1}{8\pi}L(s), \\ k_2(s) &= \frac{1}{8\pi}\left(1 - \frac{4M_\pi^2}{s}\right)L(s), \\ k_3(s) &= \frac{3}{16\pi}\frac{M_\pi^2}{\sqrt{s(s-4M_\pi^2)}}L^2(s), \\ k_4(s) &= \frac{1}{16\pi}\frac{M_\pi^2}{\sqrt{s(s-4M_\pi^2)}}\left\{1 + \sqrt{\frac{s}{s-4M_\pi^2}}L(s) \right. \\ &\quad \left. + \frac{M_\pi^2}{s-4M_\pi^2}L^2(s)\right\}, \end{aligned} \quad (5.8)$$

with[11]

$$L(s) = \ln\frac{1 - \sqrt{\frac{s-4M_\pi^2}{s}}}{1 + \sqrt{\frac{s-4M_\pi^2}{s}}} [s \geq 4M_\pi^2]. \quad (5.9)$$

The polynomials $\xi_I^{(i)}(s)$ have been worked out in Ref. [46]. We will use them in the form given in terms of subthreshold parameters in Eq. (C.8) of Ref. [44]. Their expressions in terms of the scattering lengths can be obtained from the formulas (F.8) to (F.11) given in Appendix F of that same reference, upon taking the limit where the neutral and charged pion masses coincide. Note that the function $k_4(s)$ appears only in the P-wave projection $\psi_1(s)$, and the polynomials $\xi_0^{(4)}(s)$ and $\xi_2^{(4)}(s)$ vanish identically. Due to the relation

$$\left(\frac{s}{M_\pi^2} - 4\right)k_4(s) = k_0(s) + 2k_1(s) + \frac{1}{3}k_3(s), \quad (5.10)$$

[10]It is useful, for what follows, to keep in mind that the functions $\tilde{\varphi}(s)$ and $\varphi(s)$ all simply become first-order polynomials in s when $M_{\pi^0} = M_\pi$.

[11]Note that for $s \geq 4M_\pi^2$, one has

$$\bar{J}(s) = \frac{1}{16\pi^2}\left[2 + \sqrt{1 - \frac{4M_\pi^2}{s}}(L(s) + i\pi)\right].$$

there is an ambiguity in the definition of the polynomials $\xi_1^{(i)}(s)$. This, however, does not matter in practice, and $\psi_1(s)$ is well defined.

Following Ref. [46], the expressions of the various functions $W_0(s)$ and $W_1(s)$ can be written in terms of integrals

$$\bar{K}_i(s) = \frac{s}{\pi}\int_{4M_\pi^2}^{\infty}\frac{dx}{x}\frac{k_i(x)}{x-s-\mathrm{i}0}. \tag{5.11}$$

These integrals can be expressed in terms of the function $\bar{J}(s)$, and the corresponding formulas are given in Eq. (3.49) of Ref. [46].

We may now display, for each function $\mathcal{W}(s)$ appearing in Table II, its NNLO contribution $\mathcal{W}^{\pi\pi}(s)$. These expressions read

$$\begin{aligned}
\mathcal{W}_{++}^{\pi\pi}(s) &= \tilde{\varphi}_0^{++}(s)\frac{M_\pi^4}{F_\pi^4}\sum_{i=0}^{3}\xi_2^{(i)}(s)\bar{K}_i(s),\\
\mathcal{W}_{+-}^{(0)\pi\pi}(s) &= \frac{1}{3}\tilde{\varphi}_0^{+-}(s)\frac{M_\pi^4}{F_\pi^4}\sum_{i=0}^{3}[2\xi_0^{(i)}(s)+\xi_2^{(i)}(s)]\bar{K}_i(s)\\
&\quad -\frac{1}{3}\tilde{\varphi}_0^{x}(s)\frac{M_\pi^4}{F_\pi^4}\sum_{i=0}^{3}[\xi_0^{(i)}(s)-\xi_2^{(i)}(s)]\bar{K}_i(s),\\
\mathcal{W}_{+-}^{(1)\pi\pi}(s) &= -\frac{B_{++}}{96\pi F_\pi^2}\frac{M_\pi^4}{F_\pi^4}\sum_{i=0}^{4}\xi_1^{(i)}(s)\bar{K}_i(s),
\end{aligned} \tag{5.12}$$

$$\begin{aligned}
\mathcal{W}_{x}^{\pi\pi}(s) &= \frac{1}{3}\tilde{\varphi}_0^{x}(s)\frac{M_\pi^4}{F_\pi^4}\sum_{i=0}^{3}[\xi_0^{(i)}(s)+2\xi_2^{(i)}(s)]\bar{K}_i(s)\\
&\quad -\frac{2}{3}\tilde{\varphi}_0^{+-}(s)\frac{M_\pi^4}{F_\pi^4}\sum_{i=0}^{3}[\xi_0^{(i)}(s)-\xi_2^{(i)}(s)]\bar{K}_i(s),\\
\mathcal{W}_{0+}^{(0)\pi\pi}(s) &= \tilde{\varphi}_0^{0+}(s)\frac{M_\pi^4}{F_\pi^4}\sum_{i=0}^{3}\xi_2^{(i)}(s)\bar{K}_i(s),\\
\mathcal{W}_{0+}^{(1)\pi\pi}(s) &= \frac{B_x}{96\pi F_\pi^2}\frac{M_\pi^4}{F_\pi^4}\sum_{i=0}^{4}\xi_1^{(i)}(s)\bar{K}_i(s),
\end{aligned} \tag{5.13}$$

$$\begin{aligned}
\mathcal{W}_{L;x}^{\pi\pi}(s) &= \frac{1}{3}\tilde{\varphi}_0^{L;x}(s)\frac{M_\pi^4}{F_\pi^4}\sum_{i=0}^{3}[2\xi_0^{(i)}(s)+\xi_2^{(i)}(s)]\bar{K}_i(s)\\
&\quad -\frac{1}{3}\tilde{\varphi}_0^{L;00}(s)\frac{M_\pi^4}{F_\pi^4}\sum_{i=0}^{3}[\xi_0^{(i)}(s)-\xi_2^{(i)}(s)]\bar{K}_i(s),\\
\mathcal{W}_{L;+0}^{(0)\pi\pi}(s) &= \tilde{\varphi}_0^{L;+0}(s)\frac{M_\pi^4}{F_\pi^4}\sum_{i=0}^{3}\xi_2^{(i)}(s)\bar{K}_i(s),\\
\mathcal{W}_{L;+0}^{(1)\pi\pi}(s) &= \frac{B_x^L}{96\pi F_\pi^2}\frac{M_\pi^4}{F_\pi^4}\sum_{i=0}^{4}\xi_1^{(i)}(s)\bar{K}_i(s),
\end{aligned} \tag{5.14}$$

$$\begin{aligned}
\mathcal{W}_{L;00}^{\pi\pi}(s) &= \frac{1}{3}\tilde{\varphi}_0^{L;00}(s)\frac{M_\pi^4}{F_\pi^4}\sum_{i=0}^{3}[\xi_0^{(i)}(s)+2\xi_2^{(i)}(s)]\bar{K}_i(s)\\
&\quad -\frac{2}{3}\tilde{\varphi}_0^{L;x}(s)\frac{M_\pi^4}{F_\pi^4}\sum_{i=0}^{3}[\xi_0^{(i)}(s)-\xi_2^{(i)}(s)]\bar{K}_i(s),
\end{aligned} \tag{5.15}$$

and finally,

$$\begin{aligned}
\mathcal{W}_{S;x}^{(1)\pi\pi}(s) &= \frac{B_x^S}{48\pi F_\pi^2}\frac{M_\pi^4}{F_\pi^4}\sum_{i=0}^{4}\xi_1^{(i)}(s)\bar{K}_i(s),\\
\mathcal{W}_{S;+0}^{(0)\pi\pi}(s) &= \tilde{\varphi}_0^{S;+0}(s)\frac{M_\pi^4}{F_\pi^4}\sum_{i=0}^{3}\xi_2^{(i)}(s)\bar{K}_i(s),\\
\mathcal{W}_{S;+0}^{(1)\pi\pi}(s) &= -\frac{B_x^S}{96\pi F_\pi^2}\frac{M_\pi^4}{F_\pi^4}\sum_{i=0}^{4}\xi_1^{(i)}(s)\bar{K}_i(s).
\end{aligned} \tag{5.16}$$

B. NLO partial waves of the $P\pi \to \pi\pi$ amplitudes and the functions $\mathcal{W}^{P\pi}(s)$

Above the physical threshold [or equivalently for $M_P^2 < (\sqrt{s}-M_{\pi,\pi^0})^2$], the partial-wave projections of the $P\pi\to\pi\pi$ amplitudes in the form given by Eqs. (3.11) and (3.12) are defined as integrals over the scattering angle, cf. Eq. (3.9). This integration can be traded for an integration over the Mandelstam variable t, upon using relation (3.7). Starting from the one-loop expression of the amplitude given in Sec. IV B, and written in the form shown in Eqs. (3.11) and (3.12), this leads to

$$\begin{aligned}
t_0(s) &= \mathcal{W}_0(s) + \frac{1}{64\pi K(s)}\int_{t_-}^{t_+}dt[\mathcal{P}(s,t,3s_0-t-s)+\mathcal{P}(s,3s_0-t-s,t)]\\
&\quad +\frac{1}{2K(s)}\int_{t_-}^{t_+}dt\{\mathcal{W}_0^t(t)+\mathcal{W}_0^u(t)-3(2s+t-3s_0)[\mathcal{W}_1^t(t)+\mathcal{W}_1^u(t)]\},\\
t_1(s) &= 2K(s)\mathcal{W}_1(s) + \frac{1}{128\pi K^2(s)}\int_{t_-}^{t_+}dt(2t+s-3s_0)[\mathcal{P}(s,t,3s_0-t-s)-\mathcal{P}(s,3s_0-t-s,t)]\\
&\quad +\frac{1}{4K^2(s)}\int_{t_-}^{t_+}dt(2t+s-3s_0)\{\mathcal{W}_0^t(t)-\mathcal{W}_0^u(t)-3(2s+t-3s_0)[\mathcal{W}_1^t(t)-\mathcal{W}_1^u(t)]\}
\end{aligned} \tag{5.17}$$

for the corresponding S- and P-wave projections. The limits of integration are given by

$$t_\pm(s) = \frac{3s_0 - s}{2} \pm K(s), \tag{5.18}$$

where $K(s)$ is the Kacser function defined in general by the formula (3.8). This t-integral representation of the partial-wave projections is well suited for the analytic continuation in M_P^2 mentioned above.

In the above formulas, all $\mathcal{W}$ functions stand for the one-loop expressions worked out in Sec. IV B. Making the connection with the discussion at the end of Sec. III, the contributions from direct rescattering (the first diagram in Fig. 2) are contained in the functions $\mathcal{W}_{0,1}(s)$, whereas rescattering in the crossed channels (the second diagram, with the fish topology, in Fig. 2) is contained in the integrals involving the functions $\mathcal{W}_{0,1}^{t,u}(t)$. The integrals over the polynomial parts present no difficulty. For the polynomial given in Eq. (4.42), one obtains

$$\begin{aligned}&\frac{1}{4K(s)}\int_{t_-}^{t_+} dt[\mathcal{P}(s,t,3s_0-t-s)+\mathcal{P}(s,3s_0-t-s,t)]\\&=A+B\frac{s-s_0}{F_\pi^2}+\left(C+\frac{D}{2}\right)\frac{(s-s_0)^2}{F_\pi^4}+\frac{2}{3}D\frac{K^2(s)}{F_\pi^4},\end{aligned} \tag{5.19}$$

and for the polynomial $P_x^S(s,t,u)$ given in Eq. (4.46),

$$\begin{aligned}&\frac{1}{4K^2(s)}\int_{t_-}^{t_+} dt(2t+s-3s_0)[\mathcal{P}_x^S(s,t,3s_0-t-s)\\&\quad-\mathcal{P}_x^S(s,3s_0-t-s,t)]\\&\quad=\frac{4}{3}\left[\frac{B_x^S}{F_\pi^2}-\frac{D_x^S}{F_\pi^4}(s-s_0)\right]K(s).\end{aligned} \tag{5.20}$$

As for the remaining integrals, for equal-mass pions, some simplifications occur. For instance, the three functions $\bar{J}(s)$, $\bar{J}_0(s)$, and $\bar{J}_{\pm 0}(s)$ that appear in the expressions for the one-loop amplitudes become identical and equal to $\bar{J}(s)$. Furthermore, contributions involving the twice-subtracted function $\bar{\bar{J}}_{\pm 0}(s)$ vanish, being proportional to powers of Δ_π. From the expressions obtained at NLO, the remaining integrands can then be written as polynomials in t times the loop function $\bar{J}(t)$,

$$\begin{aligned}&\{\mathcal{W}_0^t(t)\pm\mathcal{W}_0^u(t)-3(2s+t-3s_0)[\mathcal{W}_1^t(t)\pm\mathcal{W}_1^u(t)]\}_{\mathcal{O}(E^4)}\\&\quad=\left[\sum_{n=0}^{2}\tilde{w}_\pm^{(n)}\left(\frac{t}{F_\pi^2}\right)^n+\frac{\mathcal{B}_\pm}{3}\frac{s(t-4M_\pi^2)}{F_\pi^4}\right]\bar{J}(t),\end{aligned} \tag{5.21}$$

so that one obtains

$$\begin{aligned}t_0(s) &= \mathcal{W}_0(s)+\frac{1}{64\pi K(s)}\int_{t_-}^{t_+} dt[\mathcal{P}(s,t,3s_0-t-s)+\mathcal{P}(s,3s_0-t-s,t)]\\&\quad+\frac{1}{2K(s)}\int_{t_-}^{t_+} dt\sum_{n=0}^{2}\left[\tilde{w}_+^{(n)}+(2-n)\frac{\mathcal{B}_+}{3}\frac{s}{F_\pi^2}\left(-2\frac{M_\pi^2}{F_\pi^2}\right)^{1-n}\right]\left(\frac{t}{F_\pi^2}\right)^n\bar{J}(t),\end{aligned} \tag{5.22}$$

$$\begin{aligned}t_1(s) &= 2K(s)\mathcal{W}_1(s)+\frac{1}{128\pi K^2(s)}\int_{t_-}^{t_+} dt(2t+s-3s_0)[\mathcal{P}(s,t,3s_0-t-s)-\mathcal{P}(s,3s_0-t-s,t)]\\&\quad+\frac{1}{4K^2(s)}\int_{t_-}^{t_+} dt\sum_{n=0}^{2}\tilde{w}_-^{(n)}(2t-3s_0)\left(\frac{t}{F_\pi^2}\right)^n\bar{J}(t)\\&\quad+\frac{s}{4K^2(s)}\int_{t_-}^{t_+} dt\sum_{n=0}^{2}\left[\tilde{w}_-^{(n)}+\frac{\mathcal{B}_-}{3}\left(-2\frac{M_\pi^2}{F_\pi^2}\right)^{1-n}\frac{n(n-3)2^{3-n}M_\pi^2-(n-2)(s-3s_0)}{F_\pi^2}\right]\left(\frac{t}{F_\pi^2}\right)^n\bar{J}(t).\end{aligned} \tag{5.23}$$

The coefficients $\tilde{w}_\pm^{(n)}$ and $\mathcal{B}_\pm$ are process dependent, and their expressions for the various channels are collected in Appendix D.

Following the same path in the case of the partial-wave projections of the $\pi\pi$ amplitudes, we would obtain the expressions for the functions $\psi_I(s)$ explicitly; namely, in the case of equal-mass pions, we would reproduce the formulas (5.6)–(5.9) from the previous subsection. The situation in the case of the processes $P\pi \to \pi\pi$ is more involved, for the reasons already explained previously. The main difference from the case of $\pi\pi$ scattering (and the source of the complication) lies in the integration itself. In the case of $\pi\pi$ scattering, the above integrals are computed in the usual way, with the limits of integration given by $t_+(s) = 0$ and $t_-(s) = -(s - 4M_\pi^2)$. In the case of the partial-wave projections of the $P\pi \to \pi\pi$ amplitudes, we have to perform an analytic continuation in M_P^2 from $M_P = M_\pi$ to $M_P > 3M_\pi$ keeping s real and above the two-pion unitarity threshold. During the process of this analytic continuation, the physical threshold of the $P\pi \to \pi\pi$ scattering moves above the two-pion unitarity threshold, and the unphysical region appears, where the limits of

integration (5.18) become complex. Finally, also the decay region emerges. The correct prescription for such analytic continuation corresponds to approaching the real values of M_P^2 from the upper complex half-plane, i.e., taking $M_P^2 \to M_P^2 + i\delta$. It fixes the position of the end points infinitesimally below or above the real axis when necessary, as described in detail in Ref. [68] for the equal-mass pions. As a result, we get in this case

$$t_\pm(s) = \frac{3s_0 - s}{2} + \mathcal{K}_\pm(s), \tag{5.24}$$

where $\mathcal{K}_\pm(s)$ is defined as

$$\mathcal{K}_\pm(s) = \begin{cases} \mp|K(s)|, & s > M_+^2 \\ \pm i|K(s)|, & M_+^2 > s > M_-^2 \\ \pm|K(s)| \pm i\delta, & M_-^2 > s > \frac{1}{2}\Delta_{P\pi} \\ \pm|K(s)| + i\delta, & \frac{1}{2}\Delta_{P\pi} > s > 4M_\pi^2, \end{cases} \tag{5.25}$$

and $K(s)$ denotes the Kacser function for the equal-mass pions. According to the general definition (3.8), it reads

$$K^2(s) = \frac{1}{4}\left(1 - \frac{4M_\pi^2}{s}\right)\lambda_{P\pi}(s). \tag{5.26}$$

In the above formulas, we have introduced the shorthand notation $M_\pm = M_P \pm M_\pi$ and $\Delta_{P\pi} = M_P^2 - M_\pi^2$. At the same time, the path of integration itself has to be deformed into the complex-t plane in order that the integration avoids the two-pion unitarity cut.

As shown in Appendix B, the required contour integrals of $t^n\bar{J}(t)$, with $n = 0, 1, 2, 3$, can be easily computed in closed form. Note that the integrands of (5.22) and (5.23) are analytic functions. A detailed analysis of the analytic structure of these integrands reveals (cf. Appendix B) that in the case of equal-mass pions, the above contour integrals can be obtained upon taking the difference at the end points of the primitives of the functions occurring in these integrals. The results can be written compactly as (recall that the condition $s \geq 4M_\pi^2$ holds)

$$\pi \int_{t_-(s)}^{t_+(s)} dt t^n \bar{J}(t) = \frac{2K(s)}{\sigma(s)} \sum_{i=0}^{3} \kappa_i^{(n)}(s)\tilde{k}_i(s), \tag{5.27}$$

where the functions $\tilde{k}_i(s)$ are similar to the functions $k_i(s)$ introduced in Eq. (5.8) in the case of the $\pi\pi$ partial-wave projections:

$$\begin{aligned} \tilde{k}_0(s) &= \frac{1}{16\pi}\sigma(s), \qquad \tilde{k}_1(s) = \frac{1}{16\pi}L(s), \\ \tilde{k}_2(s) &= \frac{1}{16\pi}\sigma(s)s\frac{M(s)}{\lambda_{P\pi}^{1/2}(s)}, \\ \tilde{k}_3(s) &= -\frac{1}{16\pi}M_\pi^2\frac{M(s)}{\lambda_{P\pi}^{1/2}(s)}L(s). \end{aligned} \tag{5.28}$$

Actually, $k_0(s) = \tilde{k}_0(s)$ and $k_1(s) = 2\tilde{k}_1(s)$, but we prefer to keep different notations for them, such as to clearly separate the present discussion from the case of the $\pi\pi$ scattering amplitude; of course, in the limit $M_P \to M_\pi$, $\tilde{k}_2(s) \to k_1(s)/2$ and $\tilde{k}_3(s) \to -k_3(s)/3$. These expressions involve the functions $\sigma(s)$ and $L(s)$, already defined in Eqs. (4.14) and (5.9), respectively. An additional function $M(s)$ appears. For $s > 4M_\pi^2$, it is defined as

$$\begin{aligned} M(s) &= -\ln\left[1 - \frac{\Delta_{P\pi}}{s} + \frac{\lambda_{P\pi}^{1/2}(s)}{s}\right] \\ &\quad - \ln\left[1 - \frac{\Delta_{P\pi}}{s} - \frac{\lambda_{P\pi}^{1/2}(s)}{s}\right]^{-1} \\ &= -2\ln\left[1 - \frac{\Delta_{P\pi}}{s} + \frac{\lambda_{P\pi}^{1/2}(s)}{s}\right] + \ln\frac{4M_\pi^2}{s}. \end{aligned} \tag{5.29}$$

Another issue is raised by these expressions, namely, the determination of the square root of the triangle function $\lambda_{P\pi}(s)$. Nevertheless, an inspection of the formula given above for the function $M(s)$ shows that the functions $\tilde{k}_i(s)$ in Eq. (5.27) do not depend on the way one defines $\lambda_{P\pi}^{1/2}(s)$. Given the discussion preceding Eq. (5.27), it seems actually natural to define $\lambda_{P\pi}^{1/2}(s)$ as the square root of the function $\lambda(s, M_P^2 + i\delta, M_\pi^2)$, which we will assume to be the case in the remainder of this section. The functions $\tilde{k}_n(s)$ for $n = 2, 3$ are represented in Fig. 10 in Appendix C, both for $M_P < M_\pi$, where they are real, and for $M_P > M_\pi$, where an imaginary part appears.[12]

The functions $\kappa_i^{(n)}(s)$, for $i = 0, 1, 2$, are not polynomials in s, but have the following general structure,

$$\kappa_i^{(n)}(s) = \bar{\kappa}_i^{(n)}(s) + c_i^{(n)}\frac{\Delta_{P\pi}}{s} + d_i^{(n)}\frac{\Delta_{P\pi}^2}{s^2}, \tag{5.30}$$

where $\bar{\kappa}_i^{(n)}(s)$ are now polynomials in s and $c_i^{(n)}$, $d_i^{(n)}$ are numerical coefficients. The polynomials $\bar{\kappa}_i^{(n)}(s)$ are given by

[12]Up to trivial changes in the labels and normalization factors, $\tilde{k}_n(s)$ are identical with the functions $\mathcal{F}_i(s)$ defined in Eqs. (A.7) to (A.11) of Ref. [36]. For $n = 0, 1$ they furthermore coincide with the imaginary parts of the corresponding functions $\tilde{K}_n(z)$ shown in Fig. 11.

$$\bar{\kappa}_0^{(0)}=3,\quad \bar{\kappa}_0^{(1)}=\frac{1}{4}(-5s+5M_P^2+11M_\pi^2),$$
$$\bar{\kappa}_0^{(2)}=\frac{7}{9}(s-M_P^2)^2+\frac{9}{2}M_\pi^2(M_P^2+M_\pi^2-s),$$
$$\bar{\kappa}_0^{(3)}=\frac{721}{144}s^2M_\pi^2-\frac{1442}{144}M_P^2M_\pi^2s-\frac{231}{16}M_\pi^4s+\frac{153}{16}M_\pi^6+\frac{883}{144}M_P^4M_\pi^2+\frac{195}{16}M_P^2M_\pi^4+\frac{9}{16}(M_P^2-s)^3,$$
$$\bar{\kappa}_1^{(0)}=\frac{1}{2},\quad \bar{\kappa}_1^{(1)}=\frac{1}{4}(M_P^2+M_\pi^2-s),$$
$$\bar{\kappa}_1^{(2)}=\frac{1}{6}[(s-M_P^2)^2-M_\pi^2(5s+2M_\pi^2-7M_P^2)],$$
$$\bar{\kappa}_1^{(3)}=\frac{M_\pi^2}{24}[25s^2-(56M_P^2+53M_\pi^2)s+43M_P^4+67M_P^2M_\pi^2-53M_\pi^4]+\frac{1}{8}(M_P^2-s)^3,$$
$$\bar{\kappa}_2^{(0)}=\frac{1}{2},\quad \bar{\kappa}_2^{(1)}=-\frac{1}{4}(s-2M_P^2),$$
$$\bar{\kappa}_2^{(2)}=\frac{1}{6}[s^2-s(3M_P^2+4M_\pi^2)+3(M_P^4+2M_P^2M_\pi^2-M_\pi^4)],$$
$$\bar{\kappa}_2^{(3)}=\frac{M_\pi^2}{12}[11s^2-10s(3M_P^2+2M_\pi^2)+30M_P^4+18M_P^2M_\pi^2-24M_\pi^4]-\frac{1}{8}(s^3-4s^2M_P^2+6sM_P^4-4M_P^6),$$
$$\bar{\kappa}_3^{(0)}=1,\quad \bar{\kappa}_3^{(1)}=M_\pi^2,\quad \bar{\kappa}_3^{(2)}=2M_\pi^4,\quad \bar{\kappa}_3^{(3)}=5M_\pi^6. \tag{5.31}$$

The only nonvanishing coefficients $d_i^{(n)}$ are

$$d_1^{(3)}=\frac{M_\pi^4}{4}\Delta_{P\pi},\qquad d_2^{(2)}=\frac{M_\pi^2}{6}\Delta_{P\pi},$$
$$d_2^{(3)}=\frac{M_\pi^2}{12}(3M_P^2+5M_\pi^2)\Delta_{P\pi}, \tag{5.32}$$

while the nonvanishing coefficients $c_i^{(n)}$ read

$$c_0^{(2)}=-\frac{7}{9}M_\pi^2\Delta_{P\pi},\quad c_0^{(3)}=-\frac{M_\pi^2}{72}(81M_P^2+239M_\pi^2)\Delta_{P\pi},$$
$$c_1^{(1)}=-\frac{1}{2}M_\pi^2,\quad c_1^{(2)}=-\frac{1}{2}M_\pi^2(M_P^2+M_\pi^2),$$
$$c_1^{(3)}=-\frac{1}{4}M_\pi^2(2M_P^4+7M_P^2M_\pi^2+M_\pi^4),$$
$$c_2^{(0)}=-\frac{1}{2},\quad c_2^{(1)}=-\frac{\Delta_{P\pi}}{4},\quad c_2^{(2)}=-\frac{1}{6}(M_P^2+5M_\pi^2)\Delta_{P\pi},$$
$$c_2^{(3)}=-\frac{1}{24}(3M_P^4+34M_P^2M_\pi^2+59M_\pi^4)\Delta_{P\pi}. \tag{5.33}$$

1. S-wave projections

From expression (5.22) for the one-loop S-wave projection, we can extract its dispersive part $\tilde{\psi}_0(s)$ as

$$\tilde{\psi}_0(s)=t_0^{1\text{loop}}(s)-\mathrm{i}\mathrm{Abs}t_0^{1\text{loop}}(s). \tag{5.34}$$

In accord with Eq. (3.13), for $s>4M_\pi^2$, we have $\mathrm{Abs}t_0^{1\text{loop}}(s)=\mathrm{Abs}\mathcal{W}_0^{1\text{loop}}(s)$, where $\mathcal{W}_0^{1\text{loop}}(s)$ denotes the one-loop expression of $\mathcal{W}_0(s)$ constructed through the first iteration in Sec. IV B. Then, using (5.22), we get finally

$$\sigma(s)\tilde{\psi}_0(s)=\frac{\sigma(s)}{16\pi}\left\{16\pi\mathrm{Disp}\mathcal{W}_0^{1\text{loop}}(s)+\frac{C}{F_\pi^4}(s-s_0)^2+\frac{D}{F_\pi^4}\left[\frac{2}{3}K^2(s)+\frac{(s-s_0)^2}{2}\right]\right\}+\frac{1}{\pi}\sum_{i=0}^{3}\left\{\sum_{n=0}^{2}\tilde{w}_+^{(n)}\frac{\kappa_i^{(n)}(s)}{F_\pi^{2n}}+\frac{\mathcal{B}_+}{3F_\pi^4}\frac{s}{F_\pi^2}\frac{\kappa_i^{(1)}(s)-4M_\pi^2\kappa_i^{(0)}(s)}{F_\pi^2}\right\}\tilde{k}_i(s). \tag{5.35}$$

The expression of $\mathrm{Abs}\mathcal{W}_0(s)$ at next-to-leading order involves the product

$$\mathrm{Abs}\mathcal{W}_0(s)\sim\sigma(s)\varphi_0(s)\tilde{\psi}_0(s)\theta(s-4M_\pi^2), \tag{5.36}$$

where $\varphi_0(s)$ is a first-order polynomial in s. The next step consists in constructing a function in the complex-s plane, which has a cut along the positive real axis, and whose discontinuity is given by Eq. (5.36). This is straightforward for the contribution between the first curly brackets in Eq. (5.35) since

$$\sigma(s)\mathrm{Re}\bar{J}(s)=8\pi\mathrm{Im}\bar{J}^2(s). \tag{5.37}$$

For the remaining terms, given by the sum in Eq. (5.35), this can be achieved in the following way. Let us introduce functions defined through dispersive integrals of the functions $\tilde{k}_i(s)$,

$$\tilde{K}_i(s)=\frac{s}{\pi}\int_{4M_\pi^2}^{\infty}\frac{dx}{x}\frac{\tilde{k}_i(x)}{x-s-\mathrm{i}0},$$
$$\tilde{\tilde{K}}_i(s)=\frac{s^2}{\pi}\int_{4M_\pi^2}^{\infty}\frac{dx}{x^2}\frac{\tilde{k}_i(x)}{x-s-\mathrm{i}0}=\tilde{K}_i(s)-s\tilde{K}_i'(0). \tag{5.38}$$

Then, the function

$$
\begin{aligned}
&[\varphi_0 \odot \tilde{\xi}_0](s) \\
&= \frac{1}{16\pi^2 F_\pi^2}[\varphi_0(s)-\varphi_0(0)]\sum_{n=0}^{2}\tilde{w}_+^{(n)}\sum_{i=0}^{3}\kappa_i^{(n)}(s)\tilde{K}_i(s) \\
&+ \frac{1}{16\pi^2 F_\pi^2}\varphi_0(0)\sum_{n=0}^{2}\tilde{w}_+^{(n)}\sum_{i=0}^{3}\left[\kappa_i^{(n)}(s)-d_i^{(n)}\frac{\Delta_{P\pi}^2}{s^2}\right]\tilde{K}_i(s) \\
&+ \frac{s\mathcal{B}_+}{16\pi^2 F_\pi^2}\varphi_0(s)\sum_{i=0}^{3}[\kappa_i^{(1)}(s)-4M_\pi^2\kappa_i^{(0)}(s)]\tilde{K}_i(s) \\
&+ \frac{1}{16\pi^2 F_\pi^2}\varphi_0(0)\sum_{n=0}^{2}\tilde{w}_+^{(n)}\sum_{i=0}^{3}d_i^{(n)}\frac{\Delta_{P\pi}^2}{s^2}\tilde{\tilde{K}}_i(s)
\end{aligned}
\tag{5.39}
$$

has a discontinuity along the positive real axis given by the sum in Eq. (5.35), multiplied by $\varphi_0(s)$. Notice that all the functions $\tilde{k}_i(x)$ are bounded on the real axis by $\ln x$ as $x \to +\infty$ since

$$
\lim_{x\to+\infty}\tilde{k}_i(x) = \left\{\frac{1}{16\pi};\frac{1}{16\pi}\ln\frac{M_\pi^2}{x};\frac{1}{16\pi}\ln\frac{M_\pi^2}{x};-\frac{1}{16\pi}\frac{M_\pi^2}{x}\ln^2\frac{M_\pi^2}{x}\right\}. \tag{5.40}
$$

Therefore, the once-subtracted dispersive integrals in Eq. (5.38) are convergent, and the functions $\tilde{\tilde{K}}_i(s)$ are defined without ambiguity. Actually, the dispersive integral for $\tilde{k}_3(x)$ would already converge without subtraction. Finally, one easily finds expressions in terms of $\bar{J}(s)$ [36,46] for the two first functions, i.e., $\tilde{K}_0(s) = \bar{J}(s)$, and

$$
\tilde{K}_1(s) = \frac{1}{2}\frac{s}{s-4M_\pi^2}\left[16\pi^2\bar{J}^2(s) - 4\bar{J}(s) + \frac{1}{4\pi^2}\right]. \tag{5.41}
$$

2. P-wave projections

The dispersive part of the P-wave projection can be obtained as

$$
\begin{aligned}
\tilde{\psi}_1(s) &= t_1^{1\text{loop}}(s) - \mathrm{i}\mathrm{Abs}t_1^{1\text{loop}}(s) \\
&= t_1^{1\text{loop}}(s) - 2\mathrm{i}K(s)\mathrm{Abs}\mathcal{W}_1^{1\text{loop}}(s),
\end{aligned}
\tag{5.42}
$$

where we used (3.13). Starting from the structure of $\mathrm{Abs}\mathcal{W}_1(s)$, i.e.,

$$
\mathrm{Abs}\mathcal{W}_1(s) \sim \sigma(s)\frac{\varphi_1(s)}{2K(s)}\tilde{\psi}_1(s)\theta(s-4M_\pi^2), \tag{5.43}
$$

one may notice that $\tilde{\psi}_1(s)$ occurs in $\mathrm{Abs}\mathcal{W}_1(s)$ through the combination [$\varphi_1(s)$ is proportional to $s-4M_\pi^2$][13]

$$
\begin{aligned}
\frac{\sigma(s)(s-4M_\pi^2)}{2K(s)}\tilde{\psi}_1(s) &= \frac{\sigma(s)(s-4M_\pi^2)}{32\pi}\left[\mathrm{Disp}\mathcal{W}_1^{1\text{loop}}(s) - \frac{D_x^S}{F_\pi^4}(s-s_0)\right] + \frac{1}{\pi}\sum_{n=0}^{3}\tilde{w}_-^{(n)}\sum_{i=0}^{3}\frac{2\kappa_i^{(n+1)}(s)-3s_0\kappa_i^{(n)}(s)}{F_\pi^{2n}}\frac{s\tilde{k}_i(s)}{\lambda_{P\pi}(s)} \\
&+ \frac{1}{\pi}\sum_{i=0}^{3}\left\{\sum_{n=0}^{3}\tilde{w}_-^{(n)}\frac{\kappa_i^{(n)}(s)}{F_\pi^{2n}} + \frac{\mathcal{B}_-}{3F_\pi^4}[2\kappa_i^{(2)}(s) + (s-3s_0-8M_\pi^2)\kappa_i^{(1)}(s) - 4M_\pi^2(s-3s_0)\kappa_i^{(0)}(s)]\right\}\frac{s^2\tilde{k}_i(s)}{\lambda_{P\pi}(s)},
\end{aligned}
\tag{5.44}
$$

The main difference from the previous case of the S-wave projection lies in the presence of additional polynomial $\lambda_{P\pi}(s)$ in the denominator of the right-hand side. This feature can be handled by writing

$$
\lambda_{P\pi}(s) = (s-M_+^2)(s-M_-^2), \qquad M_\pm = M_P \pm M_\pi, \tag{5.45}
$$

and by using the decomposition of a product of fractions. As a result, we define the additional functions

$$
\begin{aligned}
\tilde{K}_i^{(\lambda)}(s) &= \frac{1}{4}\left[\frac{M_\pi^2}{s-M_+^2}\left(\tilde{K}_i(s) - \frac{s}{M_+^2}\tilde{K}_i(M_+^2)\right)\right. \\
&\left. - \frac{M_\pi^2}{s-M_-^2}\left(\tilde{K}_i(s) - \frac{s}{M_-^2}\tilde{K}_i(M_-^2)\right)\right] \\
&\equiv \frac{s}{\pi}\int_{4M_\pi^2}^{\infty}\frac{dx}{x}\frac{M_P M_\pi^3}{\lambda_{K\pi}(x)}\frac{\tilde{k}_i(x)}{x-s-\mathrm{i}0},
\end{aligned}
\tag{5.46}
$$

which are actually characterized (but not entirely) by the conditions $\tilde{K}_i^{(\lambda)}(0) = 0$ and their absorptive parts along the cut on the positive real axis

$$
\mathrm{Abs}\tilde{K}_i^{(\lambda)}(s) = \frac{M_P M_\pi^3}{\lambda_{K\pi}(s)}\tilde{k}_i(s)\theta(s-4M_\pi^2). \tag{5.47}
$$

[13] In this formula, the second term in the rectangular brackets is present only for $K_S\pi^0 \to \pi^+\pi^-$ scattering; see Appendix D.

Then, the discontinuity along the real positive axis of the function

$$\tilde{\xi}_1(s)=\frac{1}{\pi}\sum_{n=0}^{2}\frac{s\tilde{w}_-^{(n)}}{M_P M_\pi^3}\sum_{i=0}^{3}\tilde{K}_i^{(\lambda)}(s)\frac{2\kappa_i^{(n+1)}+(s-3s_0)\kappa_i^{(n)}(s)}{F_\pi^{2n}}$$
$$+\frac{1}{\pi}\sum_{i=0}^{3}\frac{\mathcal{B}_-}{3}[2\kappa_i^{(2)}(s)+(s-3s_0-8M_\pi^2)\kappa_i^{(1)}(s)$$
$$-4M_\pi^2(s-3s_0)\kappa_i^{(0)}(s)]\frac{s^2}{M_P M_\pi^3 F_\pi^4}\tilde{K}_i^{(\lambda)}(s) \tag{5.48}$$

reproduces the terms displayed in Eq. (5.44).

VI. SECOND ITERATION: $P\to\pi^0\pi^0\pi^0$ WITH $M_\pi\neq M_{\pi^0}$

We next consider the second iteration in the case where the difference between neutral and charged pion masses is taken into account, but for the two processes where all the external pions are neutral, i.e., $K_L\to\pi^0\pi^0\pi^0$ and $\eta\to\pi^0\pi^0\pi^0$. These amplitudes are fully symmetric under exchanges of the three Mandelstam variables, and are described by the polynomial of the form (5.1)

$$\mathcal{P}(s,t,u)=A+\frac{C}{F_\pi^4}[(s-s_0)^2+(t-s_0)^2+(u-s_0)^2]$$
$$+\frac{E}{F_\pi^6}[(s-s_0)^3+(t-s_0)^3+(u-s_0)^3]+\mathcal{O}(E^8) \tag{6.1}$$

and a single function (see Table II) that we call simply $\mathcal{W}_{L,00}(s)$. Its expression at one loop is given in Eq. (4.41). According to (5.3), at two loops, the absorptive part of $\mathcal{W}_{L,00}(s)$ is determined in terms of the dispersive parts of the $\ell=0$ partial-wave projections of the one-loop amplitudes $\mathcal{M}_{00}^L$, $\mathcal{M}_x^L$ and A_{00}, A_x. However, these have now to be calculated for $M_\pi\neq M_{\pi^0}$. Regarding the $\pi\pi$ amplitudes A_{00}, A_x, this has already been done in Ref. [44], where explicit expressions can be found, see Sec. IV A therein. As discussed below, in the case of the amplitudes $\mathcal{M}_{00}^L$ and $\mathcal{M}_x^L$, this calculation does not raise any difficulties of principle, although the resulting formulas become much more complicated than in the case of the equal-mass pions.

A. NLO partial waves of the $P\pi^0\to\pi^0\pi^0$ amplitude

The additional algebraic complexity generated by $M_\pi\neq M_{\pi^0}$ is, in this case, compensated to some extent by the absence of a P-wave. Discarding the contribution from the polynomial part, which is trivial to handle, we need to compute two types of integrals, cf. (4.41). The first type is analogous to the one in Eq. (5.27), but involves now the function $\bar{J}_0(s)$ instead of $\bar{J}$, while at the same time the limits of integration become

$$t_\pm^{\pi^0}(s)=\frac{3s_0^{\pi^0}-s}{2}+\mathcal{K}_{\pi^0;\pm}(s), \tag{6.2}$$

with $s_0^{\pi^0}\equiv M_{\pi^0}^2+M_P^2/3$, and $\mathcal{K}_{\pi^0;\pm}(s)$ is the same function as $\mathcal{K}_\pm(s)$, defined in Eq. (5.25), but with the charged pion mass replaced by the neutral one. The result of this integration is given by the formula (5.27), provided one replaces the functions $\kappa_i^{(n)}(s)$ and $\tilde{k}_i(s)$ by functions $\kappa_{\pi^0;i}^{(n)}(s)$ and $\tilde{k}_i^{\pi^0}(s)$, respectively, obtained from the former upon performing everywhere the substitution $M_\pi\to M_{\pi^0}$, e.g.,

$$\pi\int_{t_-^{\pi^0}(s)}^{t_+^{\pi^0}(s)}dt t^n\bar{J}_0(t)=\frac{2K_{\pi^0}(s)}{\sigma_0(s)}\sum_{i=0}^{3}\kappa_{\pi^0;i}^{(n)}(s)\tilde{k}_i^{\pi^0}(s). \tag{6.3}$$

The second type of integral that is needed is of a new type. It involves the loop function $\bar{J}(s)$ for charged pions, but integrated with the kinematics corresponding to neutral pions. This second integral can also be done analytically, and the result is cast into the form

$$\pi\int_{t_-^{\pi^0}(s)}^{t_+^{\pi^0}(s)}dt t^n\bar{J}(t)=\frac{2K_{\pi^0}(s)}{\sigma_0(s)}\sum_{i=0}^{3}\kappa_{\nabla;i}^{(n)}(s)\tilde{k}_{\nabla;i}(s). \tag{6.4}$$

The set of functions $\tilde{k}_{\nabla;i}(s)$ in terms of which it is expressed differs from the set $\tilde{k}_i(s)$ given in Eq. (5.28). Explicitly, they read

$$\tilde{k}_{\nabla;0}(s)=\frac{1}{16\pi}\sigma_0(s),$$
$$\tilde{k}_{\nabla;1}(s)=\frac{1}{8\pi}\frac{\sigma_0(s)}{M_\pi^2}[t_+^{\pi^0}(s)\sigma_+(s)\ln\tau_+(s)+t_-^{\pi^0}(s)\sigma_-(s)\ln\tau_-(s)],$$
$$\tilde{k}_{\nabla;2}(s)=\frac{1}{8\pi}\sigma(s)s\frac{1}{\lambda_{P\pi}^{1/2}(s)}[t_+^{\pi^0}(s)\sigma_+(s)\ln\tau_+(s)$$
$$-t_-^{\pi^0}(s)\sigma_-(s)\ln\tau_-(s)],$$
$$\tilde{k}_{\nabla;3}(s)=-\frac{1}{16\pi}\frac{M_\pi^2}{\lambda_{P\pi}^{1/2}(s)}[\ln^2\tau_+(s)-\ln^2\tau_-(s)], \tag{6.5}$$

with $\sigma_\pm(s)\equiv\sigma(t_\pm^{\pi^0}(s))$ and, likewise, $\tau_\pm(s)\equiv\tau(t_\pm^{\pi^0}(s))$, where

$$\tau_\pm(s)=\frac{\sigma_\pm(s)-1}{\sigma_\pm(s)+1}. \tag{6.6}$$

In the limit $M_{\pi^0}\to M_\pi$, one recovers the previous set of functions:

$$\tilde{k}_{\nabla;0}(s)\to\tilde{k}_0(s),\qquad \tilde{k}_{\nabla;3}(s)\to\tilde{k}_3(s),$$
$$\tilde{k}_{\nabla;1}(s)\to\left(\frac{3s_0-s}{M_\pi^2}-4\frac{\Delta_{P\pi}}{s}\right)\tilde{k}_1(s)-\frac{\lambda_{P\pi}(s)}{sM_\pi^2}\tilde{k}_1(s),$$
$$\tilde{k}_{\nabla;2}(s)\to\tilde{k}_1(s)+\left(1-\frac{\Delta_{P\pi}}{M_\pi^2}\right)\tilde{k}_2(s). \tag{6.7}$$

As for the functions $\kappa^{(n)}_{\nabla;i}(s)$, one has $\kappa^{(n)}_{\nabla;3}(s)=\kappa^{(n)}_{3}(s)$, and the remaining ones are given by

$$\begin{aligned}
\kappa^{(0)}_{\nabla;0}&=3,\quad \kappa^{(1)}_{\nabla;0}=\frac{1}{4}(-5s+5M_P^2+15M_{\pi^0}-4M_\pi^2),\\
\kappa^{(2)}_{\nabla;0}&=\frac{7}{9}(s-M_P^2)^2-\frac{7}{9}M_{\pi^0}^2\frac{\Delta^2_{P\pi^0}}{s}-\frac{1}{6}[(s-M_P^2)(28M_{\pi^0}^2-M_\pi^2)\\
&\quad+12M_\pi^4+3M_\pi^2M_{\pi^0}^3-42M_{\pi^0}^4],\\
\kappa^{(3)}_{\nabla;0}&=\frac{9}{16}(3s_0^{\pi^0}-s)^3-\frac{M_\pi^2}{18}(3s_0^{\pi^0}-s)^2-\frac{5}{12}M_\pi^4(3s_0^{\pi^0}-s)\\
&\quad-5M_\pi^6-\frac{9}{8}M_{\pi^0}^2(3s_0^{\pi^0}-s)\frac{\Delta^2_{P\pi^0}}{s}+\frac{1}{18}M_\pi^2M_{\pi^0}^2\frac{\Delta^2_{P\pi^0}}{s},\\
\kappa^{(0)}_{\nabla;1}&=0,\quad \kappa^{(1)}_{\nabla;1}=\frac{M_\pi^2}{8},\\
\kappa^{(2)}_{\nabla;1}&=\frac{M_\pi^2}{12}(M_\pi^2+2M_{\pi^0}^2-s),\\
\kappa^{(3)}_{\nabla;1}&=\frac{M_\pi^2}{16}(s-3s_0^{\pi^0})^2+\frac{M_\pi^4}{24}(s-3s_0^{\pi^0})\\
&\quad-\frac{5}{24}M_\pi^6-\frac{1}{16}M_\pi^2M_{\pi^0}^2\frac{\Delta^2_{P\pi^0}}{s},\\
\kappa^{(0)}_{\nabla;2}&=\frac{1}{2},\quad \kappa^{(1)}_{\nabla;2}=-\frac{1}{8}(s-M_P^2+4M_\pi^2-3M_{\pi^0}^2),\\
\kappa^{(2)}_{\nabla;2}&=\frac{1}{12}(s-3s_0^{\pi^0})^2-\frac{1}{6}M_{\pi^0}^2\frac{\Delta^2_{P\pi^0}}{s}\\
&\quad+\frac{M_\pi^2}{12}(s-M_P^2-3M_{\pi^0}^2-12M_\pi^2),\\
\kappa^{(3)}_{\nabla;2}&=\frac{1}{16}(3s_0^{\pi^0}-s)^3-\frac{M_\pi^2}{24}(3s_0^{\pi^0}-s)^2-\frac{5}{24}M_\pi^4(3s_0^{\pi^0}-s)\\
&\quad-\frac{5}{2}M_\pi^6-\frac{3}{16}M_{\pi^0}^2(3s_0^{\pi^0}-s)\frac{\Delta^2_{P\pi^0}}{s}+\frac{1}{12}M_\pi^2M_{\pi^0}^2\frac{\Delta^2_{P\pi^0}}{s}.
\end{aligned}\tag{6.8}$$

We were not able to find simpler expressions for the functions $\tilde{k}_{\nabla;i}(s)$, i.e., comparable to those given in Eq. (5.28). The origin of the difficulty can, for instance, be understood upon considering the square of the functions $\sigma_\pm(s)$,

$$\sigma^2_\pm(s)=\frac{s}{s-4M_{\pi^0}^2}\frac{M_\pi^2}{M_{\pi^0}^2}\left(\frac{s-4M_{\pi^0}^2\pm 2\mathcal{K}_{\pi^0}(s)}{\Delta_{P\pi^0}}\right)^2-\frac{\Delta_\pi}{M_{\pi^0}^2}\left(1-\frac{4M_{\pi^0}^2}{s}\right),\tag{6.9}$$

and comparing it to the expression for $\sigma_{T_\pm}(s)$ given in Eq. (B22): as $\Delta_\pi\to 0$, $\sigma_\pm(s)\to 1/\sigma_{T_\pm}(s)$, but no such simple expression is available when $\Delta_\pi\neq 0$.

B. NLO S-wave projection of the $P\pi^0\to\pi^+\pi^-$ amplitude

The one-loop representation of the $P\pi^0\to\pi^+\pi^-$ amplitude is given by Eqs. (4.38) and (4.40). In order to obtain the corresponding S-wave projection, we need to compute the contour integrals involving the functions $\bar{J}_{\pm 0}$ with the end points given by

$$t^x_\pm(s)=\frac{3s_0^x-s}{2}+\mathcal{K}_{x;\pm}(s),\tag{6.10}$$

where now $3s_0^x=M_P^2+M_{\pi^0}^2+2M_\pi^2$ and

$$\mathcal{K}_{x;\pm}(s)=\begin{cases}\mp|K_x(s)|, & s>M_{+x}^2\\ \pm i|K_x(s)|, & M_{+x}^2>s>M_{-x}^2\\ \pm|K_x(s)|\pm i\delta, & M_{-x}^2>s>\frac{M_\pi}{M_\pi+M_{\pi^0}}\Delta_{P\pi^0}\\ \pm|K_x(s)|+i\delta, & \frac{M_\pi}{M_\pi+M_{\pi^0}}\Delta_{P\pi^0}>s>4M_\pi^2\end{cases}.\tag{6.11}$$

Here, $M_{\pm x}=M_P\pm M_{\pi^0}$, and $K_x(s)$ is the corresponding Kacser's function, given by

$$K_x^2(s)=\frac{1}{4}\left(1-\frac{4M_\pi^2}{s}\right)\lambda_{P\pi^0}(s).\tag{6.12}$$

Since for $s>4M_\pi^2$ the path corresponding to the movement of $t^x_\pm(s)$ in the complex t plane does not cross the cut of the function $\bar{J}_{\pm 0}(t)$, the contour integrals can be again calculated as the differences of the corresponding primitive functions at the above end points, as described in Appendix B. In analogy with (6.4), we express them in terms of elementary functions $\tilde{k}_{+;i}(s)$ as

$$\pi\int_{t^x_-(s)}^{t^x_+(s)}dt t^n\bar{J}(t)=\frac{2K_x(s)}{\sigma(s)}\sum_{i=0}^{3}\kappa^{(n)}_{+;i}(s)\tilde{k}_{+;i}(s).\tag{6.13}$$

The explicit form of the latter functions reads

$$\begin{aligned}
\tilde{k}_{+;0}(s)&=\frac{1}{16\pi}\sigma(s),\qquad \tilde{k}_{+;1}(s)=\frac{1}{16\pi}L(s),\\
\tilde{k}_{+;2}(s)&=\frac{1}{16\pi}\sigma(s)s\frac{M(s)}{\lambda^{1/2}_{P\pi^0}(s)},\\
\tilde{k}_{+;3}(s)&=-\frac{1}{16\pi}\frac{\Sigma_\pi}{2}\frac{M(s)}{\lambda^{1/2}_{P\pi^0}(s)}L(s),\\
\tilde{k}_{+;4}(s)&=-\frac{1}{16\pi}\Delta_\pi\frac{\mathcal{J}(\tau^x_+(s))-\mathcal{J}(\tau^x_-(s))}{\lambda^{1/2}_{P\pi^0}(s)},
\end{aligned}\tag{6.14}$$

where $\Sigma_\pi\equiv M_\pi^2+M_{\pi^0}^2$, $\Delta_\pi\equiv M_\pi^2-M_{\pi^0}^2$, and the functions $L(s)$ and $\sigma_(s)$ are given by (5.9) and (4.14), respectively. In the above formulas,

$$\tau^x_\pm(s)=\frac{\sigma_{\pm 0}(t^x_\pm(s))-1}{\sigma_{\pm 0}(t^x_\pm(s))+1},\qquad \sigma_{\pm 0}(t)=\sqrt{\frac{t-(M_\pi+M_{\pi^0})^2}{t-(M_\pi-M_{\pi^0})^2}}.\tag{6.15}$$

In the limit of equal-mass pions, we recover the functions $\tilde{k}_i$, namely, $\tilde{k}_{+;i}(s) \to \tilde{k}_i(s)$ for $i = 1, \ldots, 3$. The new function $\tilde{k}_{+;4}(s)$, which vanishes in the limit $M_{\pi^0} \to M_\pi$, is defined in terms of the function $\mathcal{J}(\tau)$,

$$\mathcal{J}(\tau) = \log\frac{M_{\pi^0}}{M_\pi}\log\tau + \mathrm{Li}_2\left(1-\frac{M_{\pi^0}}{M_\pi}\tau\right) - \mathrm{Li}_2\left(1-\frac{M_\pi}{M_{\pi^0}}\tau\right). \tag{6.16}$$

Here, we assume the standard definition of the dilogarithm, with a cut along the interval $(1,\infty)$ of the real axis and $\mathrm{Li}_2(x) = \mathrm{Li}_2(x - \mathrm{i}0)$ for $x > 1$. Let us denote for short

$$\xi = \frac{M_\pi^2}{\Delta_\pi}\frac{\Delta_{P\pi^0}^2}{\Delta_{P\pi^+}^2}. \tag{6.17}$$

Then, the rational functions $\kappa_{+;i}^{(n)}(s)$ are given by

$$\kappa_{+;0}^{(-2)} = -\frac{1}{2\Delta_{P\pi^+}\Delta_\pi}\frac{s}{s-\xi}\log\frac{M_{\pi^0}}{M_\pi}\left(\frac{s}{s-\xi}\frac{s-2\Sigma_\pi-\Delta_{P\pi^0}}{\Delta_{P\pi^+}}+1\right), \quad \kappa_{+;0}^{(-1)} = -\frac{1}{\Delta_{P\pi^+}}\frac{s}{s-\xi}\frac{\Sigma_\pi}{\Delta_\pi}\log\frac{M_{\pi^0}}{M_\pi},$$

$$\kappa_{+;0}^{(0)} = 2-\frac{\Sigma_\pi}{\Delta_\pi}\log\frac{M_{\pi^0}}{M_\pi}, \quad \kappa_{+;0}^{(1)} = \frac{1}{4}[3(M_P^2-s)+4M_\pi^2+M_{\pi^0}^2] - \frac{1}{2}\frac{\Sigma_\pi}{\Delta_\pi}\log\frac{M_{\pi^0}}{M_\pi}\left(8\frac{M_\pi^2M_{\pi^0}^2}{\Sigma_\pi}+\Delta_{P\pi^0}-s\right),$$

$$\kappa_{+;0}^{(2)} = \frac{1}{36}\left[16s^2 - s(32\Delta_{P\pi^0}+61\Sigma_\pi) + 16\Delta_{P\pi^0}^2 + \Delta_{P\pi^0}^2(77M_\pi^2+45M_{\pi^0}^2) + 4(9\Sigma_\pi^2+4M_\pi^2M_{\pi^0}^2) - 16M_\pi^2\frac{\Delta_{P\pi^0}^2}{s}\right]$$
$$-\frac{1}{6}\frac{\Sigma_\pi}{\Delta_\pi}\log\frac{M_{\pi^0}}{M_\pi}\left[2s^2+2\Delta_{P\pi^0}^2 - s\left(4\Delta_{P\pi^0}+5\Sigma_\pi+12\frac{M_\pi^2M_{\pi^0}^2}{\Sigma_\pi}\right) + \Delta_{P\pi^0}\left(3\Sigma_\pi+4\frac{M_\pi^2+4M_{\pi^0}^2}{\Sigma_\pi}\right) + 32M_\pi^2M_{\pi^0}^2 - 3M_\pi^2\frac{\Delta_{P\pi^0}^2}{s}\right],$$

$$\kappa_{+;1}^{(-2)} = \frac{1}{2\Delta_{P\pi^+}\Delta_\pi}\frac{1}{s-\xi}\left[\frac{s}{2} - \frac{2\Delta_{P\pi^0}M_\pi^2 - s\Delta_\pi}{\Delta_\pi}\left(\frac{\Sigma_\pi}{\Delta_\pi} - \frac{s}{s-\xi}\frac{s-2\Sigma_\pi-\Delta_{P\pi^0}}{\Delta_{P\pi^+}}\right)\right], \quad \kappa_{+;1}^{(-1)} = \frac{2\Delta_{P\pi^0}M_\pi^2 - s\Delta_\pi}{2\Delta_{P\pi^+}\Delta_\pi(s-\xi)}, \quad \kappa_{+;1}^{(0)} = \frac{1}{2},$$

$$\kappa_{+;1}^{(1)} = \frac{1}{4s}(s-2M_\pi^2)(\Delta_{P\pi^0}-s), \quad \kappa_{+;1}^{(2)} = \frac{1}{12}\left\{(s-\Delta_{P\pi^0})\left[2s+2\frac{\Delta_{P\pi^0}}{s} - 6\frac{\Delta_{P\pi^+}}{s} - (2M_P^2+9M_\pi^2+3M_{\pi^0}^2)\right] - 2M_{\pi^0}^2\frac{\Delta_{P\pi^0}}{s}\right\},$$

$$\kappa_{+;2}^{(-2)} = \frac{1}{4\Delta_{P\pi^+}\Delta_\pi}\left[s-\Delta_{P\pi^0} + \frac{\Delta_{P\pi^0}\Sigma_\pi - s\Delta_\pi}{\Delta_\pi}\left(\frac{\Sigma_\pi}{\Delta_\pi} - \frac{s}{s-\xi}\frac{s-2\Sigma_\pi-\Delta_{P\pi^0}}{\Delta_{P\pi^+}}\right)\right], \quad \kappa_{+;2}^{(-1)} = -\frac{\Delta_{P\pi^0}\Sigma_\pi - s\Delta_\pi}{2\Delta_{P\pi^+}\Delta_\pi(s-\xi)},$$

$$\kappa_{+;2}^{(0)} = \frac{1}{2}\left(1-\frac{\Delta_{P\pi^0}}{s}\right), \quad \kappa_{+;2}^{(1)} = -\frac{1}{4}\left(s-2M_P^2+\frac{\Delta_{P\pi^0}}{s}\right),$$

$$\kappa_{+;2}^{(2)} = \frac{1}{12}\left\{6M_{\pi^0}^2\Sigma_\pi\frac{\Delta_{P\pi^0}^2}{s} + \left(1-\frac{\Delta_{P\pi^0}}{s}\right)\left[2s^2 - s(4M_P^2+5\Sigma_\pi) + 2\Delta_{P\pi^0}^2\right.\right.$$
$$\left.\left. + \Delta_{P\pi^0}(7M_\pi^2+3M_{\pi^0}^2) + 6M_{\pi^0}^2\Sigma_\pi + 2(3M_{\pi^0}^2\Sigma_\pi - M_\pi^2\Delta_{P\pi^0})\frac{\Delta_{P\pi^0}}{s}\right]\right\}, \quad \kappa_{+;3}^{(-2)} = 0, \quad \kappa_{+;3}^{(-1)} = -\frac{1}{\Sigma_\pi}, \quad \kappa_{+;3}^{(0)} = 1,$$

$$\kappa_{+;3}^{(1)} = 2\frac{M_\pi^2M_{\pi^0}^2}{\Sigma_\pi}, \quad \kappa_{+;3}^{(2)} = 2M_\pi^2M_{\pi^0}^2, \quad \kappa_{+;4}^{(-2)} = 2\frac{M_\pi^2M_{\pi^0}^2}{\Delta_\pi^4}, \quad \kappa_{+;4}^{(-1)} = \frac{\Sigma_\pi}{\Delta_\pi^2}, \quad \kappa_{+;4}^{(0)} = -1, \quad \kappa_{+;4}^{(1)} = \kappa_{+;4}^{(2)} = 0. \tag{6.18}$$

Let us note that the single and the double poles that appear in the coefficients $\kappa_{+;i}^{(n)}$ for $s = \xi$ for $n < 0$, are in fact spurious artifacts corresponding to the partition of the integrals in Eq. (6.13) into the individual terms. In the full sum on the right-hand side of (6.13), the various pole contributions cancel each other. Note also that the analogous integrals which are necessary for the calculation of the dispersive parts of the NLO partial-wave projections of the pion scattering amplitudes A_{00} and A_x, and which are given explicitly in Sec. IV B of Ref. [44], can be formally obtained from the above formulas in the limit $M_P \to M_{\pi^0}$. This limit requires, however, enlarging the definition of the function $L(s)$ to the region $4M_{\pi^0}^2 < s < 4M_\pi^2$, namely, to set in this region

$$L(s) = \log(1-\sigma(s)) - \log(1+\sigma(s)), \tag{6.19}$$

where we assume the principal branch of the logarithm with a cut on the interval $(-\infty, 0)$ along the real axis, and $\log(x) = \log(x + \mathrm{i}0)$ for $x < 0$.

Using the above results for the integrals (6.3), (6.4), and (6.13), it is now a straightforward task to calculate the corresponding S-wave projections of the amplitudes $\mathcal{M}_{00}^L$, $\mathcal{M}_x^L$ at NLO and, with the help of (5.3), to construct the absorptive part of the function $\mathcal{W}_{00}$. The construction of the full two-loop amplitude $\mathcal{M}_{00}^L$ then proceeds along the same lines as in the case of equal-mass pions described in detail in the previous section. Despite the higher algebraic complexity, from a numerical perspective, the dispersive

integrals similar to the ones that define the functions $\tilde{K}_i(s)$, but now featuring the functions $\tilde{k}_{\nabla;i}(s)$ and $\tilde{k}_{+;i}(s)$ in the role of absorptive parts, present no particular problem.

VII. CONCLUSIONS

The primary purpose of this study was to present a detailed account of the dispersive approach to the construction of $P\pi \to \pi\pi$, $P = K^{\pm}, K_L, K_S, \eta$, scattering amplitudes that possess all the correct analytic properties at the order two loops in the low-energy expansion. It generalizes the representation of the two-loop $\pi\pi$ amplitudes first constructed in Ref. [45] to the case where the masses are distinct, and with one of the mesons (P) unstable through decay into three pions. As compared to $\pi\pi$ scattering, this last aspect makes the discussion of the analytic properties significantly more involved. We have, therefore, tried to provide the necessary information on these aspects. Most notably, we have extended the existing discussions [79,85] to the case where the charged and the neutral pions have different masses. The most remarkable feature is the apparition of an anomalous threshold as soon as the final state contains charged pions. This requires a modification of both the dispersion relations that provide the starting point of our construction and of the manner in which the projection on the partial waves of the one-loop amplitudes is performed. We plan to come back to these delicate issues in a forthcoming paper.

We would like to point out that our approach applies as soon as an expansion under which the counting rules (3.10) are valid is available. This is, in particular, the case of the combined chiral and $1/N_C$ expansion [56,86,87]. Within this framework, our construction would apply to further processes, like $\eta' \to \eta\pi\pi$, which was recently studied in high-precision experiments [88–90].

From a practical point of view, the two-loop amplitudes constructed this way depend on a certain number of subtraction constants, which can be put in one-to-one correspondence with the Dalitz-plot parameters (slopes and curvatures). These representations could, therefore, be used in order to analyze experimental high-statistics data for the decay distribution of the $P \to \pi\pi\pi$ processes. The number of parameters to be fitted, for instance, is the same as in the usual Dalitz-plot expansions, but the inclusion of the correct analytic properties might allow for better fits. Alternatively, these representations can also be useful in order to extract information on fundamental quantities, like the quark-mass ratio R, or the $\pi\pi$ scattering lengths, from the data. In the former case, we have already illustrated this in Ref. [36], and we plan to redo a similar analysis using more recent high-statistics data on the Dalitz-plot distribution of $\eta \to \pi\pi\pi$ [15–18].

ACKNOWLEDGMENTS

This work is supported in part by Grant No. 40652ZE, financed by the French Ministry of Foreign Affairs and the French Ministry for Higher Education, Research and Innovation, and by Grant No. 8J18FR039, financed by the Czech Ministry of Education, Youth and Sports, both within the framework of the bilateral PHC Barrande Mobility Program 2018, and by the Czech Science Foundation Project No. GACR 18-17224S. We also acknowledge useful discussions with J. Gasser, B. Kubis, H. Leutwyler, and E. Passemar.

APPENDIX A: ANOMALOUS THRESHOLDS

In this Appendix, we summarize the analysis of the physical-sheet singularities of the diagrams with the "fish" topology; see Fig. 3. Whereas the analysis of Refs. [79,85] addresses the situation where all the pions have the same mass, the more general analysis presented here holds for any combinations, allowed by conservation of the electric charge, of charged and neutral pions as external and internal states. This analysis rests on the study of the Landau singularities [91,92], which is summarized in the monography [77]. For more details of this analysis, we also refer to Ref. [55].

We first recall that, as far as the structure of the singularities is concerned, one can consider the following dispersive representation of the fish diagram in terms of the standard triangle diagram [85,93],

$$\int_{\mu_0^2}^{\infty} d\mu^2 \rho(\mu^2) \int \frac{\mathrm{d}^4 q_1}{(2\pi)^4} \frac{1}{(k_1^2 - m_1^2)(k_2^2 - m_2^2)(k_3^2 - \mu^2)}, \quad \text{(A1)}$$

where the possible values of μ_0 are $2M_{\pi^0}$, $M_\pi + M_{\pi^0}$, or $2M_\pi$. The precise form of the spectral density $\rho(\mu^2)$ is not important here. It suffices to know that it provides an adequate renormalization of the ultraviolet divergence in the subgraph, but brings in no further singularity, the only additional singularity being a possible end point singularity at the lower end of the μ^2 integration. After the introduction of Feynman parameters and integration over q_1, one obtains an integrand whose denominator $\mathcal{D}$ reads [94,95]

$$-\mathcal{D} = \beta^T Y \beta - i\epsilon, \quad \text{(A2)}$$

where $\beta^T = (\beta_1, \beta_2, \beta_3)$, $0 \le \beta_i \le m_i$, and Y is the symmetric 3×3 matrix with entries

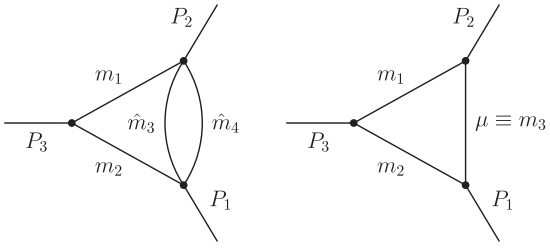

FIG. 3. The general diagram with the fish topology (left) and its reduction to the corresponding triangle diagram (right).

$$y_{ii}=1, \quad y_{ij}=\frac{m_i^2+m_j^2-P_k^2}{2m_i m_j}, \quad i\neq j, \quad k\neq i,j. \tag{A3}$$

In what follows, the masses m_i are real and strictly positive numbers. The virtualities P_k^2 of the external lines can be arbitrary complex numbers. Then, the path of integration over the β_i variables need not be distorted if one of the y_{ij}, $i\neq j$, is kept real, while the remaining two are given negative imaginary parts. In this setting, the $i\epsilon$ contribution to $\mathcal{D}$ is not necessary, provided $\mathcal{D}$ is defined as the boundary value when these imaginary parts tend to zero [77].

The Landau conditions [91,92] read

$$\beta_i\frac{\partial\mathcal{D}}{\partial\beta_i}=0 \quad \text{for each internal line } i=1,2,3, \tag{A4}$$

$$\mathcal{D}=0. \tag{A5}$$

The first three equations can be rewritten as

$$\begin{pmatrix}\beta_1 & 0 & 0\\ 0 & \beta_2 & 0\\ 0 & 0 & \beta_3\end{pmatrix} Y\beta=0. \tag{A6}$$

The leading Landau singularity (LLS), corresponding to $\beta_1\beta_2\beta_3\neq 0$, is then given by the condition

$$\det Y = 1+2y_{12}y_{23}y_{31}-y_{12}^2-y_{23}^2-y_{31}^2=0. \tag{A7}$$

The nonleading Landau singularities (NLLSs), corresponding to the vanishing of exactly one β_i, require $y_{jk}=\pm 1$, $j\neq k$, $i\neq j,k$. They represent both normal and anomalous thresholds. Finally, the second-type (or non-Landau) singularity (NLS) curve is given by

$$\lambda(P_1^2,P_2^2,P_3^2)=0. \tag{A8}$$

Not all the singularities derived from the Landau conditions do occur on the physical sheet. Before starting a more detailed analysis for the identification of the physical-sheet Landau singularities, it is useful to identify the domains where $\mathcal{D}$ never vanishes in the undistorted region of parametric integration. Apart from the case already mentioned, when two y_{ij} variables are given negative imaginary parts, such singularity-free domains are, for instance,

(i) SF1: domains where all the y_{ij} are real and positive; this means (for all $m_i>0$) that all $P_k^2\leq m_i^2+m_j^2$;
(ii) SF2: domains where, simultaneously, one of the variables y_{ij}, $i\neq j$, is greater than unity, a second one is greater than zero, and the third one strictly greater than -1.

We will split the discussion upon considering two types of triangle diagrams; see Fig. 4. In the first one, we will call it a π-diagram, the on-shell conditions for the external lines are, say, $P_i^2=M_i^2$, $i=1,2$, where M_1 and M_2 are not necessarily equal, but correspond to a pion mass, M_π or M_{π^0}, whereas $P_3^2=s$ is a free variable. The second case corresponds to, say, $P_2^2=M_P^2$, whereas $P_1^2=M_1^2$ and $P_3^2=s$ are as before. We refer to this situation as a P-diagram. In both cases, the internal lines are restricted to neutral or charged pions. A brief discussion of other intermediate states is to be found at the end of this Appendix. Furthermore, since we are interested in the singularities as s varies in the complex plane, all other quantities, like M_1 and M_2 will be kept at their physical values, unless we are forced to modify them. In particular, unless unavoidable, we will keep the integration over μ^2 fixed to occur along the straight line $\mu^2\geq\mu_0^2$ on the real axis. Since in any case we have $\mu^2\geq 4M_{\pi^0}^2>\Delta_\pi$, we observe that the condition

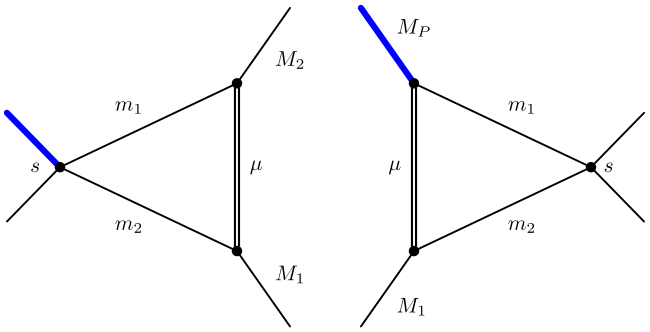

FIG. 4. The two types of fish/triangle diagrams contributing to the $P\pi\to\pi\pi$ amplitudes. On the left diagram, the heavy external meson line is combined with an external pion line into the kinematic variable s (π-diagram). On the right diagram, the heavy meson line is an isolated external line (P-diagram). All external and internal lines are charged or neutral pion lines, except for the thick external line corresponding to the P meson, and the internal double line, which denotes to the dispersive loop corresponding to the exchange of a pion pair.

$$y_{23}\equiv\frac{m_2^2+\mu^2-M_1^2}{2m_2\mu}>0 \tag{A9}$$

is always satisfied.

1. Physical-sheet singularities of the π-diagrams

The analysis for the π-diagrams, which, since the momentum of the meson P is hidden inside the variable s, will also hold for $\pi\pi$ scattering, turns out to be quite straightforward. Indeed, in this case, we also have

$$y_{13}\equiv\frac{m_1^2+\mu^2-M_2^2}{2m_1\mu}>0. \tag{A10}$$

Combined with the conditions (A9) and SF1, we at once conclude that we need to worry only about the singularities occurring for $s>m_1^2+m_2^2$.

Next, conservation of the electric charge tells us either that $M_1 = M_2$ and $m_1 = m_2$ hold simultaneously or that $M_1 \neq M_2$ and $m_1 \neq m_2$ hold simultaneously. It leads only to four possibilities for the charge assignments of the corresponding states:

(i) $M_1 = M_2 = m_1 = m_2 \equiv M$: Then, we study the amplitudes with fixed $\mu \geq 2M_{\pi^0}$, and the singularity-safe domain for the physical amplitude is for $s \leq 2M^2$. The LLS occurs for $s=0$ and $s = 4M^2 - \mu^2$. The NLLSs are $s = 0$ and $s = 4M^2$ from $y_{12} = \pm 1$, and $\mu^2 = 4M^2$ from $y_{13,23} = +1$, the case $y_{13,23} = -1$ being excluded for positive masses, cf. Eqs. (A9) and (A10). There appears no new singularity from pinching at infinity, Eq. (A8). At $\mu^2 = 4M^2$, there is no singularity on the physical sheet. As expected, it means that the only relevant singularities are in s, and since only the normal threshold singularity $s = 4M^2$ does not belong to the safe region in s, the only relevant singularity for the physical amplitudes is this normal threshold.

(ii) $M_1 = M_2 \equiv M$, $m_1 = m_2 \equiv m$, $M \neq m$: μ is fixed with $\mu \geq m + M = M_{\pi^0} + M_{\pi^\pm}$, so that $y_{13} \geq 1$, $y_{23} \geq 1$ and the condition SF2 is satisfied for $s < 4m^2$. Therefore, physical-sheet singularities only occur for $s \geq 4m^2$. On the other hand, the possible singular points are the LLS at

$$s = 0, \quad \text{or} \quad s = -\frac{\lambda(\mu^2, m^2, M^2)}{\mu^2} < 0 \tag{A11}$$

and the NLLSs at $s = 0$, $s = 4m^2$ (from $y_{12} = \pm 1$), or for $\mu^2 = (M \pm m)^2$, and finally, there appears, in addition, a NLS at $s = 4M^2$. Therefore, in this case, in addition to the normal threshold $s = 4m^2$, there occurs a NLS at $s = 4M^2$, i.e., at the beginning of the physical region, provided $M = M_{\pi^\pm}$ and $m = M_{\pi^0}$.

(iii) $M_1 = m_1 = M_{\pi^\pm}$, $M_2 = m_2 = M_{\pi^0}$: again $\mu \geq M_{\pi^0} + M_{\pi^\pm}$, and no singularity appears on the physical sheet for $s < (M_{\pi^\pm} + M_{\pi^0})^2$. All the possible singularities are

$$s = \frac{\Delta_\pi^2}{\mu^2}, \qquad s = 2\Sigma_\pi - \mu^2, \tag{A12}$$

both bounded from above by $(M_\pi - M_{\pi^0})^2$, from the LLS and

$$s = (M_\pi \pm M_{\pi^0})^2, \qquad \mu^2 = (M_\pi \pm M_{\pi^0})^2 \tag{A13}$$

from the NLLSs and NLS. Thus, on the physical sheet, we find only the normal threshold singularity at $s = (M_\pi + M_{\pi^0})^2$.

(iv) $M_1 = m_2 = M_{\pi^\pm}$, $M_2 = m_1 = M_{\pi^0}$: $\mu \geq 2M_{\pi^0}$, $y_{13} \geq 1$, $y_{23} > 0$, and thus no singularity occurs on the physical sheet for $s < (M_{\pi^\pm} + M_{\pi^0})^2$. The singularities in this case read

$$s = \Sigma_\pi - \frac{\mu^2}{2} \pm \frac{\sqrt{(\mu^2 - 4M_{\pi^\pm}^2)(\mu^2 - 4M_{\pi^0}^2)}}{2} \tag{A14}$$

from the LLS, with both solutions smaller than $\Sigma_\pi < (M_{\pi^\pm} + M_{\pi^0})^2$ whenever they are real, and

$$s = (M_\pi \pm M_{\pi^0})^2, \quad \mu^2 \in \{0, 4M_\pi^2, 4M_{\pi^0}^2\} \tag{A15}$$

from the NLLSs, with no new constraint from the NLS. The only singularity lying on the physical sheet is the normal threshold $s = (M_\pi + M_{\pi^0})^2$.

In conclusion, the only π-diagram where there appears an anomalous threshold on the physical sheet is the diagram with $M_1 = M_2 = M_{\pi^\pm}$, $m_1 = m_2 = M_{\pi^0}$, and $\mu_0 = M_{\pi^\pm} + M_{\pi^0}$, which has a non-Landau singularity at $s = 4M_{\pi^\pm}^2$, close to the beginning of the physical region $s \geq 4M_{\pi^0}^2$.

2. Physical-sheet singularities of the *P*-diagrams

We next consider the second type of diagrams from Fig. 4, which we call P-diagrams and which needs more careful analysis. Since $\mu_0 \geq 2M_{\pi^0} > \Delta_\pi$, the condition (A9) is always satisfied. The singularities are most conveniently discussed through their localization on curves lying in the (M_P^2, s) plane.

In the following, we denote $M_1 \equiv m_5$. For the LLS, we obtain from Eq. (A7) ($\Delta_{25} = m_2^2 - m_5^2$, $\Delta_{P1} = M_P^2 - m_1^2$)

$$\begin{aligned}\Sigma\colon\ 2\mu^2 s = &-\mu^4 + \mu^2(M_P^2 + m_1^2 + m_2^2 + m_5^2) + \Delta_{25}\Delta_{P1} \\ &\pm \lambda^{1/2}(\mu^2, M_P^2, m_1^2)\lambda^{1/2}(\mu^2, m_2^2, m_5^2).\end{aligned} \tag{A16}$$

The subleading singularities read

$$\begin{aligned}\sigma_{s\pm}\colon\ & s = (m_1 \pm m_2)^2, \\ \sigma_{P\pm}\colon\ & M_P^2 = (\mu \pm m_1)^2, \\ \sigma_{\mu\pm}\colon\ & \mu^2 = (m_2 \pm m_5)^2.\end{aligned} \tag{A17}$$

The second-type singularity may occur on the curve

$$\Gamma\colon\ s = (M_P \pm m_5)^2. \tag{A18}$$

As before, in the end, we are interested in the analytic properties in s with M_P and all the other masses fixed at their physical value. However, in the case $M_P > 3M_\pi$, we need to perform an analytic continuation in some other variable from the values where the diagram is analytic. Inspired by the analysis of Kacser and Bronzan [68,79], we start by considering an analytic continuation in the external variables P_i^2, and we deform the integration contour in μ

from the original line $\mu \geq \mu_0$ only when forced to do so. The singularity curve $\sigma_{\mu-}$ is, therefore, again irrelevant, and the curve $\sigma_{\mu+}$, corresponding to the anomalous subleading threshold, can be avoided, in the cases of interest here, by the addition of a small imaginary part to μ^2 without any change of the analytic structure in s.

For the diagrams under consideration, the domains where the β integrations do not need to be deformed from the original physical integration contour are the following:

(a) Im$s > 0$ together with Im$M_P^2 > 0$.
(b) SF1 holds; the condition (A9) holds automatically, and the domain $y_{12}, y_{13} \geq 0$ corresponds to $s \leq m_1^2 + m_2^2$ together with $M_P^2 \leq \mu^2 + m_1^2$.
(c) SF2 holds; this happens, in particular, when
-(c1) $\mu \geq (m_5 + m_2)$ and $M_P^2 \leq \mu^2 + m_1^2$; we can go with s up to $s < (m_1 + m_2)^2$;
-(c2) $\mu \geq (m_5 + m_2)$, $M_P^2 < (\mu + m_1)^2$, and $s \leq m_1^2 + m_2^2$;
-(c3) $M_P^2 \leq (\mu - m_1)^2$, and $s < (m_1 + m_2)^2$;
-(c4) $M_P^2 \leq (\mu + m_1)^2$, and $s \leq (m_1 - m_2)^2$.

Therefore, we see that the anomalous thresholds σ_{s-} and σ_{P-} bring no singularity to the physical sheet, but for $M_P > 3M_\pi$, there are always some parts of Σ and Γ which do not belong to the regions (b) or (c), and thus we need to perform the analysis very carefully, in order to see whether it is possible to continue the amplitude there without the appearance of singularities. The answer depends on the relative positions of the individual singularity curves. An important observation is that the remaining curves of potential singularities meet only at the following points:

$A_{1,2} = \Sigma \cap \Gamma$:

$$M_P^2 = \mu^2 + m_1^2 + \frac{\lambda(\mu^2, m_2^2, m_5^2)}{2m_5^2} \pm \frac{(\mu^2 + m_5^2 - m_2^2)\sqrt{\lambda(\mu^2, m_2^2, m_5^2) + 4m_1^2 m_5^2}}{2m_5^2},$$
$$s = s(A_{1,2}), \tag{A19}$$

$B = \Sigma \cap \sigma_{P+}$:

$$M_P^2 = (\mu + m_1)^2, \quad s = m_1^2 + m_2^2 + \frac{m_1}{\mu}(\mu^2 + m_2^2 - m_5^2), \tag{A20}$$

$C = \Sigma \cap \sigma_{s+}$:

$$M_P^2 = \mu^2 + m_1^2 + \frac{m_1}{m_2}(\mu^2 + m_2^2 - m_5^2),$$
$$s = m_1^2 + m_2^2 + \frac{m_1}{\mu}(\mu^2 + m_2^2 - m_5^2), \tag{A21}$$

$D_{1,2} = \Gamma \cap \sigma_{P+}$:

$$M_P^2 = (\mu + m_1)^2, \qquad s = (\mu + m_1 \pm m_5)^2, \tag{A22}$$

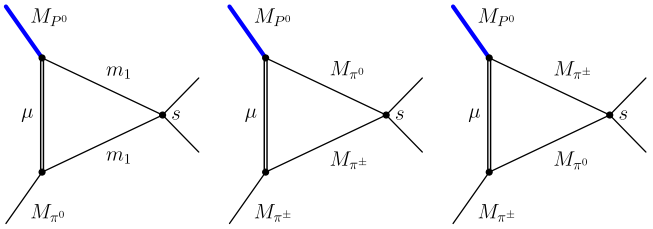

FIG. 5. The P-diagrams contributing to the $P^0\pi \to \pi\pi$ amplitudes. The assignments of the lines are as in Fig. 4.

$E_{1,2} = \Gamma \cap \sigma_{s+}$:

$$M_P^2 = (m_1 + m_2 \pm m_5)^2, \quad s = (m_1 + m_2)^2. \tag{A23}$$

We proceed with the analysis of the individual diagrams. The distinct types of diagrams with the neutral P^0 are displayed in Fig. 5.

a. Analytic properties of the first diagram from Fig. 5

For the first of these diagrams ($m_2 = m_1$, $m_5 = M_{\pi^0}$), the singularity curves are [$\Delta_{10} = m_1^2 - M_{\pi^0}^2$]:

(1) LLS curve Σ:

$$2\mu^2 s = -\mu^4 + \mu^2(M_P^2 + M_{\pi^0}^2 + 2m_1^2) + \Delta_{10}\Delta_{P1} \pm \lambda^{1/2}(\mu^2, M_P^2, m_1^2)\lambda^{1/2}(\mu^2, M_{\pi^0}^2, m_1^2). \tag{A24}$$

(2) NLLS curves:

$$\sigma_{s-}: \ s = 0, \qquad \sigma_{s+}: \ s = 4m_1^2,$$
$$\sigma_{P\pm}: \ M_P^2 = (\mu \pm m_1)^2. \tag{A25}$$

(3) NLS curves:

$$\Gamma: \ s = (M_P \pm M_{\pi^0})^2. \tag{A26}$$

The integration contour for the dispersive loop is the line $\mu \geq (M_{\pi^0} + m_1)$. For $m_1 = M_{\pi^0}$, the situation simplifies into the one studied by Kacser and Bronzan in Refs. [68,79]. However, the relative position of the curves is the same also for $m_1 = M_{\pi^\pm}$ as is depicted in Fig. 6, and one therefore expects that also the singularity structure will remain the same.

Since $\mu \geq (M_{\pi^0} + m_1)$, the denominator $\mathcal{D}$ of the parametric integrand does not vanish for $\beta_i \geq 0$ also in the regions (c1) and (c2), and the contribution of this diagram is without singularities on the physical sheet for all s and M_P^2 on the left of or below the dashed lines in Fig. 6. Since the normal-threshold lines σ_{s+} and σ_{P+} correspond to the singularity curves with one of the β_i equal to zero and the other two positive, the only part of the real section of the singularity curve Σ where $\mathcal{D}$ vanishes for all $\beta_i > 0$ is the arc between the points B and C, and this remains true

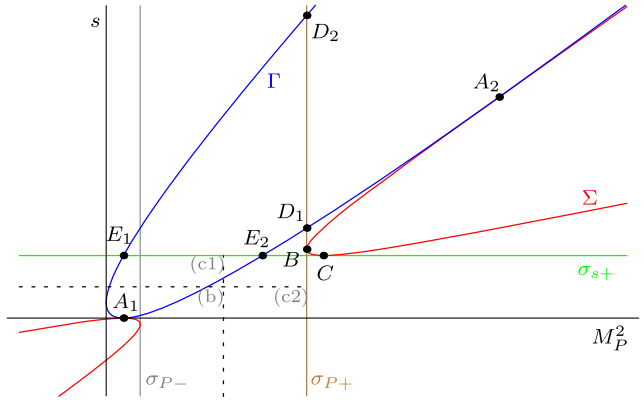

FIG. 6. The real sections of the singularity curves for the diagrams without the occurrence of the anomalous threshold on the physical Riemann sheet. For the labels of the curves, as well as for those of the points of intersections, see the main text.

for the appropriate complex surface connected to this real arc. All the other parts of Σ are nonsingular since we can continue the integral analytically in the following way. We start in the domain (c1), where the integration contour in β_i is the original one, and we add a small positive imaginary part to both s and M_P^2 [coming so to the domain (a)], which is nonsingular for any values of s and M_P^2 without the need of deformation of the contour. This way, we can reach any point where the singularity does not occur for positive β_i, upon letting the added imaginary parts tend to zero (without deformation of the integration curve).

However, the arc BC is connected to the nonsingular lower-left part of Σ by a continuous complex part of Σ [77]. Since all intersections of Σ with the other curves are just the real points from above, by performing the analytic continuation from the lower-left part by the path along Σ, we do not pass through any branch cut until we come to the real arc BC, where either σ_{P+} or σ_{s+} have to be crossed. Similarly, in all the points of Γ, the loop integral can be defined by analytic continuation along this complex curve. Therefore, there are no complex singularities in this case, and the only singularities occurring for the diagram considered on the physical sheet are the normal thresholds σ_{s+} and σ_{P+}, together with the anomalous threshold on the real arc BC, cf. Ref. [77]. (Note that on the section BC, the loop integral can be made analytic without the appearance of singularities by deforming the integration contour of the parametric integration to $\beta_1\beta_2 < 0$.)

The singularity at this anomalous threshold occurs only for $M_P^2 \in ((\mu + m_1)^2, 2\mu^2 + 2m_1^2 - M_{\pi^0}^2)$. Upon adding to μ^2 a small negative imaginary part, we can avoid this singularity. The only point where this is not possible is the end point of the integration, $\mu = M_{\pi^0} + m_1$.

In conclusion, for the fish diagram connected with the first diagram of Fig. 5, the anomalous threshold singularity in the s plane appears only for $M_P^2 = (M_{\pi^0} + 2m_1)^2$. Since $M_P > 3.5M_\pi$ for the physical values of the masses of the $K^\pm$, K_L, K_S, and η masses, this condition is never fulfilled.[14] For the physical masses, the only singularities appearing for this diagram are, therefore, just the regular normal thresholds. The important observation is that we obtain the correct physical analytic continuation of the amplitude also on the leading singularity curve by taking $M_P^2 \to M_P^2 + i\delta$, where δ is a small positive number.

b. Analytic properties of the second diagram from Fig. 5

The singularity curves for the second of these diagrams ($m_1 = M_{\pi^0}$, $m_2 = m_5 = M_{\pi^\pm}$) read:

(1) LLS curve Σ:

$$2s = M_P^2 + M_{\pi^0}^2 + 2M_{\pi^\pm}^2 - \mu^2 \pm \lambda^{1/2}(\mu^2, M_P^2, M_{\pi^\pm}^2)\sigma(\mu^2). \quad \text{(A27)}$$

(2) NLLS curves:

$$\sigma_{s\pm}\colon s = (M_\pi \pm M_{\pi^0})^2, \quad \sigma_{P\pm}\colon M_P^2 = (\mu \pm M_{\pi^0})^2. \quad \text{(A28)}$$

(3) NLS curves:

$$\Gamma\colon s = (M_P \pm M_{\pi^\pm})^2. \quad \text{(A29)}$$

For $\mu \geq 2M_{\pi^\pm}$, the relative position of these curves is again the one depicted in Fig. 6, and thus, by the same procedure as in the previous case, we obtain the contributions whose singularities on the physical sheet are just the normal thresholds. However, the integration in the dispersive loop starts at $\mu = 2M_{\pi^0} < 2M_{\pi^\pm}$. For these values of μ, the real section of the curves moves into the situation depicted in Fig. 7, and the analytic continuation proceeds as follows. The original integration contour in parametric space is free of singularities in the domain (b), i.e., on the left of and below the dashed lines of Fig. 7. We can continue the contribution of this diagram along the ellipsis Σ further up to B and C without the appearance of the singularities on the physical sheet, even without deforming the original integration contour, similarly to the previous case, since the only part of the real section of Σ which corresponds to $\beta_i > 0$ is the arc BC. In order to avoid singularities also on this arc, we would need to deform the integration contour there. However, all paths from the parts we have identified to be nonsingular to the arc BC along Σ pass through a singularity curve, either σ_{P+} or σ_{s+}. Since the curve Σ is

[14]Note that for the physical masses and for μ corresponding to the end point, even the extremal value of the position of C, $M_P^2 = 5M_{\pi^\pm}^2 + \frac{M_{\pi^\pm}}{M_{\pi^0}}(5M_{\pi^\pm}^2 - M_{\pi^0}^2)$ corresponds to $M_P \approx 423$ MeV. For the kaons and the eta, we can, therefore, altogether ignore this complication with the BC section.

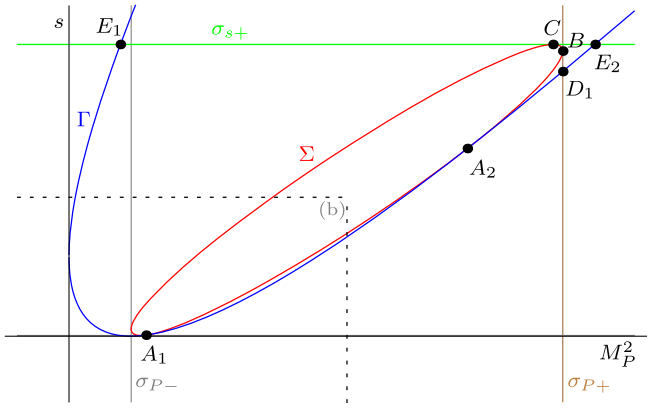

FIG. 7. The real sections of the singularity curves for the diagrams where the anomalous threshold occurs on the physical Riemann sheet. For the labels of the curves, as well as for those of the points of intersections, see the main text.

here real for real M_P^2, for any complex singularity curve in β-space, there exists a complex conjugated one, and therefore if we want to evade the complex singularities on one side, we encounter the complex conjugated one, cf. Ref. [77]. We have, therefore, no way how to avoid singularities on the arc BC. This diagram thus possesses on the physical sheet, in addition to the normal threshold, also the anomalous threshold (A27) on the arc BC and on all the corresponding complex surfaces.

We can try to avoid these singularities by the addition of a small imaginary part also to μ^2. However, this does again not work for the end point of the μ^2 integration, in this case for $\mu = 2M_{\pi^0}$. Even though the real arc BC is again to the left of the physical value of M_P^2 for both the kaons and the eta, the singular complex surface connected with this arc extends to the region where $M_P > 3M_{\pi^0}$. We are, therefore, left with two complex conjugated anomalous thresholds in s for the physical $M_P > 3M_{\pi^0}$,

$$2s = M_P^2 + 2M_{\pi^\pm}^2 - 3M_{\pi^0}^2 \pm \lambda^{1/2}(M_P^2, M_{\pi^\pm}^2, 4M_{\pi^0}^2)\sigma(4M_{\pi^0}^2). \quad \text{(A30)}$$

Thus, for the amplitudes to which this diagram contributes, the starting point of our construction, the dispersive representation of Eq. (3.5), requires appropriate modifications in order to include the contributions from these anomalous thresholds.

c. Analytic properties of further diagrams

We have seen that the appearance of the anomalous thresholds on the physical sheet is connected with the position of the real section of the curve Σ between the subleading curves $\sigma_{s\pm}$ and the $\sigma_{P\pm}$, in which case we cannot evade the corresponding normal threshold branch cuts when trying to avoid the singularities Σ on the complex surfaces connected with the arc BC. We can, therefore, observe a simple condition for this appearance of the anomalous threshold. It occurs on the physical sheet only in the case (A16) is real in the interval $M_P^2 \in ((\mu - m_1)^2, (\mu + m_1)^2)$. Since the first triangle function appearing there is imaginary on this interval, the condition means that the second triangle function $\lambda(\mu^2, m_2^2, m_5^2)$ has to be imaginary as well. This happens in the interval $\mu^2 \in ((m_2 - m_5)^2, (m_2 + m_5)^2)$.

From this condition, we can formulate the following simple rule of thumb, stating that the $\pi\pi$ fish diagram has the anomalous threshold singularity on the physical sheet in the variable s only in the case when in the corresponding triangle diagram one of the other vertices (than the one adjacent to s) is stable and the second one is unstable, when we take for μ its end point value μ_0. The vertex is called unstable if the masses on the adjoining lines are such that at least one of them is greater than the sum of the other two. Note that this rule does not take into account the singularity on the real arc BC of Fig. 6 (we have found that for the pion lines, this singularity never occurs) and the non-Landau singularities, as is obvious from its application to the π-diagrams (the only unstable mass there can be μ, which appears in both vertices; i.e., this rule tells there is no anomalous threshold for all π-diagrams). However, in our previous analysis, we have also taken its existence into account, and it does not change the above conclusion.

Since the vertex with M_P in P-diagrams is always unstable for $\mu = \mu_0$, the anomalous threshold appears only in the case $\mu_0 < (m_2 + m_5)$. Furthermore, since m_2 and m_5 are pion masses and conservation of the electric charge has to be respected, the only possibility is $\mu_0 = 2M_{\pi^0}$ and $m_2 = m_5 = M_{\pi^\pm}$.

In conclusion, the only P-diagrams possessing the anomalous threshold singularity on the physical sheet for the physical values of M_P and of the pion masses are those depicted in Fig. 8. These diagrams contribute to the processes $P^0 \to \pi^0\pi^+\pi^-$, $P^+ \to \pi^-\pi^+\pi^+$, and $P^+ \to \pi^+\pi^0\pi^0$. Therefore, besides the case $M_\pi = M_{\pi^0}$, the only $P \to \pi\pi\pi$ decay processes with $M_\pi \neq M_{\pi^0}$ where no such singularity occurs are the processes $P^0 \to \pi^0\pi^0\pi^0$, with $P^0 = K_L$ or $P^0 = \eta$. Kacser's prescription can be extended to these cases; i.e., the required analytic continuation in

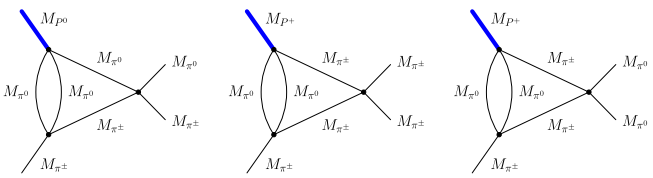

FIG. 8. The complete set of P-diagrams possessing an anomalous threshold singularity on the physical Riemann sheet for the physical values of the masses M_P, M_π, and M_{π^0}.

M_P^2, $\bar{M}_P^2 \to M_P^2 + i\delta$, $\bar{M}_P < 3M_{\pi^0}$, $\delta > 0$, can be performed without encountering any singularity.

3. Fish diagrams with other-than-pion internal lines

The same analysis can be performed for fish diagrams containing other mesons, kaons, and η's, in internal lines. Naturally, then it can happen that there will occur anomalous threshold singularity for some value of M_P. However, thanks to the hierarchy of the masses prohibiting decays of the type $P \to P'\pi$, where P and P' are kaons or η's, the physical mass M_P will each time be smaller than the mass where such anomalous threshold singularity can occur. In other words, in all the cases, the physical mass M_P is to the left of the points B and C in one of the situations from Figs. 6 and 7; i.e., it lies in the region where the anomalous threshold singularity does not appear on the physical sheet. The inclusion of these other internal lines does, therefore, not change the conclusions of our analysis from the previous sections.

APPENDIX B: INTEGRALS OF THE $\bar{J}$ FUNCTIONS

In order to compute the partial-wave projections of the one-loop amplitudes, we need to perform the integrals occurring in Eq. (5.17). Actually, in order to avoid the cuts on the positive real axis, the integration has to be performed along a path in the complex plane [79],

$$\int_{t_-(s)}^{t_+(s)} dt \to \int_{\mathcal{C}(t_-(s),t_+(s))} dt, \tag{B1}$$

starting at $t_-(s)$ and ending at $t_+(s)$. It turns out that the complex path $\mathcal{C}(t_-(s), t_+(s))$ can always be chosen such that there exists an open neighborhood of it that also avoids the cut. This follows from the analysis of Ref. [79] in the equal-mass case, and also holds for $M_\pi \neq M_{\pi^0}$ when the singularities of the integrands consist only of the normal branch cut, starting at $s = 4M_\pi^2$ or $s = 4M_{\pi^0}^2$, i.e., when there is no anomalous threshold [55]. Then, a result of complex analysis [96] tells us that the integral is correctly evaluated in the usual way, i.e., upon taking the difference of the end point values of the primitive function, provided, of course, that the latter exists. Given this result, our task in this Appendix will be to construct the required primitive functions, and then, as a second step, to evaluate them at the end points $t_\pm(s)$. It will be enough to give the results for the function $\bar{J}_{\pm 0}(t)$ defined in Eq. (4.13); the expressions corresponding to the two other cases, $\bar{J}(t)$ and $\bar{J}_0(t)$, can easily be obtained upon taking the appropriate limits in the pion masses. More specifically, we denote the ratio of the pion masses by q,

$$q = \frac{M_{\pi^0}}{M_\pi}, \tag{B2}$$

and the two other cases will be obtained simply by taking the limit $q \to 1$ in the end. We thus first need to know the following primitive functions:

$$I_{\pm 0}^{(n)}(t) = 16\pi^2 \int dt t^n \bar{J}_{\pm 0}(t), \quad \text{for } n = -1, \ldots, 3;$$
$$I_{\pm 0}^{(-2)}(t) = 16\pi^2 \int dt \frac{\bar{\bar{J}}_{\pm 0}(t)}{t^2}. \tag{B3}$$

These then need to be evaluated at the corresponding end points. We address these two separate issues in turn in the remainder of this Appendix.

1. Primitive functions

Writing the function $\bar{J}_{\pm 0}(t)$ in the form

$$\bar{J}_{\pm 0}(t) = \frac{1}{16\pi^2}\left[1 + \left(\frac{\Delta_q}{t} - \frac{\Sigma_q}{\Delta_q}\right)\ln q + \frac{t-\mu_{-q}}{t}\sigma_q(t)\ln\frac{\sigma_q(t)-1}{\sigma_q(t)+1}\right], \tag{B4}$$

with

$$\mu_q = M_\pi^2(1+q)^2, \qquad \Sigma_q = M_\pi^2(1+q^2), \qquad \Delta_q = M_\pi^2(1-q^2) \tag{B5}$$

and

$$\sigma_q(t) = \sqrt{\frac{t-\mu_q}{t-\mu_{-q}}}, \tag{B6}$$

suggests performing the following transformation of the variable:

$$\tau = \frac{\sigma_q(t)-1}{\sigma_q(t)+1}. \tag{B7}$$

The function $\sigma_q(t)$ is defined in the complex t plane, with a cut on the real axis, from μ_{-q} to μ_q, and with $\sigma_q(t \pm i\epsilon) = \pm i\sqrt{(\mu_q - t)/(t-\mu_{-q})}$ when t lies on this cut. This transformation then maps the complex plane with the cut (μ_{-q}, μ_q) onto the unit disk. As illustrated in Fig. 9, the points slightly above the cut $(t + i\epsilon)$ are mapped slightly below the upper semicircle, while the points slightly below this cut $(t - i\epsilon)$ are mapped slightly above the lower semicircle (the points lying exactly on the upper and on the lower semicircles have to be identified). The ray $(\mu_q + i\epsilon, \infty + i\epsilon)$, where the branch cut of the one-loop

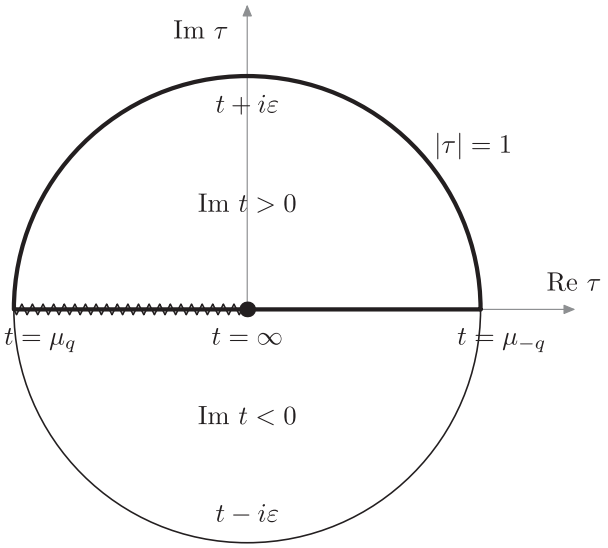

FIG. 9. Conformal transformation (B7) mapping the complex t plane onto the unit disk in the τ plane. The points on the upper and on the lower semicircles are identified. In the transformed plane, the one-loop functions to which the transformation corresponds have their branch cut located on the line segment $\tau \in (-1 + i\epsilon, 0 + i\epsilon)$.

function is located, is mapped onto line segment $(-1 + i\epsilon, 0 + i\epsilon)$. The inverse transformation

$$t(\tau) = M_\pi^2(\tau - q)\left(\frac{1}{\tau} - q\right), \tag{B8}$$

with

$$\sigma_q(t) = \frac{1+\tau}{1-\tau}, \qquad dt = \frac{qM_\pi^2}{\tau^2}(1-\tau^2)d\tau, \tag{B9}$$

can be continued to the whole complex τ plane and satisfies

$$t(\tau) = t(1/\tau). \tag{B10}$$

This means that the points τ and $1/\tau$ should be identified, which also implies the identification of τ and $\tau^\star = 1/\tau$ on the unit-disk boundary of Fig. 9.

Expressed in terms of the variable τ, the one-loop function $\bar{J}_{\pm 0}$ reads

$$16\pi^2\bar{J}_{\pm 0}(\tau) = 1 - \frac{\Sigma_q}{\Delta_q}\log q - \frac{\tau(1-q^2)}{(\tau-q)(\tau q-1)}\log q + \frac{q(1-\tau^2)}{(\tau-q)(\tau q-1)}\log\tau. \tag{B11}$$

Its analyticity in the unit disk with the segment $\langle -1, 0\rangle$ removed and the symmetry property $\bar{J}_{\pm 0}(\tau) = \bar{J}_{\pm 0}(1/\tau)$ become manifest in this expression. The expression that mixes the two variables,

$$16\pi^2\bar{J}_{\pm 0}(t) = 1 + \left(\frac{\Delta_q}{t} - \frac{\Sigma_q}{\Delta_q}\right)\log q + q\frac{M_\pi^2}{t}\frac{\tau^2-1}{\tau}\log\tau, \tag{B12}$$

allows obtaining its derivative in a simple way,

$$16\pi^2\frac{d}{dt}(t\bar{J}_{\pm 0}(t)) = \frac{1+\tau^2}{1-\tau^2}\log\tau - \frac{1+q^2}{1-q^2}\log q, \tag{B13}$$

which in turn makes it easy to check the primitive functions given here. Finally, we introduce the following function,

$$\mathcal{J}(\tau) = \log q\log\tau + \mathrm{Li}_2(1-q\tau) - \mathrm{Li}_2\left(1 - \frac{\tau}{q}\right), \tag{B14}$$

which appears in the results of the integration.

Having prepared all the necessary ingredients, we present here a list of all primitive functions that are needed for the computation of the S and P partial waves of the one-loop amplitudes:

$$\begin{aligned}
I^{(1)}_{\pm 0}(t) &= 8\pi^2\bar{J}_{\pm 0}(t)t(t-\Sigma_q) + \frac{t^2}{4} - 2q^2M_\pi^4 t\frac{\log q}{\Delta_q} \\
&\quad + q^2M_\pi^4\log^2\tau, \\
I^{(2)}_{\pm 0}(t) &= \frac{8\pi^2}{3}\bar{J}_{\pm 0}(t)t(2t^2 - \Sigma_q t - (\Sigma_q^2 + 8q^2M_\pi^4)) \\
&\quad + \frac{t^3}{9} + \frac{\Sigma_q t^2}{12} - 2q^2M_\pi^4 t\left(\frac{t}{3} + \Sigma_q\right)\frac{\log q}{\Delta_q} \\
&\quad + q^2M_\pi^4\Sigma_q\log^2\tau, \\
I^{(3)}_{\pm 0}(t) &= \frac{t^4}{16} + \Sigma_q\frac{t^3}{18} + \frac{t^2}{24}(\Sigma_q^2 + 6q^2M_\pi^4) \\
&\quad + q^2M_\pi^4(\Sigma_q^2 + q^2M_\pi^4)\log^2\tau \\
&\quad - q^2M_\pi^4 t\left[\frac{t^2}{3} + \frac{5\Sigma_q t}{6} + 2(\Sigma_q^2 + q^2M_\pi^4)\right]\frac{\log q}{\Delta_q} \\
&\quad + \frac{4\pi^2}{3}\bar{J}_{\pm 0}(t)t(3t^3 - \Sigma_q t^2 - (\Sigma_q^2 + 6q^2M_\pi^4)t \\
&\quad - \Sigma_q(\Sigma_q^2 + 26q^2M_\pi^4)), \\
I^{(0)}_{\pm 0}(t) &= 16\pi^2\bar{J}_{\pm 0}(t)t + t + \frac{\Sigma_q}{2}\log^2\tau - \Delta_q\mathcal{J}(\tau), \\
I^{(-1)}_{\pm 0}(t) &= -16\pi^2\bar{J}_{\pm 0}(t) - \frac{1}{2}\log^2\tau - 2 + \frac{\Sigma_q}{\Delta_q}\mathcal{J}(\tau), \\
I^{(-2)}_{\pm 0}(t) &= 8\pi^2\bar{J}_{\pm 0}(t)\left(\frac{\Sigma_q}{\Delta_q^2} - \frac{1}{t}\right) - \frac{\Sigma_q}{\Delta_q^2} + \frac{13}{36qM_\pi^2} \\
&\quad + \frac{2q^2M_\pi^4}{\Delta_q^3}\mathcal{J}(\tau).
\end{aligned} \tag{B15}$$

We have adjusted the free integration constants in these primitive functions, such as to ensure that all of them exhibit a smooth limit for the ratio of pion masses q going to unity, and to make them vanish at $t = 0$ (in this limit).

2. End point evaluation in the case $M_{\pi^0} = M_\pi$

In order to perform the explicit calculation of the partial-wave projections, we should now evaluate the preceding primitives at the end points given in Eq. (5.18). In general, this procedure produces complicated expressions. However, in particular cases, like for equal-mass pions, the situation simplifies somewhat. We will, therefore, treat this case in some detail in what follows. For definiteness, we consider the case of the charged pion. The corresponding expressions for the neutral pion are obtained from those given below by substituting M_π by M_{π^0} in all formulas.

Introducing

$$T_\pm(s) = \frac{4M_\pi^2 - t_\pm(s)}{2M_\pi^2} \tag{B16}$$

and

$$\sigma_{T_\pm}(s) = \frac{1}{\sigma(t_\pm(s))} = \sqrt{\frac{T_\pm(s)-2}{T_\pm(s)}}, \tag{B17}$$

we obtain

$$\begin{aligned} \tau(t_\pm(s)) &= T_\pm(s) - 1 - T_\pm(s)\sigma_{T_\pm}(s), \\ \frac{1}{\tau(t_\pm(s))} &= T_\pm(s) - 1 + T_\pm(s)\sigma_{T_\pm}(s) \end{aligned} \tag{B18}$$

and

$$L_{T_\pm}(s) = \log\tau(t_\pm(s)) \equiv \log\left(\frac{1-\sigma_{T_\pm}(s)}{1+\sigma_{T_\pm}(s)}\right). \tag{B19}$$

Inserting these relations into the primitive functions in the limit $q = 1$, and using the simplification $T_\pm\sigma_{T_\pm}^2 = T_\pm - 2$, we arrive at rather simple expressions

$$\begin{aligned} I^{(1)}(t_\pm) &= M_\pi^4[(T_\pm-2)(5T_\pm-8) \\ &\quad + 2T_\pm(T_\pm-1)\sigma_{T_\pm}L_{T_\pm} + L_{T_\pm}^2], \\ I^{(2)}(t_\pm) &= \frac{M_\pi^6}{9}[2(T_\pm-2)(7T_\pm-8)(11-4T_\pm) \\ &\quad - 12T_\pm(T_\pm-3)(2T_\pm-1)\sigma_{T_\pm}L_{T_\pm} + 18L_{T_\pm}^2], \\ I^{(3)}(t_\pm) &= \frac{M_\pi^8}{9}[(T_\pm-2)(81{T_\pm}^3 - 482{T_\pm}^2 + 941T_\pm - 512) \\ &\quad + 6T_\pm(6{T_\pm}^3 - 34{T_\pm}^2 + 59T_\pm - 15)\sigma_{T_\pm}L_{T_\pm} \\ &\quad + 45L_{T_\pm}^2], \\ I^{(0)}(t_\pm) &= M_\pi^2[6(2-T_\pm) - 2T_\pm\sigma_{T_\pm}L_{T_\pm} + L_{T_\pm}^2], \\ I^{(-1)}(t_\pm) &= -4 - \frac{2T_\pm}{T_\pm-2}\sigma_{T_\pm}L_{T_\pm} - \frac{1}{2}L_{T_\pm}^2, \\ I^{(-2)}(t_\pm) &= \frac{1}{18M_\pi^2}\left[\frac{4(2T_\pm-1)}{T_\pm-2} + \frac{3{T_\pm}^2}{(T_\pm-2)^2}\sigma_{T_\pm}L_{T_\pm}\right]. \end{aligned} \tag{B20}$$

Finally, it is also useful to notice the relations

$$\begin{aligned} 16\pi^2\bar{J}(t_\pm) &= 2 + \frac{L_{T_\pm}}{\sigma_{T_\pm}}, \\ 16\pi^2\bar{\bar{J}}(t_\pm) &= 2 + \frac{L_{T_\pm}}{\sigma_{T_\pm}} - \frac{t_\pm}{6M_\pi^2}. \end{aligned} \tag{B21}$$

The link with the expressions given in Eqs. (5.27), (5.28), and (5.31) is then provided by the relations

$$\begin{aligned} \sigma_{T_\pm}(s) &= \frac{\Delta_{P\pi}\sigma(s)}{s - 4M_\pi^2 \pm 2K(s)}, \\ L_{T_\pm}(s) &= \frac{1}{2}[L(s) \mp M(s)]. \end{aligned} \tag{B22}$$

APPENDIX C: PROPERTIES OF THE FUNCTIONS $\tilde{k}_i(s)$ AND $\tilde{K}_i(s)$

In this Appendix, we discuss some properties of the functions $\tilde{k}_i(s)$, $\tilde{K}_i(s)$, and $\tilde{K}_i^{(\lambda)}(s)$, introduced in Eqs. (5.28), (5.38), and (5.46), respectively. We briefly address their analytic properties and also provide graphical representations. We display the functions $\tilde{k}_i(s)$, with $i = 2$, 3, on the real axis in Fig. 10 [the real parts of those with $i = 0$, 1 coincide with the imaginary parts of $\tilde{K}_i(z)$].

The functions $\tilde{K}_i(z)$ are defined as dispersive integrals in the complex plane,

$$\tilde{K}_i(z) = \frac{z^n}{\pi}\int_{4M_\pi^2}^\infty \frac{dx}{x^n}\frac{\tilde{k}_i(x)}{x-z}, \tag{C1}$$

and the physical value corresponds to $z = s + \mathrm{i}0$, which is shown in Fig. 11. For z which is not located on the integration contour, the only potential singularities of the integrand are those of the function $\tilde{k}_i(x)$ where $4M_\pi^2 < x < \infty$. The functions $\tilde{k}_0(s)$ and $\tilde{k}_1(s)$ do not present any particular problem. They already occur in the simpler situation provided by $\pi\pi$ scattering, and the two functions $\tilde{K}_0(s)$ and $\tilde{K}_1(s)$ can be expressed in terms of the function $\bar{J}(s)$ [see Eq. (5.41)], which has no other singularity than a cut along the positive-s real axis, starting at $s = 4M_\pi^2$. In the case of $\tilde{k}_2(s)$ and $\tilde{k}_3(s)$, there are two possibly problematic points, namely, $x = (M_P \pm M_\pi)^2 = M_\pm^2$. Closer inspection reveals that only $x = M_-^2$ corresponds to a singularity, as can actually also be seen directly in Fig. 10. This singularity is, however, integrable since the integrand in Eq. (C1) behaves as $(x - M_\pm^2)^{-1/2}$ in the vicinity of this point. It means the $\tilde{K}_i(z)$, defined by the original contour, is at least analytic in the complex plane with the exception of the part of the real axis for which $z > 4M_\pi^2$. For $z \to 4M_\pi^2$, we have a nonintegrable end point singularity. Therefore, this point constitutes a branch point of $\tilde{K}_i(z)$. For z real, $z \neq M_\pm^2$ we can deform the integration contour in (C1), such as to avoid the singularity $(x-z)^{-1}$, in an appropriate way, depending

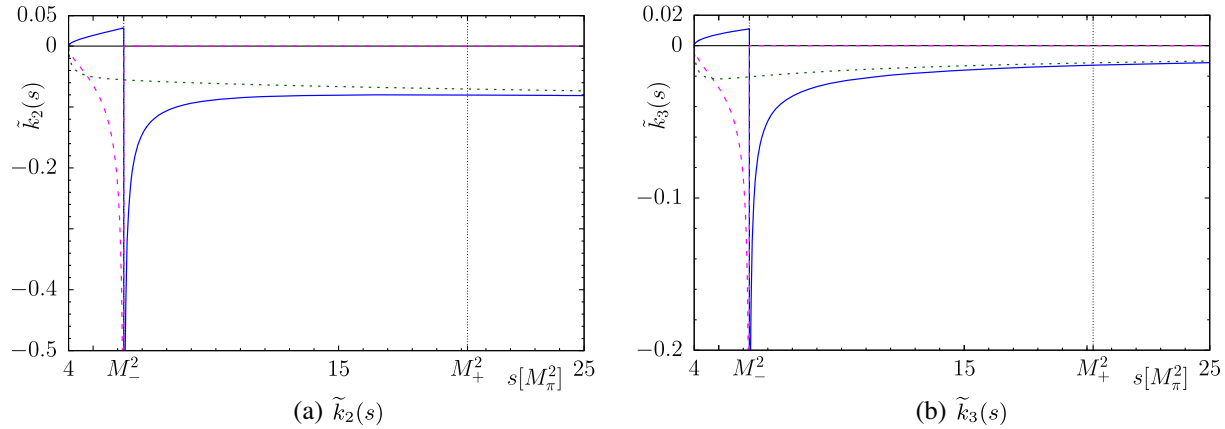

(a) $\widetilde{k}_2(s)$ (b) $\widetilde{k}_3(s)$

FIG. 10. The real (solid curve in blue) and the imaginary (dashed curve in magenta) parts of functions $\tilde{k}_{2,3}(s)$ for $M_P = 3.5M_\pi + \mathrm{i}0$. For comparison, also the real part of these functions for $M_P = 2.9M_\pi$ (dotted curve in green) is plotted (in this case, their imaginary part is zero). The abscissas show s in units of M_π^2. The vertical lines indicate the positions of $s = M_\pm^2$.

on whether we approach the contour from below or from above. The only dangerous point is the true singularity of $\tilde{k}_i(x)$, i.e., $z = M_-^2$. Because we made the analytic continuation $M_P^2 + \mathrm{i}\delta$, this singularity is, in fact, avoided by contour deformation when we approach $z = M_-^2$ from the upper complex half-plane because then there is no pinch

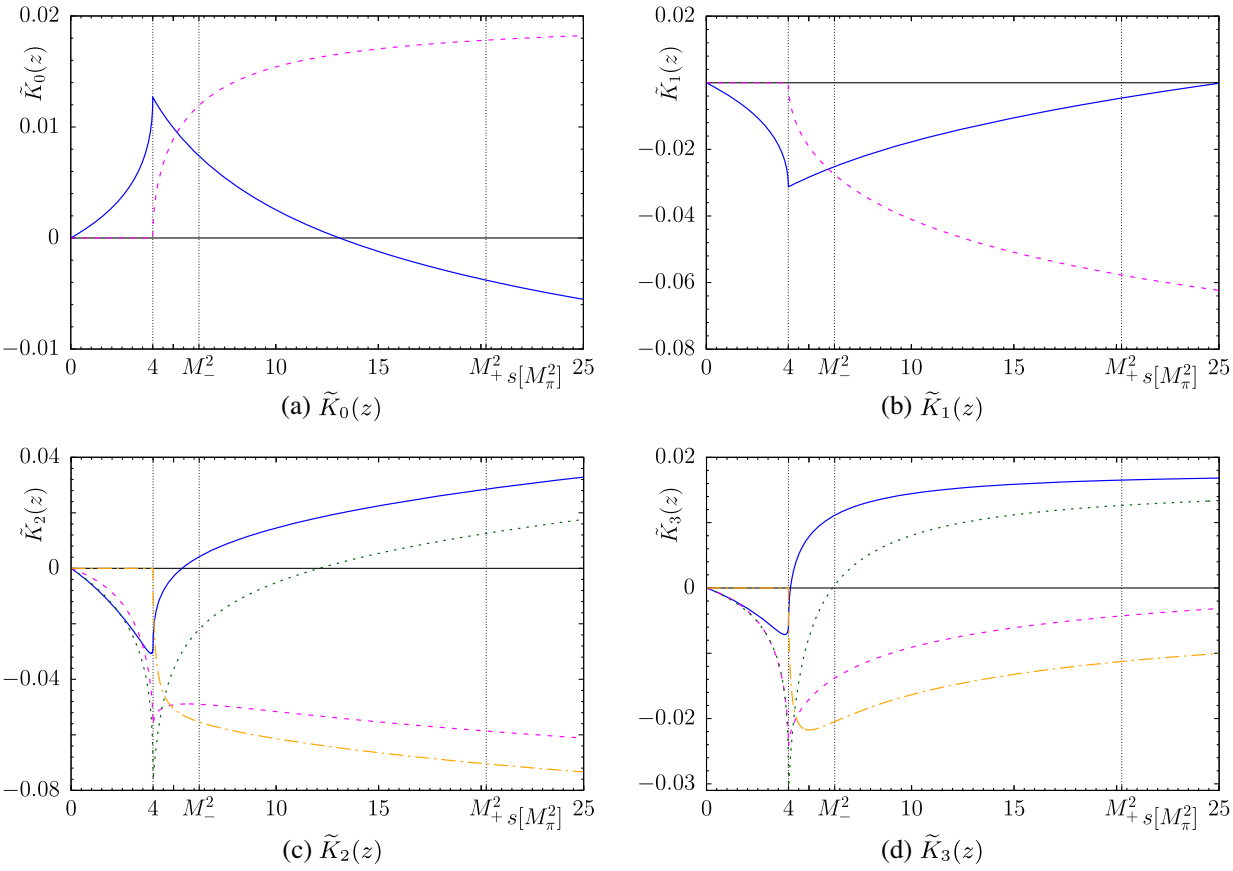

(a) $\widetilde{K}_0(z)$ (b) $\widetilde{K}_1(z)$

(c) $\widetilde{K}_2(z)$ (d) $\widetilde{K}_3(z)$

FIG. 11. The real (solid curve in blue) and the imaginary (dashed curve in magenta) parts of functions $\tilde{K}_i(z)$, $z = s + \mathrm{i}0$, for $M_P = 3.5M_\pi + \mathrm{i}\delta$. For comparison, the real (dotted curve in green) and the imaginary (dot-dashed curve in orange) parts of functions $\tilde{K}_{2,3}(s)$ for $M_P = 2.9M_\pi$ are also plotted. The abscissas show s in units of M_π^2. The positions of $s = \{4M_\pi^2, M_-^2, M_+^2\}$ are indicated by the vertical lines.

of the contour, and thus even this point is, in fact, regular. However, when we approach this point from below, the contour is pinched, and the singularity cannot be avoided by means of the contour deformation. Nevertheless, this singularity lies on the second sheet. Of course, these arguments rest on the fact that the discontinuities $\tilde{k}_i(z)$ have good analytic properties, which allows deforming the contour without encountering other singularities of these functions.

APPENDIX D: EXPRESSIONS OF THE FUNCTIONS $\mathcal{W}^{P\pi}(s)$

In this Appendix, we give the expressions of the functions $\mathcal{W}^{P\pi}(s)$, and of the corresponding coefficients $\tilde{w}_{\pm}^{(n)}$ and $\mathcal{B}_{\pm}$ for each function listed in Table II, in the case where the masses of charged and neutral pions are equal.

For the decay of a charged kaon into three charged pions, we have

$$
\begin{aligned}
\mathcal{W}_{++}^{P\pi}(s) &= \frac{\varphi_0^{++}(s)}{2}\left\{\frac{(16\pi)^2}{4}\varphi_0^{++}(s)\tilde{\varphi}_0^{++}(s)\bar{J}^2(s) + \left[\left(C_{++}+\frac{D_{++}}{2}\right)\frac{(s-s_0)^2}{F_\pi^4}+\frac{2}{3}D_{++}\frac{K^2(s)}{F_\pi^4}\right]\bar{J}(s)\right\} \\
&\quad + \frac{1}{2}[\varphi_0^{++}\odot\tilde{\xi}_0^{++}](s), \\
\mathcal{W}_{+-}^{(0)P\pi}(s) &= \varphi_0^{+-}(s)\left\{\frac{(16\pi)^2}{4}[2\tilde{\varphi}_0^{+-}(s)\varphi_0^{+-}(s)+\tilde{\varphi}_0^{x}(s)\varphi_0^{x}(s)]\bar{J}^2(s)\right. \\
&\quad \left. + \left[\frac{1}{4}(C_{++}+5D_{++})\frac{(s-s_0)^2}{F_\pi^4}+\frac{1}{3}(C_{++}+D_{++})\frac{K^2(s)}{F_\pi^4}\right]\bar{J}(s)\right\} + [\varphi_0^{+-}\odot\tilde{\xi}_0^{+-}](s) \\
&\quad + \frac{\varphi_0^{x}(s)}{2}\left\{\frac{(16\pi)^2}{4}[2\tilde{\varphi}_0^{+-}(s)\varphi_0^{x}(s)+\tilde{\varphi}_0^{x}(s)\varphi_0^{00}(s)]\bar{J}^2(s) + \left[\left(C_x+\frac{D_x}{2}\right)\frac{(s-s_0)^2}{F_\pi^4}+\frac{2}{3}D_x\frac{K^2(s)}{F_\pi^4}\right]\bar{J}(s)\right\} \\
&\quad + \frac{1}{2}[\varphi_0^{x}\odot\tilde{\xi}_0^{x}](s), \\
\mathcal{W}_{+-}^{(1)P\pi}(s) &= \frac{c_{+-}}{3F_\pi^2}\left[-\frac{B_{++}c_{+-}}{18}\frac{16\pi}{2}\frac{(s-4M_\pi^2)^2}{F_\pi^4}\bar{J}^2(s)+\frac{C_{++}-D_{++}}{6}\frac{(s-4M_\pi^2)(s-s_0)}{F_\pi^4}\bar{J}(s)+\tilde{\xi}_1^{+-}(s)\right]
\end{aligned}
\tag{D1}
$$

with

$$
\frac{\mathcal{B}_{+;++}}{2} = -\mathcal{B}_{\pm;+-} = -\mathcal{B}_{-;+-} = B_{++}c_{+-}, \qquad \mathcal{B}_{-;++} = 0, \tag{D2}
$$

and

$$
\begin{aligned}
\tilde{w}_{+;++}^{(0)} &= \left[A_x - \frac{B_x}{3}\frac{M_K^2+3M_\pi^2}{F_\pi^2}\right]\left(a_x - b_x\frac{4M_\pi^2}{F_\pi^2}\right) + 2\left[A_{++}+\frac{B_{++}}{6}\frac{M_K^2+3M_\pi^2}{F_\pi^2}\right]\left(a_{+-}-b_{+-}\frac{4M_\pi^2}{F_\pi^2}\right) \\
&\quad + \frac{4}{3}B_{++}c_{+-}\frac{M_\pi^2(M_K^2+3M_\pi^2)}{F_\pi^4}, \\
\tilde{w}_{+;++}^{(1)} &= b_x\left[A_x - \frac{B_x}{3}\frac{M_K^2+3M_\pi^2}{F_\pi^2}\right] + B_x\left(a_x - b_x\frac{4M_\pi^2}{F_\pi^2}\right) + 2b_{+-}\left[A_{++}+\frac{B_{++}}{6}\frac{M_K^2+3M_\pi^2}{F_\pi^2}\right] \\
&\quad - B_{++}\left(a_{+-}-b_{+-}\frac{4M_\pi^2}{F_\pi^2}\right) - \frac{B_{++}c_{+-}}{3}\frac{M_K^2+7M_\pi^2}{F_\pi^2}, \\
\tilde{w}_{+;++}^{(2)} &= B_x b_x - b_{+-}B_{++} + \frac{B_{++}c_{+-}}{3},
\end{aligned}
\tag{D3}
$$

$$\tilde{w}^{(0)}_{\pm;+-} = \left[\frac{A_x}{2} - \frac{B_x}{6}\frac{M_K^2+3M_\pi^2}{F_\pi^2}\right]\left(\mathrm{a}_x - \mathrm{b}_x\frac{4M_\pi^2}{F_\pi^2}\right) + \left[A_{++} + \frac{B_{++}}{6}\frac{M_K^2+3M_\pi^2}{F_\pi^2}\right]\left(\mathrm{a}_{+-} - \mathrm{b}_{+-}\frac{4M_\pi^2}{F_\pi^2}\right)$$
$$-\frac{2}{3}B_{++}\mathrm{c}_{+-}\frac{M_\pi^2(M_K^2+3M_\pi^2)}{F_\pi^4} \pm \frac{1}{2}\left[A_{++} - \frac{B_{++}}{3}\frac{M_K^2+3M_\pi^2}{F_\pi^2}\right]\left(\mathrm{a}_{++} - \mathrm{b}_{++}\frac{4M_\pi^2}{F_\pi^2}\right),$$
$$\tilde{w}^{(1)}_{\pm;+-} = \frac{\mathrm{b}_x}{2}\left[A_x - \frac{B_x}{3}\frac{M_K^2+M_\pi^2+2M_{\pi^0}^2}{F_\pi^2}\right] + \frac{B_x}{2}\left(\mathrm{a}_x - \mathrm{b}_x\frac{4M_\pi^2}{F_\pi^2}\right) - \frac{B_{++}}{2}\left(\mathrm{a}_{+-} - \mathrm{b}_{+-}\frac{4M_\pi^2}{F_\pi^2}\right)$$
$$+\frac{\mathrm{b}_{+-}}{F_\pi^2}\left[A_{++} + \frac{B_{++}}{6}\frac{M_K^2+3M_\pi^2}{F_\pi^2}\right] + \frac{B_{++}\mathrm{c}_{+-}}{6}\frac{M_K^2+7M_\pi^2}{F_\pi^2} \pm \frac{B_{++}}{2}\left(\mathrm{a}_{++} - 4\mathrm{b}_{++}\frac{M_\pi^2}{F_\pi^2}\right) \pm \frac{\mathrm{b}_{++}}{2}\left[A_{++} - \frac{B_{++}}{3}\frac{M_K^2+3M_\pi^2}{F_\pi^2}\right],$$
$$\tilde{w}^{(2)}_{\pm;+-} = \frac{1}{2}\left(B_x\mathrm{b}_x - B_{++}\mathrm{b}_{+-} - \frac{1}{3}B_{++}\mathrm{c}_{+-} \pm B_{++}\mathrm{b}_{++}\right). \tag{D4}$$

Next, for the decay of a charged kaon into one charged and two neutral pions, we obtain

$$\mathcal{W}_x^{P\pi}(s) = \varphi_0^x(s)\left\{\frac{(16\pi)^2}{4}[2\tilde{\varphi}_0^{+-}(s)\varphi_0^{+-}(s) + \tilde{\varphi}_0^x(s)\varphi_0^x(s)]\bar{J}^2(s) + \left[\frac{1}{4}(C_{++}+5D_{++})\frac{(s-s_0)^2}{F_\pi^4}\right.\right.$$
$$\left.\left.+\frac{1}{3}(C_{++}+D_{++})\frac{K^2(s)}{F_\pi^4}\right]\bar{J}(s)\right\} + [\varphi_0^x \odot \tilde{\xi}_0^{+-}](s)$$
$$+\frac{\varphi_0^{00}(s)}{2}\left\{\frac{(16\pi)^2}{4}[2\tilde{\varphi}_0^{+-}(s)\varphi_0^x(s) + \tilde{\varphi}_0^x(s)\varphi_0^{00}(s)]\bar{J}^2(s) + \left[\left(C_x + \frac{D_x}{2}\right)\frac{(s-s_0)^2}{F_\pi^4} + \frac{2}{3}D_x\frac{K_x^2(s)}{F_\pi^4}\right]\bar{J}(s)\right\}$$
$$+\frac{1}{2}[\varphi_0^{00} \odot \tilde{\xi}_0^x](s),$$
$$\mathcal{W}_{0+}^{(0)P\pi}(s) = \varphi_0^{+0}(s)\left\{\frac{(16\pi)^2}{2}\varphi_0^{+0}(s)\tilde{\varphi}_0^{0+}(s)\bar{J}^2(s)\right.$$
$$\left.-\left[\frac{1}{4}(C_x+5D_x)\frac{(s-s_0)^2}{F_\pi^4} + \frac{1}{3}(C_x+D_x)\frac{K^2(s)}{F_\pi^4}\right]\bar{J}(s)\right\} + [\varphi_0^{+0} \odot \tilde{\xi}_0^{0+}](s),$$
$$\mathcal{W}_{0+}^{(1)P\pi}(s) = \frac{\mathrm{c}_{+0}}{3F_\pi^2}\left[\frac{B_x\mathrm{c}_{+0}}{18}\frac{16\pi}{2}\frac{(s-4M_\pi^2)^2}{F_\pi^4}\bar{J}^2(s) - \frac{C_x-D_x}{6}\frac{(s-4M_\pi^2)(s-s_0)}{F_\pi^4}\bar{J}(s) + \tilde{\xi}_1^{0+}(s)\right], \tag{D5}$$

with

$$\frac{\mathcal{B}_{+;x}}{2} = \mathcal{B}_{+;0+} = B_x\mathrm{c}_{+0}, \qquad \mathcal{B}_{-;x} = \mathcal{B}_{-;0+} = 0, \tag{D6}$$

and

$$\tilde{w}_x^{(0)} = 2\left[A_x + \frac{B_x}{6}\frac{M_K^2+3M_\pi^2}{F_\pi^2}\right]\left(\mathrm{a}_{+0} - \mathrm{b}_{+0}\frac{4M_\pi^2}{F_\pi^2}\right) + \frac{4}{3}B_x\mathrm{c}_{+0}\frac{M_\pi^2(M_K^2+3M_\pi^2)}{F_\pi^4},$$
$$\tilde{w}_x^{(1)} = 2\mathrm{b}_{+0}\left[A_x + \frac{B_x}{6}\frac{M_K^2+3M_\pi^2}{F_\pi^2}\right] - B_x\left(\mathrm{a}_{+0} - \mathrm{b}_{+0}\frac{4M_\pi^2}{F_\pi^2}\right) - \frac{1}{3}B_x\mathrm{c}_{+0}\frac{M_K^2+7M_\pi^2}{F_\pi^2},$$
$$\tilde{w}_x^{(2)} = B_x\left(-\mathrm{b}_{+0} + \frac{1}{3}\mathrm{c}_{+0}\right), \tag{D7}$$

$$\tilde{w}^{(0)}_{\pm;0+} = -\left[A_x + \frac{B_x}{6}\frac{M_K^2+3M_\pi^2}{F_\pi^2}\right]\left(\mathrm{a}_{+0} - \mathrm{b}_{+0}\frac{4M_\pi^2}{F_\pi^2}\right) + \frac{2}{3}B_x\mathrm{c}_{+0}\frac{M_\pi^2(M_K^2+3M_\pi^2)}{F_\pi^4} \mp \left[A_{++} + \frac{B_{++}}{6}\frac{M_K^2+3M_\pi^2}{F_\pi^2}\right]\left(\mathrm{a}_x - \mathrm{b}_x\frac{4M_\pi^2}{F_\pi^2}\right)$$
$$\mp \left[A_x - \frac{B_x}{3}\frac{M_K^2+3M_\pi^2}{F_\pi^2}\right]\frac{\mathrm{a}_{00}}{2},$$
$$\tilde{w}^{(1)}_{\pm;0+} = -\mathrm{b}_{+0}\left[A_x + \frac{B_x}{6}\frac{M_K^2+3M_\pi^2}{F_\pi^2}\right] + \frac{B_x}{2}\left(\mathrm{a}_{+0} - \mathrm{b}_{+0}\frac{4M_\pi^2}{F_\pi^2}\right) - \frac{1}{6}B_x\mathrm{c}_{+0}\frac{M_K^2+7M_\pi^2}{F_\pi^2} \mp \mathrm{b}_x\left[A_{++} + \frac{B_{++}}{6}\frac{M_K^2+3M_\pi^2}{F_\pi^2}\right]$$
$$\pm\frac{B_{++}}{2}\left(\mathrm{a}_x - \mathrm{b}_x\frac{4M_\pi^2}{F_\pi^2}\right) \mp \frac{B_x\mathrm{a}_{00}}{2},$$
$$\tilde{w}^{(2)}_{\pm;0+} = \frac{1}{2}\left[B_x\left(\mathrm{b}_{+0} + \frac{\mathrm{c}_{+0}}{3}\right) \pm B_{++}\mathrm{b}_x\right]. \tag{D8}$$

For the amplitude of K_L decaying into one charged and two neutral pions, we have

$$\mathcal{W}^{P\pi}_{L;x}(s) = \varphi_0^{+-}(s)\left\{\frac{(16\pi)^2}{4}[2\tilde{\varphi}_0^{L;x}(s)\varphi_0^{+-}(s) + \tilde{\varphi}_0^{L;00}(s)\varphi_0^{x}(s)]\bar{J}^2(s) + \left[\left(C_x^L + \frac{D_x^L}{2}\right)\frac{(s-s_0)^2}{F_\pi^4} + \frac{2}{3}D_x^L\frac{K^2(s)}{F_\pi^4}\right]\bar{J}(s)\right\}$$
$$+ [\varphi_0^{+-}\odot\tilde{\xi}_0^{L;x}](s) + \frac{\varphi_0^x(s)}{2}\left\{C_{00}^L\left[\frac{3}{2}\frac{(s-s_0)^2}{F_\pi^4} + \frac{2}{3}\frac{K_x^2(s)}{F_\pi^4}\right]\bar{J}(s) + \frac{(16\pi)^2}{4}[2\tilde{\varphi}_0^{L;x}(s)\varphi_0^x(s) + \tilde{\varphi}_0^{L;00}(s)\varphi_0^{00}(s)]\bar{J}^2(s)\right\}$$
$$+ \frac{1}{2}[\varphi_0^x\odot\tilde{\xi}_0^{L;00}](s),$$
$$\mathcal{W}^{(0)P\pi}_{L;+0} = \varphi_0^{+0}(s)\left\{\frac{(16\pi)^2}{2}\varphi_0^{+0}(s)\tilde{\varphi}_0^{L;+0}(s)\bar{J}^2(s) - \left[\frac{1}{4}(C_x^L + 5D_x^L)\frac{(s-s_0)^2}{F_\pi^4} + \frac{1}{3}(C_x^L + D_x^L)\frac{K^2(s)}{F_\pi^4}\right]\bar{J}(s)\right\} + [\varphi_0^{+0}\odot\tilde{\xi}_0^{L;0+}](s),$$
$$\mathcal{W}^{(1)P\pi}_{L;+0} = \frac{\mathrm{c}_{+0}}{3F_\pi^2}\left[\frac{B_x^L\mathrm{c}_{+0}}{18}\frac{16\pi}{2}\frac{(s-4M_\pi^2)^2}{F_\pi^4}\bar{J}^2(s) - \frac{C_x^L - D_x^L}{6}\frac{(s-4M_\pi^2)(s-s_0)}{F_\pi^4}\bar{J}(s) + \tilde{\xi}_1^{L;+0}(s)\right] \tag{D9}$$

with

$$\frac{\mathcal{B}_{+;L;x}}{2} = \mathcal{B}_{\pm;L;+0} = B_x^L\mathrm{c}_{+0}, \qquad \mathcal{B}_{-;L;x} = 0, \tag{D10}$$

and

$$\tilde{w}^{(0)}_{L;x} = 2\left[A_x^L + \frac{B_x^L}{6}\frac{M_{K_L}^2+3M_\pi^2}{F_\pi^2}\right]\left(\mathrm{a}_{+0} - \mathrm{b}_{+0}\frac{4M_\pi^2}{F_\pi^2}\right) + \frac{4}{3}B_x^L\mathrm{c}_{+0}\frac{M_\pi^2(M_{K_L}^2+3M_\pi^2)}{F_\pi^4},$$
$$\tilde{w}^{(1)}_{L;x} = 2\mathrm{b}_{+0}\left[A_x^L + \frac{B_x^L}{6}\frac{M_{K_L}^2+3M_\pi^2}{F_\pi^2}\right] - B_x^L\left(\mathrm{a}_{+0} - \mathrm{b}_{+0}\frac{4M_\pi^2}{F_\pi^2}\right) - \frac{1}{3}B_x^L\mathrm{c}_{+0}\frac{M_{K_L}^2+7M_\pi^2}{F_\pi^2},$$
$$\tilde{w}^{(2)}_{L;x} = B_x^L\left(-\mathrm{b}_{+0} + \frac{1}{3}\mathrm{c}_{+0}\right), \tag{D11}$$

$$\tilde{w}^{(0)}_{\pm;L;+0} = -\left[A_x^L + \frac{B_x^L}{6}\frac{M_{K_L}^2+3M_\pi^2}{F_\pi^2}\right]\left(\mathrm{a}_{+0} - \mathrm{b}_{+0}\frac{4M_\pi^2}{F_\pi^2}\right) + \frac{2}{3}B_x^L\mathrm{c}_{+0}\frac{M_\pi^2(M_{K_L}^2+3M_\pi^2)}{F_\pi^4} \mp \frac{A_{00}^L}{2}\left(\mathrm{a}_x - \mathrm{b}_x\frac{4M_\pi^2}{F_\pi^2}\right)$$
$$\mp \left[A_x^L - \frac{B_x^L}{3}\frac{M_{K_L}^2+3M_\pi^2}{F_\pi^2}\right]\left(\mathrm{a}_{+-} - \mathrm{b}_{+-}\frac{4M_\pi^2}{F_\pi^2}\right),$$
$$\tilde{w}^{(1)}_{\pm;L;+0} = -\mathrm{b}_{+0}\left[A_x^L + \frac{B_x^L}{6}\frac{M_{K_L}^2+3M_\pi^2}{F_\pi^2}\right] + \frac{B_x^L}{2}\left(\mathrm{a}_{+0} - \mathrm{b}_{+0}\frac{4M_\pi^2}{F_\pi^2}\right) - \frac{1}{6}B_x^L\mathrm{c}_{+0}\frac{M_{K_L}^2+7M_\pi^2}{F_\pi^2} \mp \mathrm{b}_{+-}\left[A_x^L - \frac{B_x^L}{3}\frac{M_{K_L}^2+3M_\pi^2}{F_\pi^2}\right]$$
$$\mp B_x^L\left(\mathrm{a}_{+-} - \mathrm{b}_{+-}\frac{4M_\pi^2}{F_\pi^2}\right) \mp \frac{A_{00}^L\mathrm{b}_x}{2},$$
$$\tilde{w}^{(2)}_{\pm;L;+0} = \frac{1}{6}B_x^L(3\mathrm{b}_{+0} + \mathrm{c}_{+0} \mp 6\mathrm{b}_{+-}). \tag{D12}$$

For the decay of K_L into three neutral pions, we obtain

$$\mathcal{W}^{P\pi}_{L;00}(s) = \varphi^x_0(s)\left\{\frac{(16\pi)^2}{4}[2\tilde{\varphi}^{L;x}_0(s)\varphi^{+-}_0(s) + \tilde{\varphi}^{L;00}_0(s)\varphi^x_0(s)]\bar{J}^2(s) + \left[\left(C^L_x + \frac{D^L_x}{2}\right)\frac{(s-s_0)^2}{F^4_\pi} + \frac{2}{3}D^L_x\frac{K^2(s)}{F^4_\pi}\right]\bar{J}(s)\right\}$$
$$+ [\varphi^x_0 \odot \tilde{\xi}^{L;x}_0](s) + \frac{\varphi^{00}_0(s)}{2}\left\{\frac{(16\pi)^2}{4}[2\tilde{\varphi}^{L;x}_0(s)\varphi^x_0(s) + \tilde{\varphi}^{L;00}_0(s)\varphi^{00}_0(s)]\bar{J}^2(s) + C^L_{00}\left[\frac{3}{2}\frac{(s-s_0)^2}{F^4_\pi} + \frac{2}{3}\frac{K^2_x(s)}{F^4_\pi}\right]\bar{J}(s)\right\}$$
$$+ \frac{1}{2}[\varphi^{00}_0 \odot \tilde{\xi}^{L;00}_0](s), \tag{D13}$$

with

$$\mathcal{B}_{\pm;L;00} = 0, \tag{D14}$$

and

$$\tilde{w}^{(0)}_{L;00} = A^L_{00}\mathrm{a}_{00} + 2\left[A^L_x - \frac{B^L_x}{3}\frac{M^2_{K_L} + 3M^2_\pi}{F^2_\pi}\right]\left(\mathrm{a}_x - \mathrm{b}_x\frac{4M^2_\pi}{F^2_\pi}\right),$$
$$\tilde{w}^{(1)}_{L;00} = 2\mathrm{b}_x\left[A^L_x - \frac{B^L_x}{3}\frac{M^2_{K_L} + 3M^2_\pi}{F^2_\pi}\right] + 2B^L_x\left(\mathrm{a}_x - \mathrm{b}_x\frac{4M^2_\pi}{F^2_\pi}\right),$$
$$\tilde{w}^{(2)}_{L;00} = 2B^L_x\mathrm{b}_x. \tag{D15}$$

Finally, for the three-pion decay of K_S, we find

$$\mathcal{W}^{(1)P\pi}_{S;x} = \frac{\mathrm{c}_{+-}}{3F^2_\pi}\left[\frac{B^S_x\mathrm{c}_{+-}}{9}\frac{16\pi}{2}\frac{(s-4M^2_\pi)^2}{F^4_\pi}\bar{J}^2(s) - \frac{D^S_x}{3}\frac{(s-4M^2_\pi)(s-s_0)}{F^4_\pi}\bar{J}(s) + \tilde{\xi}^{S;x}_1(s)\right],$$
$$\mathcal{W}^{(0)P\pi}_{S;+0} = \varphi^{+0}_0(s)\left\{\frac{(16\pi)^2}{2}\varphi^{+0}_0(s)\tilde{\varphi}^{S;+0}_0(s)\bar{J}^2(s) + \frac{D^S_x}{12}\left[9\frac{(s-s_0)^2}{F^4_\pi} - 4\frac{K^2(s)}{F^4_\pi}\right]\bar{J}(s)\right\} + [\varphi^{+0}_0 \odot \tilde{\xi}^{S;0+}_0](s),$$
$$\mathcal{W}^{(1)P\pi}_{S;+0} = \frac{\mathrm{c}_{+0}}{3F^2_\pi}\left[-\frac{B^S_x\mathrm{c}_{+0}}{18}\frac{16\pi}{2}\frac{(s-4M^2_\pi)^2}{F^4_\pi}\bar{J}^2(s) + \frac{D^S_x}{6}\frac{(s-4M^2_\pi)(s-s_0)}{F^4_\pi}\bar{J}(s) + \tilde{\xi}^{S;+0}_1(s)\right], \tag{D16}$$

with

$$\mathcal{B}_{+;S;x} = 2B^S_x\mathrm{c}_{+0}, \qquad \mathcal{B}_{+;S;x} = 0, \tag{D17}$$

$$\mathcal{B}_{\pm;S;+0} = (1 \pm 2)B^S_x\mathrm{c}_{+0}, \tag{D18}$$

and

$$\tilde{w}^{(0)}_{S;x} = -B^S_x\frac{M^2_{K_S} + 3M^2_\pi}{F^2_\pi}\left(\mathrm{a}_{+0} - \mathrm{b}_{+0}\frac{4M^2_\pi}{F^2_\pi}\right) + \frac{4}{3}B^S_x\mathrm{c}_{+0}\frac{M^2_\pi(M^2_{K_S} + 3M^2_\pi)}{F^4_\pi},$$
$$\tilde{w}^{(1)}_{S;x} = 3B^S_x\left(\mathrm{a}_{+0} - \mathrm{b}_{+0}\frac{4M^2_\pi}{F^2_\pi}\right) - B^S_x\mathrm{b}_{+0}\frac{M^2_{K_S} + 3M^2_\pi}{F^2_\pi} - \frac{1}{3}B^S_x\mathrm{c}_{+0}\frac{M^2_{K_S} + 7M^2_\pi}{F^2_\pi},$$
$$\tilde{w}^{(2)}_{S;x} = B^S_x\left(3\mathrm{b}_{+0} + \frac{1}{3}\mathrm{c}_{+0}\right), \tag{D19}$$

$$\tilde{w}^{(0)}_{\pm;S;+0} = \frac{B^S_x}{2}\frac{M^2_{K_S} + 3M^2_\pi}{F^2_\pi}\left(\mathrm{a}_{+0} - \mathrm{b}_{+0}\frac{4M^2_\pi}{F^2_\pi}\right) - \frac{2}{3}B^S_x\mathrm{c}_{+0}\frac{M^2_\pi(M^2_{K_S} + 3M^2_\pi)}{F^4_\pi}(1 \pm 2),$$
$$\tilde{w}^{(1)}_{\pm;S;+0} = -\frac{3B^S_x}{2}\left(\mathrm{a}_{+0} - \mathrm{b}_{+0}\frac{4M^2_\pi}{F^2_\pi}\right) + \frac{B^S_x\mathrm{b}_{+0}}{2}\frac{M^2_{K_S} + 3M^2_\pi}{F^2_\pi} - \frac{1}{6}B^S_x\mathrm{c}_{+0}\frac{M^2_\pi(M^2_{K_S} + 7M^2_\pi)}{F^4_\pi}(1 \pm 2),$$
$$\tilde{w}^{(2)}_{\pm;S;+0} = -\frac{3}{2}B^S_x\left[\mathrm{b}_{+0} - \frac{\mathrm{c}_{+0}}{9}(1 \pm 2)\right]. \tag{D20}$$

[1] J. R. Batley *et al.* (NA48/2 Collaboration), Observation of a cusp-like structure in the $\pi^0\pi^0$ invariant mass distribution from $K^\pm \to \pi^\pm\pi^0\pi^0$ decay and determination of the $\pi\pi$ scattering lengths, Phys. Lett. B **633**, 173 (2006).

[2] J. R. Batley *et al.* (NA48/2 Collaboration), Search for direct CP violation in the decays $K^\pm \to 3\pi^\pm$, Phys. Lett. B **634**, 474 (2006).

[3] J. R. Batley *et al.* (NA48/2 Collaboration), Search for direct CP-violation in $K^\pm \to \pi^\pm\pi^0\pi^0$ decays, Phys. Lett. B **638**, 22 (2006); Erratum Phys. Lett. B **640**, 297 (2006).

[4] J. R. Batley *et al.* (NA48/2 Collaboration), Measurement of the Dalitz plot slopes of the $K^\pm \to \pi^\pm\pi^+\pi^-$ decay, Phys. Lett. B **649**, 349 (2007).

[5] J. R. Batley *et al.* (NA48/2 Collaboration), Search for direct CP violating charge asymmetries in $K^\pm \to \pi^\pm\pi^+\pi^-$ and $K\pm \to \pi^\pm\pi^0\pi^0$ decays, Eur. Phys. J. C **52**, 875 (2007).

[6] J. R. Batley *et al.*, Determination of the S-wave pi pi scattering lengths from a study of $K^\pm \to \pi^\pm\pi^0\pi^0$ decays, Eur. Phys. J. C **64**, 589 (2009).

[7] J. R. Batley *et al.* (NA48/2 Collaboration), Empirical parameterization of the $K^\pm \to \pi^\pm\pi^0\pi^0$ decay Dalitz plot, Phys. Lett. B **686**, 101 (2010).

[8] E. Abouzaid *et al.* (KTeV Collaboration), Detailed study of the $K(L) \to \pi^0\pi^0\pi^0$ Dalitz Plot, Phys. Rev. D **78**, 032009 (2008).

[9] M. Bashkanov *et al.*, Measurement of the slope parameter for the $\eta \to 3\pi^0$ decay in the $\pi\pi \to \pi\pi\eta$ reaction, Phys. Rev. C **76**, 048201 (2007).

[10] F. Ambrosino *et al.* (KLOE Collaboration), Determination of $\eta \to \pi^+\pi^-\pi^0$ Dalitz plot slopes and asymmetries with the KLOE detector, J. High Energy Phys. 05 (2008) 006.

[11] C. Adolph *et al.* (WASA-at-COSY Collaboration), Measurement of the $\eta \to 3\pi^0$ Dalitz plot distribution with the WASA detector at COSY, Phys. Lett. B **677**, 24 (2009).

[12] S. Prakhov *et al.* (Crystal Ball at MAMI and A2 Collaborations), Measurement of the slope parameter alpha for the $\eta \to 3\pi^0$ decay with the crystal ball at MAMI-C, Phys. Rev. C **79**, 035204 (2009).

[13] M. Unverzagt *et al.* (Crystal Ball at MAMI and TAPS and A2 Collaborations), Determination of the Dalitz plot parameter alpha for the decay $\eta \to 3\pi^0$ with the Crystal Ball at MAMI-B, Eur. Phys. J. A **39**, 169 (2009).

[14] F. Ambrosino *et al.* (KLOE Collaboration), Measurement of the $\eta \to 3\pi^0$ slope parameter α with the KLOE detector, Phys. Lett. B **694**, 16 (2010).

[15] P. Adlarson *et al.* (WASA-at-COSY Collaboration), Measurement of the $\eta \to \pi^+\pi^-\pi^0$ Dalitz plot distribution, Phys. Rev. C **90**, 045207 (2014).

[16] A. Anastasi *et al.* (KLOE-2 Collaboration), Precision measurement of the $\eta \to \pi^+\pi^-\pi^0$ Dalitz plot distribution with the KLOE detector, J. High Energy Phys. 05 (2016) 019.

[17] M. Ablikim *et al.* (BESIII Collaboration), Measurement of the matrix elements for the decays $\eta \to \pi^+\pi^-\pi^0$ and $\eta/\eta' \to \pi^0\pi^0\pi^0$, Phys. Rev. D **92**, 012014 (2015).

[18] S. Prakhov *et al.* (A2 Collaboration), High-statistics measurement of the $\eta \to 3\pi^0$ decay at the Mainz microtron, Phys. Rev. C **97**, 065203 (2018).

[19] H. B. Li, η and η' physics at BES-III, J. Phys. G **36**, 085009 (2009).

[20] L. Gan, Probes for fundamental QCD symmetries and a dark gauge boson via light meson decays, Proc. Sci., CD15 (**2015**) 017.

[21] J. Bijnens, P. Dhonte, and F. Borg, $K \to 3\pi$ decays in chiral perturbation theory, Nucl. Phys. **B648**, 317 (2003).

[22] J. Bijnens and F. Borg, Isospin breaking in $K \to 3\pi$ decays. 1. Strong isospin breaking, Nucl. Phys. **B697**, 319 (2004).

[23] J. Bijnens and F. Borg, Isospin breaking in $K \to 3\pi$ decays. II. Radiative corrections, Eur. Phys. J. C **39**, 347 (2005).

[24] J. Bijnens and F. Borg, Isospin breaking in $K \to 3\pi$ decays III: Bremsstrahlung and fit to experiment, Eur. Phys. J. C **40**, 383 (2005).

[25] E. Gamiz, J. Prades, and I. Scimemi, Charged kaon $K \to 3\pi$ CP violating asymmetries at NLO in CHPT, J. High Energy Phys. 10 (2003) 042.

[26] N. Cabibbo, Determination of the $a_0 - a_2$ Pion Scattering Length from $K^\pm \to \pi^+\pi^0\pi^0$ decay, Phys. Rev. Lett. **93**, 121801 (2004).

[27] N. Cabibbo and G. Isidori, Pion-pion scattering and the $K \to 3\pi$ decay amplitudes, J. High Energy Phys. 03 (2005) 021.

[28] E. Gamiz, J. Prades, and I. Scimemi, $K \to 3\pi$ final state interactions at NLO in CHPT and Cabibbo's proposal to measure $a_0 - a_2$, Eur. Phys. J. C **50**, 405 (2007).

[29] G. Colangelo, J. Gasser, B. Kubis, and A. Rusetsky, Cusps in $K \to 3\pi$ decays, Phys. Lett. B **638**, 187 (2006).

[30] J. Bijnens and K. Ghorbani, $\eta \to 3\pi$ at two loops in chiral perturbation theory, J. High Energy Phys. 11 (2007) 030.

[31] M. Bissegger, A. Fuhrer, J. Gasser, B. Kubis, and A. Rusetsky, Cusps in $K(L) \to 3\pi$ decays, Phys. Lett. B **659**, 576 (2008).

[32] M. Bissegger, A. Fuhrer, J. Gasser, B. Kubis, and A. Rusetsky, Cusps in $K(L) \to 3\pi$ decays, Prog. Part. Nucl. Phys. **61**, 178 (2008).

[33] M. Bissegger, A. Fuhrer, J. Gasser, B. Kubis, and A. Rusetsky, Radiative corrections in $K \to 3\pi$ decays, Nucl. Phys. **B806**, 178 (2009).

[34] C.-O. Gullstrom, A. Kupsc, and A. Rusetsky, Predictions for the cusp in $\eta \to 3\pi^0$ decay, Phys. Rev. C **79**, 028201 (2009).

[35] S. P. Schneider, B. Kubis, and C. Ditsche, Rescattering effects in $\eta \to 3\pi$ decays, J. High Energy Phys. 02 (2011) 028.

[36] K. Kampf, M. Knecht, J. Novotný, and M. Zdráhal, Analytical dispersive construction of $\eta \to 3\pi$ amplitude: First order in isospin breaking, Phys. Rev. D **84**, 114015 (2011).

[37] J. Gasser, B. Kubis, and A. Rusetsky, Cusps in $K \to 3\pi$ decays: A theoretical framework, Nucl. Phys. **B850**, 96 (2011).

[38] S. Descotes-Genon and B. Moussallam, Analyticity of $\eta\pi$ isospin-violating form factors and the $\tau \to \eta\pi\nu$ second-class decay, Eur. Phys. J. C **74**, 2946 (2014).

[39] M. Kolesár and J. Novotný, Convergence properties of $\eta \to 3\pi$ decays in chiral perturbation theory, Eur. Phys. J. C **77**, 41 (2017).

[40] G. Colangelo, S. Lanz, H. Leutwyler, and E. Passemar, $\eta \to 3\pi$: Study of the Dalitz Plot and Extraction of the Quark Mass Ratio Q, Phys. Rev. Lett. **118**, 022001 (2017).

[41] M. Albaladejo and B. Moussallam, Extended chiral Khuri-Treiman formalism for $\eta \to 3\pi$ and the role of the $a_0(980)$, $f_0(980)$ resonances, Eur. Phys. J. C **77**, 508 (2017).

[42] M. Kolesár and J. Novotný, Constraints on low energy QCD parameters from $\eta \to 3\pi$ and $\pi\pi$ scattering, Eur. Phys. J. C **78**, 264 (2018).
[43] G. Colangelo, S. Lanz, H. Leutwyler, and E. Passemar, Dispersive analysis of $\eta \to 3\pi$, Eur. Phys. J. C **78**, 947 (2018).
[44] S. Descotes-Genon and M. Knecht, Two-loop representations of low-energy pion form factors and $\pi\pi$ scattering phases in the presence of isospin breaking, Eur. Phys. J. C **72**, 1962 (2012).
[45] J. Stern, H. Sazdjian, and N. H. Fuchs, What π-π scattering tells us about chiral perturbation theory, Phys. Rev. D **47**, 3814 (1993).
[46] M. Knecht, B. Moussallam, J. Stern, and N. H. Fuchs, The low-energy $\pi\pi$ amplitude to one and two loops, Nucl. Phys. **B457**, 513 (1995).
[47] M. Zdráhal and J. Novotný, Dispersive approach to chiral perturbation theory, Phys. Rev. D **78**, 116016 (2008).
[48] V. Bernard, S. Descotes-Genon, and M. Knecht, Isospin breaking in the phases of the K_{e4} form factors, Eur. Phys. J. C **73**, 2478 (2013).
[49] G. Colangelo, E. Passemar, and P. Stoffer, A dispersive treatment of $K_{\ell 4}$ decays, Eur. Phys. J. C **75**, 172 (2015).
[50] K. Kampf, M. Knecht, J. Novotný, and M. Zdráhal (to be published).
[51] K. Kampf, M. Knecht, J. Novotný, and M. Zdráhal (to be published).
[52] K. Kampf, M. Knecht, J. Novotný, and M. Zdráhal, Dispersive representation of $K \to 3\pi$ amplitudes and cusps, Nucl. Phys. B, Proc. Suppl. **186**, 334 (2009).
[53] M. Zdráhal, K. Kampf, M. Knecht, and J. Novotný, Dispersive construction of two-loop $P \to 3\pi$ $(P = K, \eta)$ amplitudes, Proc. Sci., EFT09 (**2009**) 063 [arXiv:0905.4868].
[54] M. Zdráhal, K. Kampf, M. Knecht, and J. Novotný, Construction of the $\eta \to 3\pi$ (and $K \to 3\pi$) amplitudes using dispersive approach, Proc. Sci., CD09 (**2009**) 122 [arXiv:0910.1721].
[55] M. Zdráhal, Construction of pseudoscalar meson amplitudes in chiral perturbation theory using a dispersive approach, Ph.D. thesis, Charles University, Prague, 2011, https://is.cuni.cz/webapps/zzp/download/140012164.
[56] J. Gasser and H. Leutwyler, Chiral perturbation theory: Expansions in the mass of the strange quark, Nucl. Phys. **B250**, 465 (1985).
[57] J. Kambor, J. H. Missimer, and D. Wyler, The chiral loop expansion of the nonleptonic weak interactions of mesons, Nucl. Phys. **B346**, 17 (1990).
[58] J. Kambor, J. H. Missimer, and D. Wyler, $K \to 2\pi$ and $K \to 3\pi$ decays in next-to-leading order chiral, Phys. Lett. B **261**, 496 (1991).
[59] D. G. Sutherland, Current algebra and the decay $\eta \to 3\pi$, Phys. Lett. **23**, 384 (1966).
[60] J. S. Bell and D. G. Sutherland, Current algebra and $\eta \to 3\pi$, Nucl. Phys. **B4**, 315 (1968).
[61] R. Baur, J. Kambor, and D. Wyler, Electromagnetic corrections to the decays $\eta \to 3\pi$, Nucl. Phys. **B460**, 127 (1996).
[62] C. Ditsche, B. Kubis, and U.-G. Meißner, Electromagnetic corrections in $\eta \to 3\pi$ decays, Eur. Phys. J. C **60**, 83 (2009).
[63] J. A. Cronin, Phenomenological model of strong and weak interactions in chiral U(3) x U(3), Phys. Rev. **161**, 1483 (1967).
[64] J. Gasser and H. Leutwyler, $\eta \to 3\pi$ to one loop, Nucl. Phys. **B250**, 539 (1985).
[65] J. Kambor, C. Wiesendanger, and D. Wyler, Final state interactions and Khuri-Treiman equations in $\eta \to 3\pi$ decays, Nucl. Phys. **B465**, 215 (1996).
[66] A. V. Anisovich and H. Leutwyler, Dispersive analysis of the decay $\eta \to 3\pi$, Phys. Lett. B **375**, 335 (1996).
[67] N. N. Khuri and S. B. Treiman, Pion-pion scattering and $K^{\pm} \to 3\pi$ decay, Phys. Rev. **119**, 1115 (1960).
[68] C. Kacser, Analytic structure of partial-wave amplitudes for production and decay processes, Phys. Rev. **132**, 2712 (1963).
[69] G. Bonnevay, A model for final-state interactions, Nuovo Cimento **30**, 1325 (1963).
[70] J. B. Bronzan, Overlapping resonances in dispersion theory, Phys. Rev. **134**, B687 (1964).
[71] I. J. R. Aitchison, Final state interactions among three particles, Nuovo Cimento **35**, 434 (1965).
[72] A. Neveu and J. Scherk, Final-state interaction and current algebra in $K_{3\pi}$ and $\eta_{3\pi}$ decays, Ann. Phys. (N.Y.) **57**, 39 (1970).
[73] A. V. Anisovich, Dispersion relation technique for three pion system and the P wave interaction in $\eta \to 3\pi$ decay, Yad. Fiz. **58N8**, 1467 (1995) [Phys. At. Nucl. **58**, 1383 (1995)].
[74] A. Angelopoulos *et al.* (CPLEAR Collaboration), The neutral kaon decays to $\pi^+\pi^-\pi^0$: A detailed analysis of the CPLEAR data, Eur. Phys. J. C **5**, 389 (1998).
[75] A. Angelopoulos *et al.* (CPLEAR Collaboration), Physics at CPLEAR, Phys. Rep. **374**, 165 (2003).
[76] J. R. Batley *et al.* (NA48 Collaboration), A measurement of the CP-conserving component of the decay $K0(S) \to \pi^+\pi^-\pi^0$, Phys. Lett. B **630**, 31 (2005).
[77] R. J. Eden, P. V. Landshoff, D. I. Olive, and J. C. Polkinghorne, *The Analytic S-Matrix* (Cambridge University Press, Cambridge, England, 1966).
[78] J. Kennedy and T. D. Spearman, Singularities in partial-wave amplitudes for two ingoing and two outgoing particles, Phys. Rev. **126**, 1596 (1962).
[79] J. B. Bronzan and C. Kacser, Khuri-Treiman representation and perturbation theory, Phys. Rev. **132**, 2703 (1963).
[80] V. V. Anisovich and A. A. Anselm, Theory of reactions with production of three particles near threshold, Usp. Fyz. Nauk **88**, 287 (1966) [Sov. Phys. Usp. **9**, 117 (1966)].
[81] M. Tanabashi *et al.* (Particle Data Group), Review of particle physics, Phys. Rev. D **98**, 030001 (2018) and 2019 update.
[82] S. L. Adler, Consistency conditions on the strong interactions implied by a partially conserved axial vector current, Phys. Rev. **137**, B1022 (1965).
[83] S. L. Adler, Consistency conditions on the strong interactions implied by a partially conserved axial-vector current. II, Phys. Rev. **139**, B1638 (1965).
[84] M. Knecht and R. Urech, Virtual photons in low-energy $\pi\pi$ scattering, Nucl. Phys. **B519**, 329 (1998).

[85] G. Barton and C. Kacser, Some analytic properties of a decay amplitude with final state interactions. 1. The vertex diagrams in $K \to 3\pi$ decay, Nuovo Cimento **21**, 593 (1961).
[86] P. Herrera-Siklody, J. I. Latorre, P. Pascual, and J. Taron, Chiral effective Lagrangian in the large N(c) limit: The Nonet case, Nucl. Phys. **B497**, 345 (1997).
[87] R. Kaiser and H. Leutwyler, Large N(c) in chiral perturbation theory, Eur. Phys. J. C **17**, 623 (2000).
[88] M. Ablikim *et al.* (BESIII Collaboration), Measurement of the matrix element for the decay $\eta' \to \eta\pi^+\pi^-$, Phys. Rev. D **83**, 012003 (2011).
[89] P. Adlarson *et al.*, Measurement of the decay $\eta' \to \pi^0\pi^0\eta$ at MAMI, Phys. Rev. D **98**, 012001 (2018).
[90] M. Ablikim *et al.* (BESIII Collaboration), Measurement of the matrix elements for the decays $\eta' \to \eta\pi^+\pi^-$ and $\eta' \to \eta\pi^0\pi^0$, Phys. Rev. D **97**, 012003 (2018).
[91] L. D. Landau, On analytic properties of vertex parts in quantum field theory, Nucl. Phys. **13**, 181 (1959).
[92] N. Nakanishi, Ordinary and anomalous thresholds in perturbation theory, Prog. Theor. Phys. **22**, 128 (1959); A note on the ordinary and anomalous thresholds in perturbation theory, Prog. Theor. Phys. **23**, 284 (1960).
[93] J. Gasser and M. E. Sainio, Two loop integrals in chiral perturbation theory, Eur. Phys. J. C **6**, 297 (1999).
[94] B. Petersson, Reduction of a one-loop Feynman diagram with n vertices in m-dimensional Lorentz space, J. Math. Phys. (N.Y.) **6**, 1955 (1965).
[95] G. 't Hooft and M. J. G. Veltman, Scalar one loop integrals, Nucl. Phys. **B153**, 365 (1979).
[96] S. Saks and A. Zygmund, *Analytic Functions*, Monografie Matematyczne (Polskie Towarzystwo Matematyczne, Warsaw, Poland, 1952), Vol. 28; translated by E. J. Scott, 3rd rev. ed. (Elsevier Publishing, Amsterdam, Netherlands, 1971).